N°d'ordre NNT : 2017LYSEM021

THESE de DOCTORAT DE L'UNIVERSITE DE LYON

opérée au sein de

MINES Saint-Etienne

délivrée en partenariat international avec Ben Gurion University of Negev

Ecole Doctorale N° 488

Sciences, Ingénierie, Santé

Spécialité de doctorat : SCIENCES ET GENIE DES MATERIAUX

Soutenue publiquement le 14/09/2017, par :

Mathieu Dutto

Procédé micro-ondes pour l'élaboration de composites B_4C-SiC par infiltration et réaction de silicium, en vue d'applications balistiques

---

Devant le jury composé de :

Monsieur Lepetitcorps Yan	Professeur de l'université de Bordeaux, , Thermostructural Composites Laboratory CEA - SNECMA – CNRS, Bordeaux France	Président
Monsieur Bernard Frédéric	Professeur de l'UFR Sciences et Technique, Laboratoire Interdisciplinaire Carnot de Bourgogne, Dijon France	Rapporteur
Monsieur Maître Alexandre	Professeur de l'université de Limoge, SPCTS-Centre Européen de la Céramique, Limoge France	Rapporteur
Monsieur Frage Nachum	Professeur de l'université Ben Gurion, Departement of Material Engineering, Beer-Sheva, Israel	Examinateur
Monsieur Saunier Sébastien	Maître de conférence de Mines Saint-Etienne, Mines Saint-Etienne, Saint-Etienne, France	Co-Encadrant
Monsieur Sylvain Marinel	Professeur de l'Université de Caen, CRISMAT, Caen, France	Co-Directeur
Monsieur Hayun Shmuel	Professeur de l'université Ben Gurion, Departement of Material Engineering, Beer-Sheva, Israel	Co-Directeur
Madame Goeuriot Dominique	Directeur de recherche de Mines Saint-Etienne, Mines Saint-Etienne, Saint-Etienne, France	Directrice
Monsieur Barthélemy François	Ingénieur, DGA TT, Bourge, France	Invité

Acknowledgment

This work was realized with the financial support of the DGA and the MAFAT. Under the supervision of François Barthélemy from DGA and Udi Galum from MAFAT, I would like to thank them for their work.

This work was realized between three sites: Mines Saint-etienne, Ben Gurion university of Negev and, CRISMAT laboratory.

I thank Pr.Dominique Goeuriot, Pr.Sylvain Marinel, Pr.Shmuel Hayun, Pr. Nachum Frage and Dr. Sébastien Saunier for allowing me to work on this subject, and for their time and advice.

I thank Pr.Fréderic Bernard and Pr. Alexandre Maître for accepting to review my work and being part of the jury.

I thank Pr.Yan Lepetitcorps for accepting to be the president of the jury.

I would to thank Sergio Sao-joa and Matthieu Lenci for their assistance and answers to my questions.

Contents

List of figures

List of Tables

INTRODUCTION

Since the first war, mankind has never stopped trying to find new ways of killing people and new ways of countering what they just developed. From leather armor to the latest Kevlar bullet proof armor, we seek to protect humans from the weapons they use. For protection purposes, material hardness is capital. Lightness must be kept in mind to maintain some agility and save fuel consumption for light vehicles and aircraft. During the last decades pure metal and their alloys were replaced by ceramics. Because ceramics are lighter and harder, they can be used as military and body armor. This replacement had been made possible because new materials or new ways of production tougher and less brittle technical ceramic were found. Boron carbide is a good candidate due to its very high hardness (36-42GPa). It is the third hardest industrial material nowadays known after diamond and cubic boron nitride. Another very interesting point is the very low density (2.52g/cm^3) compared to the alumina (3.97g/cm^3) actually used in military bulletproof jacket. Boron carbide is resistant to corrosion and neutron embrittlement and might be used in nuclear industry as control bar in nuclear reactors.

Nevertheless, there are some disadvantages, boron carbide is very stable, and so to obtain sufficiently density for optimal properties, sintering under pressure (30-40MPa), and temperatures above to 2200°C have to be used. These costly production steps decrease the economic potential of this material. Consequently, new production methods are being intensively investigated such as spark plasma sintering or reaction bonding to bring down the cost.

In the present work, we will focus on the reaction bonding, consisting in a composite fabrication by the chemical reactions between melted silicon and boron carbide or carbon. This technique decreases the maximum needed temperature from 2200°C to 1500°C (silicon fusion temperature) and even better, doesn't need external pressure. The final material is composed of silicon carbide, residual silicon, residual boron carbide and new phase $B_{12}(B,C,Si)_3$ (named B12 hereafter). The obtained composite has a high cohesive strength (cracks are almost not deflected by the phases interface), elevated hardness, and high efficiency for ballistic impact test while maintaining a relatively low density. The major problem for high mechanical properties is the residual silicon which is fragile. The residual silicon can be reduced by controlling initial porosity. Many techniques are currently used to decrease the porosity as pre-sintering step (1900-2100°C), the use of multimodal powder mixture to increase green compact level, addition of elements to form stable silicide or to react with boron carbide to free more carbon and form more silicon carbide.

For the last couple of decades, reaction bonded boron carbide (RBBC) was intensively studied in conventional furnaces (i.e. resistive). In our case, we adapt such a method to microwave furnaces (2.45GHz and 915 MHz).

The advantage of this approach is the rapidity of the cycle, hence a considerable energy saving for the production of the composite: the boron carbide and silicon materials have a

priori dielectric properties favorable to their heating under the Electromagnetic field, thus the feasibility of this heating method for the production of RBBC should be promising. Those materials involved are non-oxide, so heating cannot occur in air because both silicon and boron carbide would oxidize. In conventional furnaces they work under vacuum to avoid this problem but in a microwave oven, a vacuum can't be used because it promotes plasma formation, which melts everything.

Therefore, our study will adapt the constraints related to the use of microwaves to the system B_4C, Si, SiC.

The studies about solid-solid or sintering reactions have shown that the microstructures of the produced materials are generally finer than those obtained by conventional heating: the diffusion processes are favored, or even the diffusion mechanisms are modified. We will therefore investigate what the technique can best bring about improved system efficiency and achieved the final microstructures.

In addition, the link between microstructure and mechanical properties is sought. Results will be discussed in the light of the conventionally made composite properties. Finally, we will conclude on the specific role of the microwave heating on the Reaction Bonded Boron Carbide elaboration process.

Chapter I: Bibliography

INTRODUCTION

The goal of this Ph.D. thesis is to study the effect of microwave heating on the fabrication parameters, microstructure and mechanical properties of reaction bonded boron composite. This thesis has also the purpose to compare both microstructures, physical and mechanical properties obtained after microwave method and conventional heating treatments. To do this study, a literature review was done in order to have an overview of the state of the art. This chapter compiles the data dealing with various aspects of the thesis subject:

- In the first part, the presentation of boron carbide is summarized including its physical properties and how to obtain pure boron carbide pieces. This will be useful for the preforms elaboration.
- The second part is devolved to the reaction bonding technique. It can be found general explanations on the reaction bonding methods and its particular application for boron carbide. The goal of this part is to understand the process of the infiltration of boron carbide by molten metals or alloys and the possible reactions. This part allows also knowing how the reaction bonding process is carried out in order to have a good work base for the thesis and select parameters: the powder, the initial porosity of the B_4C preform, the Si form, the atmosphere and heating conditions.
- In the third part, you can find explanations on the microwave heating.

In the last part, the link between microwave and different aspect of our work is presented. In particular, in terms of microwave sintering of boron carbide and reaction bonding carried out in a microwave furnace.

1 Boron Carbide

1-1 Structure and properties

Boron carbide is a solid solution which exists for the carbon content between 8.8 and 20 at% (Cf. figure I)1). The mechanical properties and lattice parameters change in this domain. In this thesis, we will concentrate on B_4C which composition is the maximum limit of carbon.

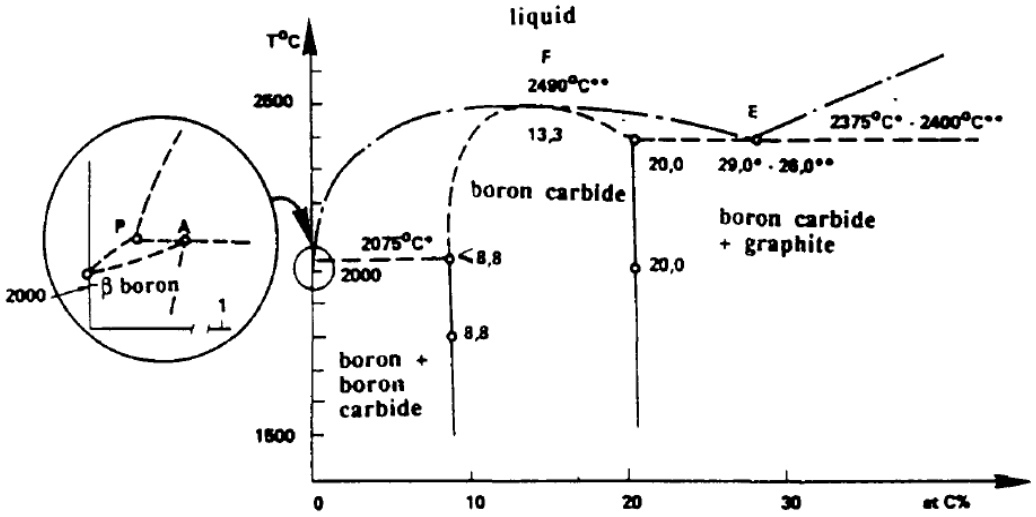

Figure I)1: Bore/carbon phase diagram [THE90]

Boron carbide lattice presents a rhombohedral structure ($D_{3d}^{\overline{5}}$, R3m). The lattice is composed of 15 atoms, and the lattice parameters for the carbon rich limit are: a=5.607Å, c=12.095Å, V=329.30Å^3 (Cf. figure I)2)[THE90].

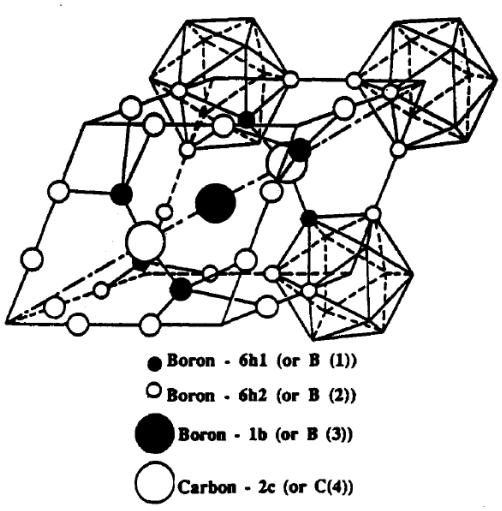

Figure I)2: Boron carbide crystalline lattice [THE90]

To produce boron carbide two reactions are possible:

- The boric acid reduction by carbon (two step reaction):

$$2\ B_2O_{3(l)} + 7\ C_{(s)} \rightarrow B_4C_{(s)} + 6\ CO_{(g)}$$

- The reaction of magnesium on boric acid and carbon:

$$2\ B_2O_{3(l)} + 6\ Mg_{(s)} + C_{(s)} \rightarrow B_4C_{(s)} + 6\ MgO_{(s)}$$

Boron carbide, which is a refractory material, gets a high melting temperature (2490°C). Thus, it is one of the known hardest materials (42GPa), just behind diamond and cubic boron nitride. B_4C presents an excellent abrasive power. It also has a low density (2.52 g/cm^3), good cold and warm mechanical properties and, a high chemical resistance in severe environments. Nevertheless, it starts to oxidize at 600°C and is sensitive to hydrolysis. Another property is that boron carbide is a good neutron absorber.

All these characteristics make it a good choice in several domains like ballistic protection (hardness and lightness) or nuclear (neutron absorber). However, its low toughness and high hardness make it difficult to cut and constrains to use expensive diamond tools. So the machining is hazardous to the workpiece because it may fracture.

Table I)1 summaries properties of pure boron carbide.

Table I)1: Physical properties of B_4C [SHA91, THE90, HAY09t]

Properties (unit)	Notation	Value
Density (g/cm^3)	ρ	2.52
Melting temperature (°C)	MT	2450
Hardness (GPa)	H	36-42
Young modulus (GPa)	E	440-471
Shear modulus (GPa)	G	186.5
Poisson coefficient	υ	0.17
Flexural strength (MPa)	Fs	300-480
Compressive strength (MPa)	Cs	2855
Toughness ($MPa.m^{1/2}$)	K_{1C}	3.2-3.6
Thermal conductivity ($W.m^{-1}.K^{-1}$)		28
Dilatation coefficient (K^{-1})	Dc	$4.5x10^{-6}$
Electrical resistivity (Ω.cm)		0.1-10
Maximum used temperature in air (°C)		540
Neutron absorption efficient section (Barns)		3850 (thermal neutron)

1-2 Boron carbide sintering

Pure non-oxide material densification without mechanical charge is very difficult. Pure dense boron carbide is very hard to obtain, because it has very strong covalent bonds, a low plasticity, a strong resistance to the grain boundary displacement (γ_b) and a weak solid state surface tension (γ_s). These properties are the exact opposite of those necessary for sintering. The oxidation of boron carbide at relatively low temperature (540°C) forms an oxide layer on the boron carbide particles, which limits further its densification. So the sintering of boron carbide is realized in an inert atmosphere (Argon). The advantage of the pressureless sintering is that it doesn't need mold, so pieces with complex forms can be considered.

1-2-1 Pressureless sintering- effect of addition

For promoting the sintering of boron carbide, it could be added some additives. These sintering aids can have the following effects:

- Change the interfacial properties, by changing the particles surface energy (γ_s) and/or the grain boundary specific energy (γ_b). The elimination of absorbed species can lead to the increase of the γ_s. In contrast, the additions of species which segregate at grain boundaries allow frequently the decrease of γ_b. In the case of boron carbide, it is well known that the elimination of the oxide layer is favorable to the densification process.

- Accelerate the transport of the matter: the objective here is to accelerate the material transfert by reducing the path of the diffusing species. This can be attained by the increase of the contact number between particles and/or by the improvement of the compact morphology homogeneity and compactness.

The sintering aids can be metals (Si, Fe, Mn, Al, Cu, Ni)[BOU85] which lead to a density close to the theoretical density (TD). But these additions can also lead to grain growth, and consequently to a decrease of mechanical properties. Another important point is that the impurity content can become too high for some applications (nuclear industry).

Some carbides, borides or oxides were studied too. As an example, for a thermal cycle between 2150 and 2280°C, the addition of 3 to 20 weight% of carbide allows obtaining a densification between 92 and 98.5% of TD. These additions decrease the bond strength. So carbides react completely with boron carbide to form boride and carbon as follows: $B_4C+Me_xC_y \rightarrow Me_xB_y+C$. The obtained carbon reduces the boron oxide on the boron carbide particles surface. Furthermore, boride and carbon well dispersed in the matrix ease the densification by delaying the grain growth. Typical carbides used are those of: Ti, Zr, Hf, V, Nb, Ta, Cr, W, Be [SCH96, RAD98, SIG98, ZAK90, PRO77]. These results are interesting but the obtained materials are composites B_4C/Me_xB_y due to the quantity of addition. Even if their mechanical properties are promising, the boron carbide grain size is relatively high (20µm).

Some oxides were also studied like stabilized zirconia [GOL01], or some borides like CrB_2 [YAM03]. The obtained materials have high densification rates and an increase of the mechanical properties was observed.

The addition of carbon was studied [SCH 80, SCH 81, BOU 85, DOL 89, SIG 91] because it has a good effect on the boron carbide densification. It seems having two different effects:

-First, reduction of the oxide layer on the boron carbide particles by the following reaction (1300°C): $B_2O_{3(l)}+7C_{(s)} \rightarrow B_4C_{(s)}+6CO_{(g)}$.

-Second, modification of the matter transport.

Some studies showed an interest for mixed additions, like carbon and silicon carbide. Indeed both achieve a specific role:

- Reduction of boron oxide by the carbon,
- Grain growth inhibition by the silicon carbide [BOU87].

This addition allows obtaining 92%d_{th} after 15min at 2175°C in argon atmosphere.

All the previous studies were carried out in an argon atmosphere but some studies were also performed in a helium/hydrogen atmosphere [LEE02]. The hydrogen was used in pre-sintering step (1350°C) for removing the boron oxide layer by the reaction:

$H_{2(g)} + B_2O_{3(l)} \rightarrow H_2O_{(g)}+B_2O_{2(g)}$. This method allows reaching a final density of 94.7% TD with a maximum temperature of 2230°C. The major drawback of this technique is the necessity to evacuate hydrogen before the sintering because H_2 prevents the densification and reacts with boron carbide to form methane.

1-2-2 Pressure Sintering

The only way to obtain high densities without sintering additive is to carry out the sintering process under a charge. Some examples are described below: Hot Pressing, Hot Isostatic Pressing and Spark Plasma Sintering.

1-2-2-1 Hot Pressing sintering (HP)

Pure dense boron carbide material can be obtained by sintering under a uniaxial mechanical pressure (30-40MPa) and at a temperature between 2100-2200°C in an argon atmosphere [THE90]. This way of production is complex and very expensive. Moreover, the obtained pieces have simple geometric form. The carbon mold has to be covered by boron nitride to prevent the reaction between carbon and boron carbide. The morphology and the size of the initial powder are important for the density and the microstructure of the sintered material. A higher density is obtained for monomodal initial powder. Higher sintering temperature carried out on irregular growth grain, twins formation. Pressure sintering can be summary by three successive reactions. First, particles reorganization, while the closed porosity is still low and constant. Second, a plastic deformation leads to a close of the open porosity. Third, decrease of the closed porosity due to the volume diffusion.

1-2-2-2 Hot Isostatic Pressing (HIP)

Sintering step is realized without pressure in order to obtain pieces in which the porosity is closed; then a post-densification is realized by hot isostatic pressing. This method allows obtaining almost dense materials (>99% of theoretical density (TD)) with a 2000°C-200MPa-2h thermal cycle with an addition of carbon (1-3 weight %). [TAR04t]

1-2-2-3 Spark Plasma Sintering (SPS)

SPS is a method allowing a very quick heating rate. The piece to be sintered is placed in a carbon die (electrical conductor). Then, a pressure is applied on the die to maintain a contact between the carbon and the piece. Heating is provided by Joule effect: a pulsed DC current is applied at the end of the die causing heating of both the die and the piece if the latter is electrically conductive. In the case of non-conductive material only the die is heated, heating is transmitted to the sample by both conduction and radiation. Applied currents are very high so the system heats quickly (≈100°C/min). Moreover, non-thermal effects seem to appear because higher densities are obtained at lower temperature than that obtained in conventional sintering. This effect isn't clearly identified yet, but some theories attempt to explain it. A local heating, on the current trajectory, which leads to very high temperature, or an electromagnetic effect that changes species diffusivity or even modifies the diffusion, and promotes the densification.

In the case of boron carbide, SPS can be used to obtain dense piece at lower temperature than in conventional furnace (1600-2200°C), and high pressure (75-80MPa) have to be used to reach highest densities. Many studies were carried out to define the optimal sintering parameters (table I)2). George, in his PhD [GEO16t], reach a final density >95% after 5min at 1750°C with a charge of 75MPa. He shows that the charge effect reaches a maximum between 50 and 75MPa (86% TD to 97% TD respectively) but higher charge doesn't change the finale density.

Table I)2: Sintering conditions and properties of "SPS boron carbide".

Materials	B_4C [VAS16, SAI14, HAY10a, LI14, BAD14, MOS13, MOS14, MOS15, NIU16, HAL15,GEO16t]			B_4C/Al_2O_3 [SUN14]	B_4C/Si [REH15]	B_4C/SiC [SAH12]
Atmosphere	Vacuum	N_2 [VAS16, BAD14]	Ar [VAS16, BAD14]		Vacuum	
Temperature (°C)	1100-2200	1800-1850		1700-1800	1700	1700-1750
Pressure (MPa)	32-75	30-100			60	40
Density (%)	65-100	95-98	98	72.8-98.8	99.4-99.8	88.3-98.8
Hardness (GPa)	0.2-37.6	24.8-42.5	22.5-38	79-90	34-36	31-35.3
Toughness ($MPa.m^{½}$)	2.6-4.6	3.2-4.5	2.2-6.1			
Young Modulus (GPa)	19-570					
Flexural strength 25°C (MPa)	316-828	300-575 [VAS16]	400-510 [VAS16]		600-620	
Flexural strength 1600°C (MPa)		460-650 [VAS16]	590 [VAS16]			

1-2-3 Conclusion

The densification of boron carbide is possible but the methods imply high temperature, high pressure or sintering additives. The high temperature and high pressure furnaces remain very expensive and the additives change the mechanical properties, and the needed impurities contents can become too high for using it. But the characteristics of boron carbide are too interesting to give up its studies. So many techniques were developed to get close to its characteristics but bypassing the direct sintering. Spark Plasma Sintering gives good

results but the form of the sample remains simple. Reaction bonding, which is used here, leads to composite but mechanical properties are sufficient for some application. This technique will be explained in the next part.

2 Reaction Bonding Boron Carbide (RBBC)

In the previous part, the properties and direct sintering of boron carbide were presented. Even if using pure boron carbide bodies is currently difficult, some methods allow using rich boron carbide pieces. In this thesis, we will concentrate on one of them: the reaction bonding.

2-1 General principle

The reaction bonding belongs to the reaction forming process family. In this method, the pieces' consolidation involves chemical reactions creating links between particles and filling the porosity, instead of neck-growth mechanism. Consequently, the piece shrinkage is almost null. It is not necessary to do post process machining, because the final form of the workpiece can be used for the reaction. The infiltration step occurs at temperature lower than the sintering temperature and it is a pressureless method, so the production cost is decreased. This method consists in the infiltration of molten metals or alloy which will react with the infiltrated ceramic porous body and/or atmosphere to form new phases. This reaction will create a chemical bond between the initial ceramic body and the infiltrating material after cooling. In the majority of cases, the infiltrated material is a ceramic material, because of the difficulties to obtain dense pieces and, the infiltrating material is a metal or alloy. This technique is already used for SiC and is named Reaction Bonded Silicon Carbide (RBSC). We describe here the RBBC: Reaction Bonded Boron Carbide, which is the subject of our work.

2-2 Reaction Bonded Boron Carbide formation

A porous preform of B_4C ceramic is infiltrated by molten metal or alloys (generally the silicon) (Cf. figure I)3). The ceramic and molten metal reacts with each other to obtain new phases (SiC and $B_{12}(B,C,Si)_3$) and leads to a consolidation of the piece. The major advantage of this method is the temperature of heat treatment that is the melting temperature of the metal or alloy used for infiltration. This is a pressure free method too, of these two points results a decreasing of the production cost.

According to the bibliography, silicon carbide is formed in RBBC from silicon and from several possible sources of carbon.

The “Reaction bonding” technique is a solid/liquid interaction method, so some parameters are important to control:

- initial porosity amount, that conditions the surface reaction (Cf. chap. I 2-3));
- porosity size, that plays a role on the matter repartition in the piece;
- preform composition and infiltrated material composition, that could change the reaction during the infiltration step (Cf. chap. I 2-3);
- atmosphere, that could change the wettability of the liquid on the substrate (Cf. chap. I 2-4);

The reactivity is explained in paragraph 2-5.

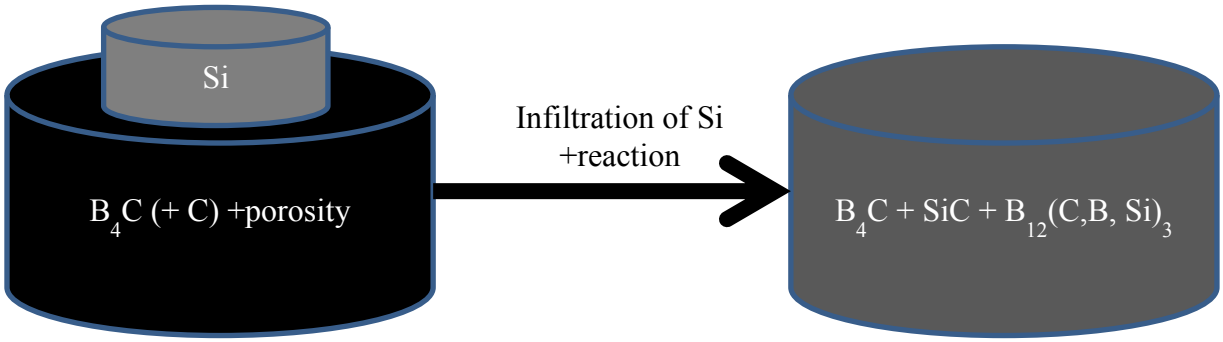

Figure I)3: Scheme of the reaction bonding

2-3 Preforms elaboration:

In the literature, it can be possible to distinguish two main families of preforms: the first one with only pure boron carbide [WAN14, TAR04, HAY09a, FRA03, CAF12, WU12, HAY10b, HAY10c, HAY10d, HAY09b, CAF14, ALM14, HAY09, KOU02, HAY08] and the other one with additions of carbon or silicon carbide [HAY06, THU13, WAN14, HAY10c, WU12, HAY10d, ZHA14a, BAR13, ZHA14b]. Except for three articles [THU13, TAR04, ALM14], the preforms are uniaxial pressed at a pressure between 10-200MPa. In the article [THU13], preforms were uniaxial pressed at 922MPa. Tariolle et al. [TAR04] used first a uniaxial compaction at 60MPa, followed by an isostatic compaction at 350MPa. The pressed samples are generally sintered in order to decrease the initial porosity: for pure boron carbide, the sintering steps were carried out at a temperature between 1900-2200°C; for the mixed powders, preforms were heated at 900°C for 5h [WAN14] or at 1550°C for 3h [WU12] (the initial porosity is not mentioned).

The addition of carbon can be realized in initial powder mixture [THU13, WAN14, WU12, ZHA14a, ZHAb] with carbon powder, or a mixture of carbon and paraffin, or resin. It could also take place after pressing or sintering by infiltration of 50/50 sugar solution [HAY10a, HAY06, HAY10b, HAY10c] then, the sugar is pyrolyzed in argon at 500°C.

The preform manufacturing is an important step which influences the behavior of the final composite. The specifications in terms of grains size, rate and size of porosity of the boron

carbide preforms is not clearly established in the literature, but we can say that the porosity of the preforms tested by the authors goes approximately from 15 to 40%. Different parameters of elaboration have to be studied:

- The initial powders: it is certain that the size of the initial powders will play a role on the microstructure of the preform. The fine powders lead to fine pores and in small quantity. Articles [DAR12, HAY08] treat of powder mixtures with various grain sizes (130,70,50,13,1µm): that facilitates the grain arrangement during pressing, and allows obtaining homogeneous samples, whose size and quantity of pores can be controlled. Despite the resulted composite is heterogeneous (large grains cohabiting with small ones), this way appears very interesting.
- Compaction: if the compaction pressure is too high, some cracks could appear in the preform after the sintering step. [DAR12]
- Debinding step: when binder or dispersant are used for compaction or mixing the powder they have to be removed in a debinding step to prevent the preform from cracks during sintering. [TAR04]
- The sintering step: direct cold compacted samples or sintered samples can be used for infiltration. [DAR12, TAR04, FRA08]
- The presence or the absence of free carbon has no influence on the final composition but the shape of SiC formed during the infiltration process depends on the carbon source. Best mechanical properties are obtained when no free carbon is added in the preform. In some cases, Si can be added in the preform. [HAY10b]

For all previous points, we decided to focus on preforms obtained with one type of powder (composition and size) compacted at 100MPa with sintering step at a temperature between 2000°C and 2200°C. Some additional samples were obtained with powder mixtures (SiC+B_4C and B_4C with different grain sizes).

2-4 Infiltration process

2-4-1 Wettability

2-4-1-1 Generality on wetting

Wettability [Larousse dictionary] is a property which characterizes the behavior of the surface of a material in the presence of a liquid. Wettability is defined by the contact angle (θ); this angle depends on the substrate, the liquid, the temperature, and the atmosphere (Cf. figure I)4). The Young-Dupré equation ties the contact angle and the three surfaces tension:

$$\gamma_{lv}cos\theta = \gamma_{sv} - \gamma_{sl} \qquad \text{Equ.1}$$

With: - γlv the liquid vapor surface tension on the free liquid surface,
- γsv the solid vapor surface tension on the free solid surface,
- γsl the solid liquid surface tension on surface between solid and liquid,

There are two types of system (substrate/liquid):

- Wetting system: partially wet for θ<90° and completely wet θ=0°. Liquid can spread on the substrate surface. Smaller θ is, more liquid will spread on the substrate.

- Non-Wetting system: 180°>θ>90°. Liquid tends to form a drop on the substrate surface. Higher θ is, more liquid will have a prefect drop form. Contact angle cannot be higher than 180°.

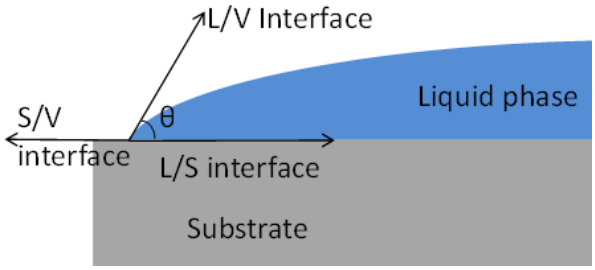

Figure I)4: Contact angle

A good wettability, smaller θ angle is mandatory in order to infiltrate the preform without any applied pressure. The wettability study can also give an idea of how the Si/B_4C interface evolved. Indeed, wettability in reaction bonded system is not simple because there are other types of wetting which play an important role.

2-4-1-2 Reactive wetting

In this case, substrate and liquid can react. Three possibilities are expected: substrate dissolves in the liquid, new phases appear at the interface between liquid and substrate or it could happen both.

2-4-1-2a Substrate dissolution

This type of wetting depends on the solubility of the substrate (S) in the liquid. If S solubility is limited, the interface can be considered flat but the surface tensions are modified.
If S solubility is not limited, the interface geometry changes, a hole appear below the liquid drop. In this case, the contact angle change followed the figure I)5

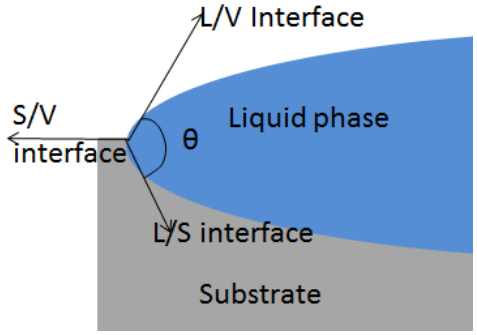

Figure I)5: Reactive wetting substrate dissolution angle

2-4-1-2b New phases precipitation

A new solid appears at the interface between the substrate and the liquid. The liquid is now in contact with the new phase. The contact angle of this new solid has to be considered. This can change the wettability; a non-wetting system can become a wetting one, for example.

2-4-1-3 Bibliography about wetting

In their Ph.D., Michael Aizenshtein and Rana Israel [AIZ05t,ISR09t] showed the importance of the porosity size for a good infiltration. When the contact angle is lower than a critical value (50° to 85° as a fonction of the porosity shape) the infiltration is spontaneous. That is the case of molten silicon. If the pore size is too small, infiltration may be difficult. It is then possible to close the porosity before a complete infiltration. In this case, non-infiltrated regions may be present in the samples, which make the piece fragile.

All the collected data show a good wettability of B_4C by molten silicon. This wettability allows the infiltration of silicon without external pressure. Moreover the wettability of reaction products (SiC, $B_{12}(B,C,Si)_3$) is good too so their formation don't be harmful for the infiltration. The influence of micro-waves on the wettability is not known, but we think a priori that it will not play a major role on the process. So no quantitative wettability studies were carried out in this thesis. The wettability of boron carbide by alloys (Cu-Si, Cu-B, 2519Al, Fe-B, Fe-C, Fe-B-C) was studied by many authors [FRO03, FRA04, AIZ08, WU14]. All studies showed a good wettability (<90°) when silicon or boron were added in these alloys. In many cases, a reactive wetting occurred with the formation of a layer between boron carbide substrate and wetting material.

Boron nitride substrates are no wetted by pure silicon, contact angle between 105° and 145°C. Boron nitride can be used as barrier to provide silicon spreading. We will use this product to protect the crucible.

2-4-2 Infiltration condition

In most cases [HAY06, WAN14, HAY10a, HAY09a, HAY10b, HAY09b, HAY10c, HAY09c, ZHA14a, ZHA14b, BAR13, HAY08], boron carbide preforms were infiltrated by silicon with a minimum purity of 98.4%. Others ones treat of the infiltration of silicon alloys with Cu, Al, Mg or of other metal (Al, Mg) or alloy (AZ91). The infiltration condition depends on the infiltrating materials: for Si the infiltration temperatures were between 1450 and 1600°C; lower temperatures were needed for alloys containing Cu (750-1100°C) and Mg (850-1000°C) due to eutectic compositions (53% atomic of Si for Mg alloys). Pure Cu didn't infiltrate boron carbide preform.

The atmospheric conditions are also influenced by the infiltrating material: for pure Si and Mg-Si alloy, the infiltration step was carried out under vacuum (1Pa≈10^{-5} mbar). Infiltration of Mg alloys was carried out under partial vacuum with a 6.6KPa of Mg vapor. Cu alloys were infiltrated under argon atmosphere. Table I)3 summarizes infiltration conditions mentioned in the bibliography.

Table I)3: Infiltration conditions in function of the molten material.

Melted materials	Atmosphere	Temperature range (°C)
Si [HAY06,WAN14,HAY10a,HAY09a,HAY10b, HAY09b,HAY10c,HAY09c,ZHA14,BAR13,HA Y08, ZHA14b]	Vacuum (1Pa≈10^{-5} mbar)	1450-1650
Cu-Si alloys [TAR04]	Argon	750-1100
Mg-Si alloys [CAF14]	Vacuum (1Pa≈10^{-5} mbar)	850-1000
Al-Si alloys [FRA03,WU12,ALM14]	Vacuum (10^{-2} Pa)	1200-1400
Mg alloys (AZ91) [CAF12,CAF14]	Partial vacuum (6.6Kpa)	850
Al and Al alloys [KOU02]	Vacuum (1-2Pa)	750-1100

2-5 Reactivity

The reactivity between silicon and boron carbide was studied by some authors [TEL90, HAY09c]. They found that the reaction can be summarized:

- As soon as the temperature reached 1000°C, B_4C can release C and incorporate Si in its structure, forming a solid solution named $B_{12}(B,C,Si)_3$
- At a temperature above 1100°C, the carbon in the B_4C powder can also react with the silicon to form β-SiC. This carbon can be in the initial B_4C powder (impurity or addition). It is also possible to make carbon additions in the preform, as described below.

Since 1380°C a ternary liquid is formed that promotes the formation of the $B_{12}(B,C,Si)_3$ phase. Between 1380°C and 1410°C, the SiC concentration is multiplied by five. At 1500°C the formation of $B_{12}(B,C,Si)_3$ is total after an annealing of 1h. To summary:

$T \geq 1000°C : B_4C + Si \rightarrow B_{12}(B,C,Si)_3 + C$

$T \geq 1100°C : C + Si \rightarrow \beta\text{-}SiC$

$T \geq 1380°C\ B,C,Si\ (L) \rightarrow \nearrow B_{12}(B,C,Si)_3$

$1380°C \leq T \leq 1410°C : \uparrow SiC$

According to Werheit et al. [WER94] and Tell [TEL90], the maximal solubility of silicon in boron carbide phase at 2323K (2050°C) is about 2.5at%. Hayun [HAY09t] used Thermo-Calc software, a model developed by Kasper [KAS96t] and extrapolation of the thermodynamic parameter to 1753K (1480°C). The result is presented in figure I)6.

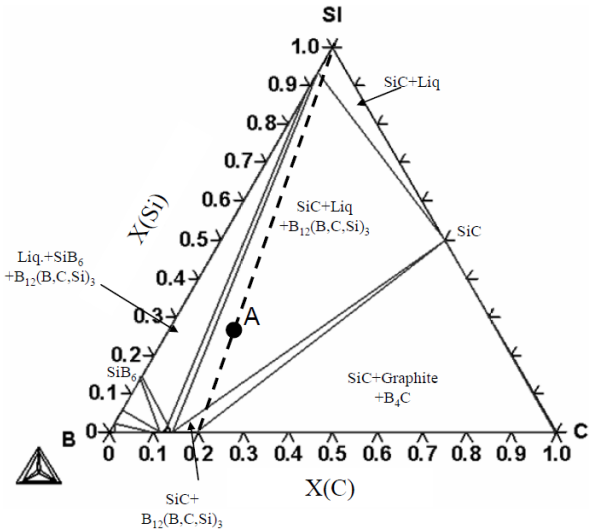

Figure I)6: Isothermal section of the B-C-Si phase diagram at1753K (calculated by Hayun[HAY09t]).

Here is cited the discussion in Hayun thesis:

"*The point A in figure 7 symbolizes the system before any interaction but after the fully infiltration. The calculation was made for 40% of porosity sample so the atomic composition is 63 at% B, 16 at% C and 21 at% Si. The dashed lines connect the Si corner (initial phases) and boron carbide (B_4C) region (initial phases). According to the model the equilibrium point of the system at 1753K is composed by SiC, $B_{12}(B,C,Si)_3$ and liquid. If the equilibrium was reached during the reaction so no more boron carbide remains after the reaction.* According to the bibliography there are almost always remaining boron carbide, Hayun explains *this by the precipitation of the newly formed B12 phase at the surface of boron carbide grain, called rim region. This layer acts like a diffusion barrier and prevent the total dissolution of the initial boron carbide particles. According to the bibliography the formation of the rim region is due to a dissolution-precipitation process [TEL90, TEL87, GUG72]. This type of core-rim structure is very often observed in composite when liquid and solid phase react to form the final composite structure. The presence of rim-core structure is observed in metal/ceramic system when ceramic is partially soluble in the liquid metal [CHE01, AND01, MOS66] and in some metal/tungsten based composite after liquid phase sintering. The formation of the core-rim structure in a solid/liquid system is attributed to the partly dissolution of original particles (B_4C) in the liquid (molten Si) and precipitation of a new solid phase ($B_{12}(B,C,Si)_3$) at the surface of the initial particles.*

The formation of a layered rim region was discussed by Chen et al.[CHEN01]. The authors suggested that the inner layer is formed as a result of the precipitation of a new phase under quasi-isothermal conditions, as long as the original ceramic phase is in contact with the liquid. The outer layer is formed during cooling when solubility of components changes. The layer resulted from congruent or stoichiometric dissolution in the liquid and its precipitation as a new phase (with new composition) determined by this new equilibrium.

If the original particles didn't dissolve in the liquid a solid state diffusion is possible the rim region growth until since the diffusion through it is too slow to continue significant growing. Boron carbide is a strong covalently bond material so its components diffuse slowly, one of the reasons it is extremely difficult to sinter, so it dissolves without any compositional changes (congruently). It dissolution in the melt conduct to the concentration of boron and carbon of: 1mole of B_4C give 4 mole of dissolved boron and 1 mole of dissolved carbon".

Hayun calculated the concentration equilibrium for the system presented before and it obtained a concentration of 8 at% of boron. He found that the maximum possible content of boron in the liquid at this temperature is 6.6 at% for higher amount the precipitation of B_{12} phase occurs. This phase precipitates at the initial boron carbide interfaces; this causes the apparition of the core (B_4C)-rim (B_{12}) structure. He also calculated the possible composition of the B_{12} phase: $B_{12}C_{1.99}Si_{0.037}$.

According to bibliography it still remains unreacted silicon in the final composite.

2-6 Microstructure-properties relationships

The Table I)4 shows the properties of composites produced by different authors with different infiltration conditions (regrouped by melted material). This shows that best mechanical properties are obtained by infiltration of "pure" silicon in boron carbide preforms. The mechanical behavior of the final composite depends on the initial preform features in terms of porosity, composition and grain size, the melted material (Cf. table I)4), the thermal cycle (dwell time, maximum temperature).

Composites infiltrated with aluminum:

In the case of composites infiltrated with Al or Al alloy, it is possible to change the mechanical properties of the composite by post infiltration heat treatment (quenching…). Therefore, after the infiltration, it is possible to shape the piece then to make an annealing to obtain better mechanical properties.

For Al-Si samples with 40% of initial porosity the hardness increased from 4,6GPa to 12.2GPa before and after a post thermal treatment respectively. In the same time, the hardness of the samples with 18% of initial porosity is stable before and after thermal treatment ≈25GPa.

Before post thermal treatment the boron carbide size plays an important role; indeed the flexural strength increases from 370±25 to 543±22 MPa when boron carbide size grows up from less than 10µm to 22-59µm. After post heat treatment, this effect is lower (622±90 MPa to 678±69 MPa).

However, the mechanical properties are lower than those obtained by silicon infiltration. Consequently, they could not be used for ballistic application.

Table I)4: Summary of the mechanical properties for boron carbide and boron carbide/carbon preform

Melted material	Initial porosity %	Young's modulus (GPa)	Flexural Strength (MPa)	Vickers Hardness (GPa)	Toughness ($MPa.m^{1/2}$)
Si [HAY06,WAN14,HAY10a,HAY09a,HAY10b,HAY09b,HAY10c,HAY09c,ZHA14a,BAR13,HAY08, ZHA14b]	20-44	300-430	210-410	16-25	3.3-4
Cu-Si [TAR04]	13-30			21±4	
Mg [CAF12]		269±4	341±16	8.7±1	
Mg90.8%-Al8.25%-Zn0.63%-Mn0.22%-Si0.035% (AZ91) [CAF12,CAF14]		295±3	327±19	11.7±2	
Al (before heat treatment) [TUN11]	43-48		370-543		
Al (after heat treatment) [TUN11]			662-678		
Al (with 2min of dwell time) [KOU02]		166-183	111-201 (tensile test)		
Al (with 15min of dwell time) [KOU02]		165-194	136-229 (tensile test)		
Al-Si (before heat treatment) [WU12,ALM14,FRA03]	16-50	216-299	201-328	4.6-25	4-5.1
Al-Si (after heat treatment) [FRA03]				12.2-25.5	
Si-Mg [CAF14]	20	356	230±22	17±3	

RBBC obtained by silicon infiltration:

The hardness of the composite infiltrated with silicon changes with the residual silicon content, it increases from 16 to 25 GPa when the residual silicon decreases from 30 to 8 vol%. The same effect was observed for Young modulus which increases from 330 to 430 MPa.

The residual silicon weakens the composite and it has to be pointed out that all authors found residual silicon after infiltration whatever the conditions.

Flexural strength seems to be independent of the residual amount of silicon but it strongly depends on the elaboration conditions of the preform: sintered (400±10MPa), monomodal powder (275MPa), multimodal powder (325MPa) or carbon added (250±25MPa).

Two teams published on the effect of particles size on the properties. One team [BAR13] worked on monomodal powder. They found linear relationship between particle size and

hardness: when particle size increases from 18.65 to 63.35µm, the hardness increases from 1261 to 1674kgf/mm^2. This is due to the number of interface boundary. Indeed, these interfaces are weaker than boron carbide particles. There are more interfaces in the imprint when initial boron carbide grain size is smaller. The effect is inverted for fracture toughness and flexural strength when particles size increases these properties respectively decrease from 5.76 to 3.4 MPa.m^{½} and from 403 to 256 MPa.

The other team [HAY09a] worked on the multimodal powder to obtain a preform with a low porosity without pre-sintering step. They obtained 25% of initial porosity using multimodal (different proportion of each size) boron carbide powder instead of 40% of initial porosity for monomodal powder. The composites were composed of four phases, residual boron carbide, residual silicon, newly formed silicon carbide and newly formed B_{12} phase. The mechanical properties were the same than that of monomodal powder samples initially pre-sintered up to 25% porosity.

Hayun et al. [HAY10b], studied the influence of the carbon source. There are two major carbon sources: carbon additions and boron carbide itself. The toughness is from 2.5 MPa.m^{½} to 3.6 MPa.m^{½} and flexural strength from 250MPa to 400MPa when only boron carbide is used in the preform. The carbon addition has no notable effect on the hardness and Young modulus, but it lowers the toughness and flexural strength. It is noteworthy that the carbon source has no effect on the composite composition but it changes the microstructure (Cf. figure I)7).

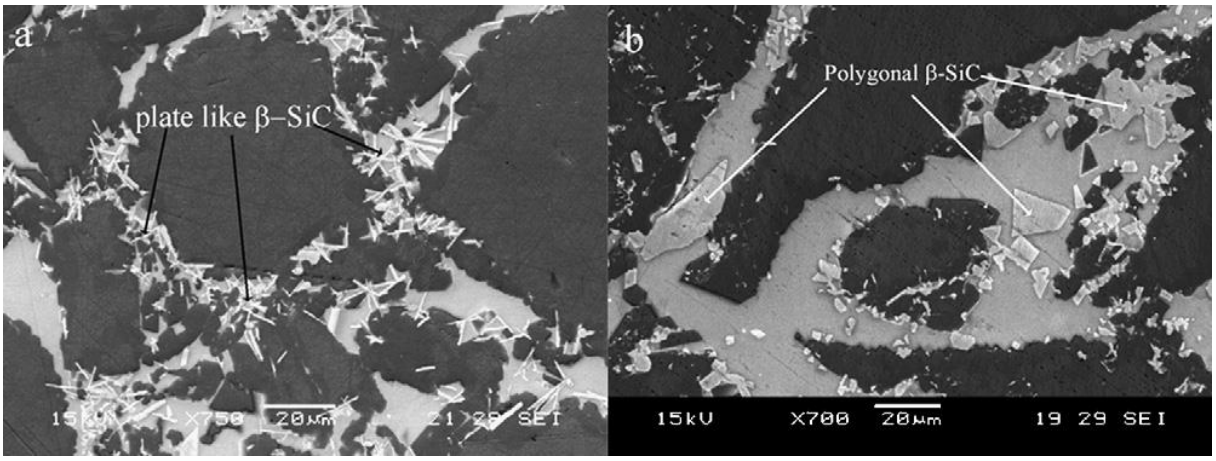

Figure I)7: SEM (secondary electron) micrograph of composites after infiltration a) without free carbon and b) free carbon addition [HAY10b]

As it can be seen on figure I)7 the final morphology of SiC is strongly influenced by the carbon source, boron carbide for Figure I)7a and carbon added for figure I)7b. The plate-like silicon carbide obtained in the case of no carbon addition is favorable to the material strengthening.

In conclusion, the silicon carbide obtained from carbon addition was less interesting for mechanical applications.

Some authors [WAN14] added SiC instead of carbon inside the preform. For example, the addition of SiC added in the initial powder lead to:
- An increase in toughness from 4.5 to 4.9 MPa.m^{½},
- A decrease in hardness from 3150 to 2800 Hv,
- A decrease in flexural strength from 320 to 240 MPa,

The effect of the temperature was also studied [ZHA14a] in the case of B_4C-Si system. Authors measured the evolution of the hardness, flexural strength and toughness for the same initial state samples. For hardness (15 to 18.5 GPa) and flexural strength (310 to 340MPa), in first time the increase of maximum temperature was profitable, in the range 1450 to 1600°C. But when temperature reached 1650°C, both measured parameters fell down, respectively 13GPa and 290 MPa. Toughness increased when temperature increased (3.3 to 4MPa.m^{½}).

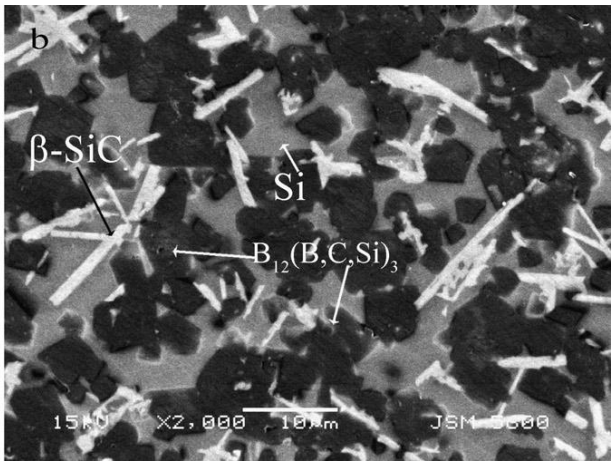

Figure I)8: SEM (secondary electron) micrograph of composite after infiltration [HAY10c]

Figure I)8 shows a typical microstructure of a sample after infiltration without carbon addition, it was composed of boron carbide (5µm) compacted. Newly formed silicon carbide (white needles) can be easily observed, the black particles were boron rich phase identified by Frage et al. as solid solution of $B_{12}(B,C,Si)_3$, and the grey area was identified as residual silicon.

Hayun [HAY10b] measured the nanohardness of the B_4C (42±3.3) and the $B_{12}(B,C,Si)_3$ (46.1±4.2) and the Young modulus of B_4C (460±23) and the $B_{12}(B,C,Si)_3$ (474±34).

The transformation of B_4C to $B_{12}(B,C,Si)_3$ seems interesting for the mechanical properties.

In his thesis [HAY09t] Hayun studied the mechanism involved in the $B_{12}(B,C,Si)_3$ formation. As mentioned before, B_{12} appears in a core-rim structure with the initial boron carbide particles. This structure is due to a dissolution/precipitation mechanism.

He also observed a highly dependence between the carbon source (free carbon or boron carbide) and the SiC morphology. TEM analysis showed that "*β-SiC always precipitate from silicon melt as single plate-like particles with the {111}$_β$ habit plane.*" He also observed an increasing of the "boron carbide" phases (residual B_4C and newly formed $B_{12}(B,C,Si)_3$) volume amount in the composite. He attributes this increase to the dissolution of the top

boron carbide layer, in direct contact with silicon; the dissolved boron carbide goes inside the preform by the silicon flow. Indeed, he observed that upper boron carbide limit is displaced to the composite core from about 150µm (Cf. figure I)9).

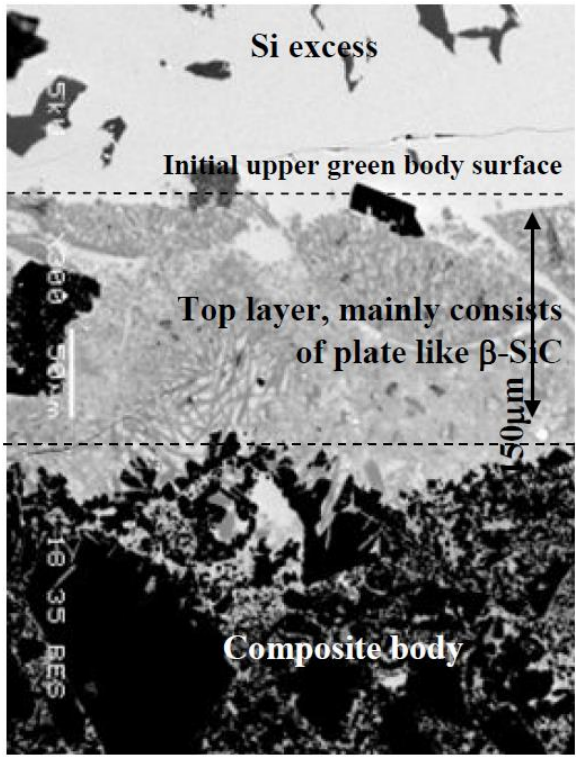

Figure I)9: [HAY09t] Top layer of the infiltrated composite

He also observed a strong interaction between the core (residual boron carbide) and rim (the newly formed $B_{12}(B,C,Si)_3$). Indeed, cracks go through the interphase without being deflect. He compared a no-pre-sintered preform and a pre-sintered one and surprisingly there were almost no mechanical properties differences. This lack of differences is attributed to the microstructure and composition similarities. In the case of pre-sintered materials, the necks formed during the sintering step are preferentially attacked by molten silicon and transformed in B_{12} that acts as a link between the residual boron carbide particles. Such a link appears also for no-pre-sintered preform with the dissolution-precipitation mechanism. Indeed, B_{12} precipitates at the boron carbide surface and could link particles. In both cases, a continuous boron carbide/B_{12} skeleton is obtained.

In all cases, a strong link between the amount of residual silicon and the mechanical properties was observed: less residual silicon causes an increase of the mechanical properties.

2-7 Conclusion

We focus our work on the use of silicon to elaborate RBBC composites.

The process:

- The way of preparation of the infiltrate metal or alloy modifies the behavior during infiltration step and final composition of the composite. The silicon can be in the form of powder, lump or pellet. It can be very pure (99.999%), or less (down to 98.4%).
- The atmosphere: vacuum is usually used, from 5.10^{-4} to 10^{-5} mbar.
- Thermal cycle: the usual temperature range is 1450-1500°C, with a dwell of 10-30 min, but higher temperatures (e.g.: 1650°C) or dwell time (up to 4h) are found in the literature.

The microstructures:

- The reaction bonding is possible, and SiC is obtained. Often, an intermediate phase $B_{12}(B,C,Si)_3$) is formed between B_4C and SiC. Residual silicon is often present, that can be removed by chemical treatments. B_4C can be totally transformed into $B_{12}(B,C,Si)_3$ phase if grains are fine in the preform.
- The form of the silicon carbide depends on the presence of carbon in the preform: if this latter is present, polygonal SiC platelets are formed. If no free carbon is present in the preform, SiC grains are platelets.

The mechanical properties:

- The infiltration temperature and the time passed at high temperature influence the final composition and the mechanical properties. For pure Si infiltration, the best temperature would be 1600°C.
- The intermediate phase $B_{12}(B,C,Si)_3$ does not affect the mechanical properties. High values for mechanical properties can be obtained: e.g. Hardness 2300±250 HV, Young modulus 400±10GPa, Flexural strength 318±20 MPa.
- The fact that the preform is sintered does not affect the final mechanical properties.

3 Microwaves Heating

3-1 Microwave heating principle

Microwave is a field of electromagnetic waves (EW) from 300MHz to 300GHz which correspond to wavelength between 1 m and 1 mm. The conventional frequencies used are: **915MHz**, **2.45GHz**, 5.8GHz and 24.125GHz. An EW plane wave is defined by two perpendicular vectors:

- Electric field vector E,
- Magnetic field vector H,

In an infinite environment without dielectric loss, the two vectors are in phase.

The wavelength (λ) is related to frequency (f) and light vacuum speed (C), and is defined by the following equation:

$$\lambda = \frac{C}{f} \qquad \text{Equ.2}$$

The EW radiance for the microwave can be produced by several sources:

- Magnetrons are the most common wave's sources. They work at a frequency between 1 and 30 GHz.
- Klystrons are used for high powered radiance source (can reach several hundred kW) in the frequency field between 0,3 and 100 GHz.

Gyrotrons allow obtaining radiance in the frequency field between 30 and 300 GHz and a maximum power of 1MW.

Microwave cavity is the limited metallic space where the sample is put; it can be single-mode or multimode.

-Multimode one is a cavity with higher size than that of the waveguide (which "transports" waves from microwave generator to cavity). In the cavity waves undergo multiple reflections. Those reflections lead to a constant distribution of the electromagnetic field, but this latter is heterogeneous. To homogenize the heating, a mixing paddle or a turntable can be used.

The mixing paddle is a metallic turning propeller which disturbs the electromagnetic field. This perturbation leads to an average distribution of the electromagnetic field. The turntable is used in home microwave, the electromagnetic field distribution is constant and heterogeneous but the sample moves inside this field where it receives an average energy.

-Single-mode cavity have particular sizes, it is adjusted by short-circuit. This allows creating a resonance phenomenon. Consequently, the sample can be put in a belly or in a node of the magnetic or electric field, which allows a finer controlled of the process. The size of samples is limited with this type of cavity.

The behavior of material with respect to EW (reflection, absorption or passage through) depends on dielectric properties of the material.

The conductor materials are generally blackout (full reflection).

The dielectric materials present different behaviors related to their complex permeability ε^*.

$$\varepsilon* = \varepsilon' - i\varepsilon'' \qquad \text{Equ.3}$$

In equation 3, the real part ε' is known as dielectric constant. The imaginary part ε'' is known as loss factor, and determines how the materials absorb the electromagnetic field. Materials with high ε'' highly absorb electric energy and so they heat quickly. On the opposite low ε'' materials are characterized by a low absorption, so there are transparent or partially transparent. Dielectric properties can change with the temperature, that's why even fully transparent material when they are heated above a critical temperature start to absorb micro-wave.

Another frequently found parameter is tanδ: loss tangent, defined by:

$$tan\delta = \frac{\varepsilon''}{\varepsilon'} \qquad \text{Equ.4}$$

The loss tangent characterizes the material and is used as indicator to describe how it dissipates microwave energy during the heating stage.

For all materials, the dielectric properties change with frequency.
For ceramics, microwave heating is due to the polarization; the electron mobility causes the energy dissipation and leads to the heating of the material. It exists different types of polarization:

-Electronic polarization: due to the displacement of the electronic cloud under electric field. This displacement creates a misalignment of the positive charge (core) and negative charge.

-Ionic polarization: due to the displacement of atoms or groups with opposite charge in equilibria position under an applied electric field. The asymmetric charge distribution between non identic atoms is a permanent dipolar moment source. If an external electric field is applied, they orient themselves in the direction of this field (orientation polarization).

-Space charge polarization: due to the blocking of the charge displacement by a physical barrier (grain boundary)

The microwave penetration depth named dp in materials is the depth where the transmitted power fall at 0.368 (1/e with e the Euler number) of its surface value. It is calculated with the following equation.

$$d_p = \sqrt{\frac{1}{f\pi\mu\sigma}} \qquad \text{Equ.5}$$

With: μ: permeability (N/A^2)
f: the frequency of the considered wave in Hz
σ: electrical conductivity (S/m)

According to the equation (5) the microwave penetration depth for a given material is a function of the wave frequency. The ratio of the penetration depth for 915MHz and 2.45GHz is the ratio of their frequency, i.e. dp_{915}= 1.64x$dp_{2.45}$. As it can be seen, a lower frequency is better for penetration depth, so for the heating homogeneity.

3-2 Three heating methods

Heating with microwave can be purchased by three ways: direct way, indirect way and hybrid.

3-2-1 Direct way

This way of heating is the one use in domestic microwaves furnaces to heat water. Samples are heated directly by the microwaves. This way of heating is characterized by a volume heating, the core of the sample is hotter than its surface. It is used when samples absorb microwaves since the room temperature. Figure I)10 shows a simplified (the influence of depth penetration is not taken into account) scheme of direct heating.

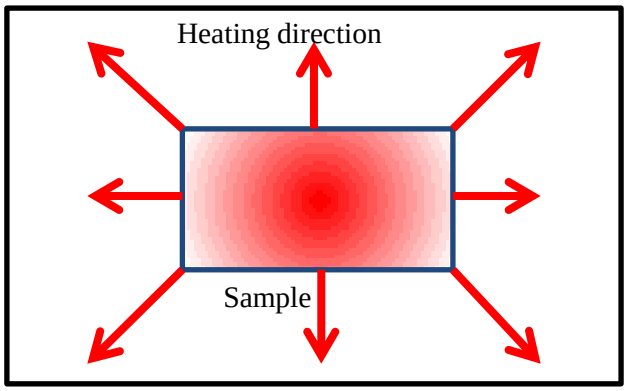

Figure I)10: Volume heating scheme

3-2-2 Indirect way

When a material does not couple with microwave, a susceptor part may be used to indirectly heat the sample. If a sufficient mass of susceptor surrounds sample, the microwave field could not attain the sample; on this way, one can heat metallic material. This way of heating is characterized by a surface heating, the surface of the sample is hotter than its core. This type of heating looks like at this one we can find in conventional furnace. Figure I)11 shows a simplified (homogenous heating) scheme of indirect heating.

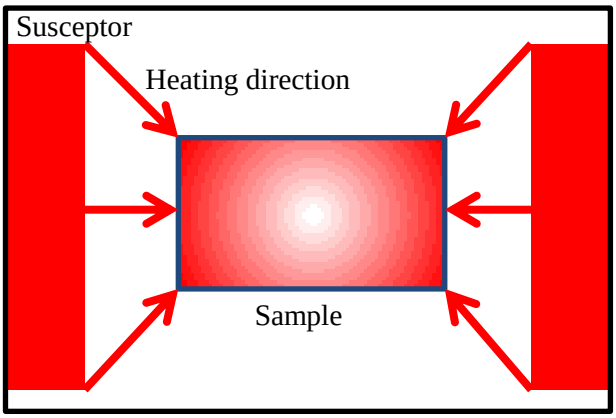

Figure I)11: Surface heating scheme

3-2-3 Hybrid

When a material couples at high temperature but not at room temperature or if its weight is not enough to heat up, we can use a susceptor to help. Microwave has to reach sample. However, the susceptor must not be too heavy or surrounds the sample. This way of heating is characterized by a mix between a surface heating and a volume heating. Figure I)12 shows a simplified (same temperature for samples and susceptor) scheme of hybrid heating.

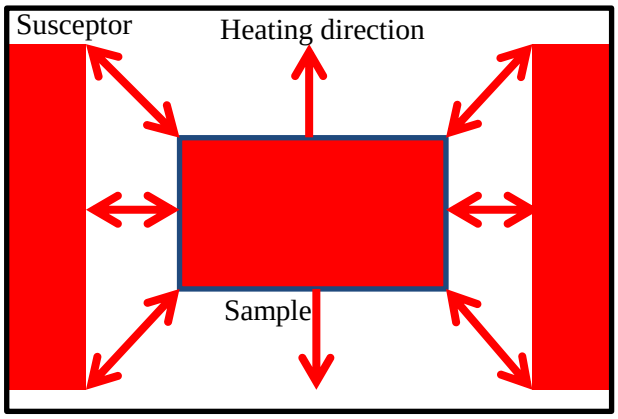

Figure I)12: Surface + Volume heating scheme = hybrid

3-3 Microwave cavity

There are different sizes of cavity from domestic microwave to bigger industrial ones (Cf. figure I)13). Currently industrial microwaves are principally used in food field or other low temperature applications.

Figure I)13: Industrial microwave furnaces

Single-mode cavity

A single-mode cavity has a particular design: a parallelepipedic tube whose cross-section is that of the waveguide. Its sizes are directly correlated to the frequency used for heating.

To calculate the minimum size of a waveguide, we can use the following equation [INT1]:

$$\lambda_c = \frac{C}{f} = 2.a_c \qquad \text{Equ.6}$$

With λc the wave length cut lower limit by the waveguide,
C the light speed,
f the frequency of the cut wave,
a_c the highest width of the waveguide section,

To allow the wave transportation with a waveguide, it has to be at least 30% higher than the a_c value calculated from the equation 5.
The smallest section width has to be the exact half of the a value.

In this type of cavity, it is possible to select which field will heat the sample. It is possible to adjust the cavity in order to place the sample in magnetic mode or electric mode. Single-mode cavity is therefore useful to know what type of field, electric or magnetic, makes it possible to heat the sample. For a single-mode furnace, the heating is very efficient if the sample is placed in a maximum field (magnetic or electric) area. At the contrary, if sample is not located at the maximum field area, heating will almost do not take place.

Multimode furnace
For multimode furnaces (like domestic microwave furnaces), the waveguide dimensions are the same than for single-mode cavity for the same frequency. Just the cavity size changes, with fewer constraints for multimode than for single-mode, the cavity size can take different values; the only thing is to check that the cavity center is in a maximum of the field. This freedom on the size allows making bigger cavity for multimode furnace. But in this type of cavity, it is impossible to select which field is used for heating. Heating is also more difficult in multimode than in single-mode, because for the same power supplied by the generator, the field will be lower on the sample. Thus, in order to study finely the microwave-matter interaction, it is preferable to use a single-mode furnace.
As previously, lower frequencies are better for penetration depth and the cavity size is directly related to wave frequency (Eq.6). According to the equation 6, a single-mode cavity 2.45GHz has a section of at least 79.43*39.715mm² is needed and 915MHz single-mode cavity has a section of at least 163.5*81.75mm² (Cf. figure I)14). The same result is found again for multimode cavity. According to these two points, a lower frequency is better to sinter large pieces.
However, the dielectric properties of the material depend on the frequency. A material could couple very well at 2.45GHz but not well at 915MHz.

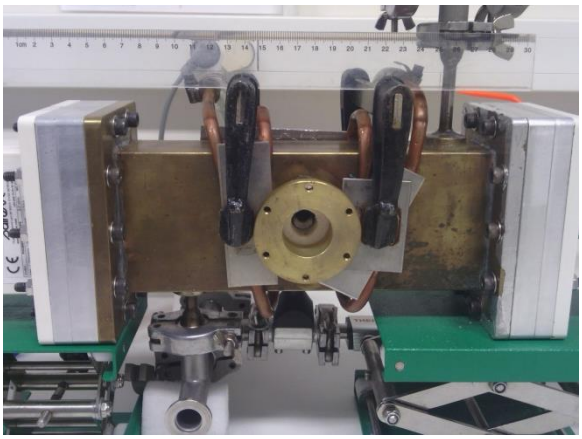

a)2.45GHz single-mode cavity (EMSE, Saint-Etienne, France)

b)915MHz single-mode cavity (CRISMAT, Caen, France)

Figure I)14: Examples of single-waves cavity

4 Microwave sintering and reaction bonding:

4-1 Microwave sintering of boron carbide

Microwave sintering of boron carbide were studied by few teams around the world. But the used frequency was above 2.45GHz. Neshpor et al. [NES 93], sintered boron carbide and silicon carbide at temperature near 1800°C during 10-15min. Samples were placed in quartz vessel filled of AlN powder because of its properties of thermal insulation and its radiation-transparency. They observed some material transferred between samples and AlN powder. Indeed, they found some Si_3N_4 and AlN inside samples. Boron carbide samples were covered by an α-BN coating after sintering. Mitsudo et al. [MIT 04] were interested, in the high frequency (24GHz), to the sintering of boron carbide. Samples were placed inside a BN crucible with a thermocouple for temperature measurements. The box is placed inside BN powder full thermal insulator made in fiber-board alumina. The sintering was performed in argon flow atmosphere. The maximum temperature is 2200°C. The best density (83% TD) was obtained at 2200°C. Mitsudo et al. [MIT 05] used the same device as previous for determine the influence of the maximum power. They realized two different thermal cycles with two maximum powers (1.5kW and 2.5kW), with the same frequency (24GHz) in such cases, the heating rate is not the same. They observed that, for the same maximal temperature, a high incident power gave better density than lower incident power, 65% TD at 1900°C for 1.5kW and 75%TD at 1900°C for 2.5kW. Even if the authors showed that the temperature involved and the frequency used for these studies make preform fabrication by microwave uninteresting and almost impossible at the actual time. We can conclude that the infiltration temperature will not cause the preform sintering. It could be considered that all observed modifications will be due to the infiltration and not of the microwave effect on the preform.

4-2 Microwave reaction bonding

4-2-1 Silicon carbide reaction bonded

Karandikar et al [KAR07], infiltrated molten Si, Al or Mg inside SiC preform. The mechanical properties obtained after the microwave treatment are the same as those obtained by a conventional way. However, the reaction bonding process made by microwaves permits to limit the process duration.

Bianchi et al. [BIA15] studied the infiltration of silicon inside SiC or carbon preform through carbon felt. They used four 2.45GHz microwaves generators. Samples were placed inside an alumina cylindrical crucible full of a mix of SiC/BN powders acting as susceptor. Preforms were placed above silicon powder and carbon felt are placed between them. Silicon reached preform, after melting, by capillarity through the carbon felt porosity. The infiltration steps were realized in an argon atmosphere with a slight over pressure. The heating rate was 6°C/s and the maximum temperature 1450°C. They successfully infiltrated SiC or C preforms by molten silicon.

4-2-2 Boron carbide reaction bonded

The micro-wave heating for infiltration step will be presented in this paragraph. For now, studied frequencies are between 2.45GHz and 24GHz microwaves.

Goldstein et al. [GOL 09] studied the reaction sintering of an Al/B_4C/SiC green body in air atmosphere. Samples were placed inside thermal insulator made of pure alumina and buried in a mixture of bubble alumina and coarse yttria. They used a maximum incident power of 2.5kW (2.45GHz); the thermal cycle didn't exceed 60min with maximum 30min at 1800-1850°C. The maximum content of B_4C didn't exceed 35% in the composite, and the final composite contains B, C, Si, Al, N and O.

Thuault et al. [THU 12], studied the infiltration of molten Si in a B_4C(85w%)/C(15w%) preform in Ar/H_2(5%) atmosphere. Samples were placed inside a cylindrical SiC suceptor embedded in BN powder inside a BN crucible. They used a maximum power of 650W (2.45GHz single-mode cavity). The power is increased by 50W steps every 10 min, the maximum reached temperature is 1500°C and a dwell of 10 min is applied. Sample shrinkage is negligible compared to the conventional sintering methods. The obtained composite was composed, followed XRD analysis, of silicon carbide, residual silicon and boron carbide phase. They found a similar value through the depth of the sample for Young modulus (309GPa) and hardness (22GPa, measured by Vickers indentation).

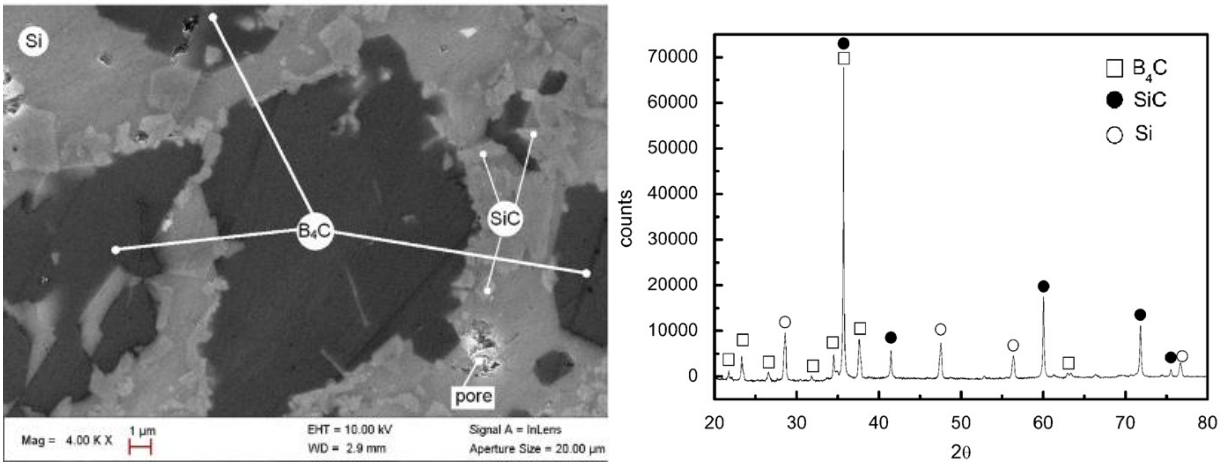

Figure I)15: Typical SEM microstructure of RBBC heated with microwaves, and XRD analysis [THU 12]

Table I)5: Mechanical properties of RBBC obtained by conventional or microwave heating

Material	Authors	Bulk density (g/cm3)	HV_{1000} (GPa)	K_{1C} ($MPa.m^{1/2}$)	Young's modulus (GPa)
Microwave heated composite	Thuault et al.	2.6	22		305-313
Conventionally heated composite	Hayun et al. [HAY 08]	2.58±0.06	22.5±1.4 (20N)	5.5±2.2	410±9

5 Conclusions:

This chapter allowed us to give information about boron carbide. Its mechanical properties are very interesting, but its covalent character makes it very difficult to densify. This is why the composites made by infiltration of molten metal and reaction is a good compromise between the temperatures of elaboration and the mechanical performance. Among the studied systems, a focus is made on the boron carbide -silicon carbide composite, known as RBBC, obtained from the infiltration of B_4C preforms by molten silicon. A team of researchers in the Material Department of Ben Gurion University has a great experience of this system by conventional heating, and has interpreted the microstructures obtained, according to the initial products: preforms of boron carbide sintered or not, sometimes from powder of different sizes, addition of carbon ...

The source of carbon in the system comes from the transformation of B_4C into a solid solution of type $B_{12}(B, C, Si)_3$. In this case, the morphology of the silicon carbide is a platelet form. If carbon additions are made, the formed SiC is polygonal. The first route is the most favorable

to the toughness of the material. The authors also noted that the solid solution of boron carbide forms at the periphery of the boron carbide grains, thus giving a core-rim structure to these grains. It should be noted that the hardness of the two boron carbide phases are equivalent. The degree of conversion of the carbide thus has no influence on the hardness of the composite.
In fact, it is the composition of silicon carbide and residual silicon which mostly condition the mechanical properties. At the end of the RBBC process, the silicon is never completely transformed. Summary table can be found in appendix I, II and III.

The application of a microwave field can modify the dissolution-precipitation mechanisms, the diffusion mechanisms implemented during the process and, thus leading to the modification of the microstructures and the mechanical properties of the final composites. This justifies this work, the results of which are presented in the chapter III.

Bibliography

[AIZ05t] : AIZENSHTEIN M., Thesis, "Interface Interaction and wetting phenomena in boron carbide-liquid metal systems", Ben Gurion University of Neguev, December 2005

[AIZ08] : AIZENSHTEIN M., MIZRAHI I., FROUMIN N., HAYUN S., DARIEL M.P., FRAGE N., " Interface interaction in the B4C/(Fe-B-C) system", Mat. Sci. Eng. A, 495, p. 70-74, 2008

[ALM14] : ALMEIDA B.A., FERRO M.C., RAVANAN A., GRAVE P.M.F., WU H-Y., GAO M-X., PAN Y., OLIVEIRA F.J., LOPES A.B., VIEIRA J.M., "Study of multi-carbide B4C-SiC/(Al,Si) reaction infiltrated composites by SEM with EBSD",IOP Conf. Series: Mat. Sci. Eng., 55, 012001, 2014

[AND01] : ANDREN H.O., "Microstructures of cemented carbides", Mater. Des., 22, 491, 2001

[BAD14] : BADICA P., BORODIANSKA H., XIE S., ZHAO T., DEMIRSKYI D., LI P., TOK A.I.Y., SAKKA Y., VASYLKIV O., "Toughness control of boron carbide obtained by spark plasma sintering in nitrogen atmosphere", Cer. Int., 40, p. 3053-3061, 2014

[BAR13] : BARICK P., JANA D.C., THIYAGARAJAN N., "Effect of particle size on the mechanical properties of reaction bonded boron carbide ceramics", Cer. Int., 39, p. 763-770, 2013

[BIA15] : BIANCHI G., VAVASSORI P., VILA B., ANNINO G., NAGLIATI M., MALLAH M., GIANELLA S., VALLE M., ORLANDI M., ORTONA A., "Reactive silicon infitrationof carbon bonded preforms embedded in powder field modifiers heated by microwaves", Cer. Int., 41, [9], p. 12439-12446, part B, 2015

[BOU85] : BOUGOIN M., Thesis, "Frittage sans charge du carbure de bore et de composite carbure de bore/carbure de silicium.Propriétés mécaniques",E.N.S des Mines de Saint-Etienne,order n°46CI,1985

[BOU87] : BOUGOIN M., THEVENOT F., "Pressurless sintering of boron carbide with an addition of polycarbosilane", J. Mat. Sci., 22, p.109-114, 1987

[CAF12] : CAFRI M., DILMAN H., DARIEL M.P., FRAGE N., "Boron carbide/magnesium composites: Processing, microstructure and properties", J. Eur. Cer. Soc., 32, p. 3477-3483, 2012

[CAF14] : CAFRI M., MALKA A., DARIEL M.P., FRAGE N., "Reaction-bonded boron carbide/magnesium-silicon composites", Int. J. Appl. Ceram. Technol., 11, [2], p.273-279, 2014

[CHE01] : CHEN L., LENGAUER W., ETTMAYER P., DREYER K., DAUB H.W., KASSEL D., "Fundamentals of liquid phase sintering for modern cermets and functionally graded cemented carbonitrides (FGCC)", Int. J. Refract. Met. Hard Mater., 18, 307, 2001

[DAR12] : DARIEL M.P, FRAGE N., "Reacition bonded Boron carbide: recent developments", Advanced in Applied Ceramics, vol 111, n°5&6, p. 301-310, 2012

[FRA03] : FRAGE N., LEVIN L., FRUMIN N., GELBSTEIN M., DARIEL M.P., "Manufacturing B4C-(Al,Si) composite materials by metal alloy infiltration", J. Mat. Pro. Tec., 143-144, p. 486-490, 2003

[FRA04] : FRAGE N., FROUMIN N., AIZENSTEIN M., DARIEL M.P, "Interface reaction in the B4C/(Cu-Si) system", Acta Materialia, 52, p. 2625-2635, 2004

[FRO03] : FROUMIN N., FRAGE N., AIZENSHTEIN M., DARIEL M.P., "Ceramic-metal interaction and wetting phenomena in the B4C/Cu system", J. Eur. Cer. Soc., 23, p. 2821-2828, 2003

[GEO16t] : Mathias Georges, Thesis, “Approche du frittage SPS de céramiques fines de carbure de bore : rôle despoudres initiales et de la mise en forme”, Matériaux. Université de Limoges, 2016. Français. NNT : 2016LIMO0132

[GOL01] : GOLDSTEIN A., GEFFEN Y., GOLDENBERG A., "Boron carbide-Zirconium boride in situ composite by reactive pressureless sintering of boron carbide-Zirconia Mixtures, J.Am.Cer.Soc, 84, [3], p642-644,2001

[GOL09] : GOLDSTEIN A., RUGINETS R., GEIFMAN L., "Carbide matrix composites by fast MW reaction-sintering in air of B4C-SiC-Al mixtures", Cer. Int., 35, p. 1297-1300, 2009

[GUG72] : GUGEL E., KIEFFER R., LEIMER G., ETTMAYER P., "Ternary system boron-carbon-silcon." Solid State chem., 364, 505, 1972

[HAL15] : HALLAM D., HEATON A., JAMES B., SMITH P., YEAMANS J., "The correlation of indentation behavior with ballistic performance for spark plasma sintered aour ceramics", J.Eur.Cer.Soc., 35, p.2243-2252, 2015

[HAY06] : HYUN S., FRAGE N., DARIEL M.P., "The morphology of ceramic phases in BxC-SiC-Si infiltrated composites", Journal of solid state chemistry, 179, p. 2875-2879, 2006

[HAY08] : HAYUN S., RITTEL D., FRAGE N., DARIEL M.P., "Static and dynamic mechanical properties of infiltrated B4C-SiC composite", Mat. Sci. Eng. A, 487, p. 405-409, 2008

[HAY09a] : HAYUN S., WEIZMANN A., DARIEL M.P., FRAGE N., "The effect of particle size distribution on the microstructure and mecahnical properties of boron carbide-based reaction-bonded composites, Int. J. Appl. Ceram. Technol., 6, [4], p. 492-500, 2009

[HAY09b] : HAYUN S., DILMAN H., DARIEL M.P., FRAGE N., "The effect of aluminum on the microstructure an phase compositionof boron carbie infiltrated wit slicon", Materials chemistry and Physics, 118, p. 490-495, 2009

[HAY09c] : HAYUN S., WEIZMANN A., DARIEL M.P., FRAGE N., "Rim region growth and its composition in the raction bonded boron carbide composites with core-rim structure.", 16th International Symposium of Boron, Borides and Related materials, Journal of Physics: Conference Series, 176, 012009, 2009

[HAY09t] : HAYUN S., Thesis, "The Inter-relationships between the static and dynamic mechanical properties and microstructure of reaction bonded boron carbide composites", Ben Gurion University of Neguev, Septembre 2009

[HAY10a] : HAYUN S., KALABUKHOV S., EZERSKY V., DARIEL M.P., FRAGE N., "Microstructural characterizationof spark plasma sintered boron carbide ceramics", Cer. Int., 36, p.451-457, 2010

[HAY10b] : HAYUN S., DILMAN H., DARIEL M.P., FRAGE N., DUB S., "The effect of carbon source on the microstructure and the mechanical properties of reaction bonded boron carbide", Advances in sintering science and technology, Book series: Ceramic Transaction, 209, p. 29-39, 2010

[HAY10c] : HAYUN S., WEIZMANN A., DARIEL M.P., FRAGE N., "Microstructural evolution during the infiltration of boron carbide with molten silicon", J. Eur. Cer. Soc., 30, p. 1007-1014, 2010

[HAY10d] : HAYUN S., DARIEL M.P., FRAGE N., ZARETSKY E., "The high-strain-rate dynamic response of boron carbide-based composites: The effect of microstructure", Acta Materialia, 58, p.1721-1731, 2010

[INT1] : http://www.radartutorial.eu/03.linetheory/tl10.fr.html

[ISR09t] : ISRAEL R., Thesis, "Etude des interactions entre silicium liquide et graphite pour applicaiton à l'élaboration du silicium photovoltaïque", Institut Polytechnique de Grenoble, Septembre 2009

[KAR07] : KARANDIKAR P.G., AGHAJANIAN M.K., AGRAWAL D., CHENG J., "Microwave assited (MASS) processing of metal ceramic and reaction bonded composites", Ceramic Enginneering and science processings, vol. 27, n°2, p. 435-446, 2007

[KAS96t] : KASPER B.,Thesis, "Phasengleichgewichte im System B-C-N-Si", University of Stuttgrat, Germany, 1996

[KOU02] : KOUZELI M., SAN MARCHI C., MORTENSEN A., "Effect of reaction on the tensile behavior of infiltrated boroncarbide-aluminum composites", Mat. Sci. Eng. A, 337, p. 264-273, 2002

[LEE02] : LEE H., SPEYER R.F., "Sintering of boron carbide heat-treated with hydrogen", J. Ame.Cer.Soc, 85, [8], p.2131-2133, 2002

[LI14] : LI X., JIANG D., ZHANG J., LIN Q., CHEN Z., HUAUNG Z., "Densification behavior and related phenomena of spark plasma sintered boron carbide", Cer. Int., 40, p.4359-4366, 2014

[MIT04] : MITSUDO S., HOSHIZUKI H., MATSUURA K., SAJI T., IDEHARA T., GLYAIN M., EREMEEV A., ZAPEVALOV V., KITANO A., NISHI H., ISHIBASHI J., "High power millimeter and submillimeter wave material processing", Plasma and Industrial Applications, p. 727-728, 2004

[MIT05] : MITSUDO S., HOSHIZUKI H., MATSUURA K., SAJI T., IDEHARA T., KITANO A., NISHI H., ISHIBASHI J., SANO S., "Non-thermal effects on B4C ceramics sintering", Plasma and industrial Applications, p.225-226, 2005

[MOS13] : MOSHTAGHIOUN B.M., CUMBERA-HERNANDEZ F.L., GOMEZ-GARCIA D., BERNARDI-MARTIN S., DOMINGUEZ-RODRIGUEZ A., MONSHI A., ABBASI M.H., "effect of spark plasma sintering parameters on microstructure and room-temperature hardness and toughness of fine-grained boron carbide (B4C), J. Eur. Cer. Soc., 33, p.361-369, 2013

[MOS14] : MOSHTAGHIOUN B.M., CUMBERA F.L., ORTIZ A.L., CASILLO-RODRIGUEZ M., GOMEZ-GARCIA D., "Additive-free superhard B4C with ultrfine-grained dense microstrucutures", J.Eur.Cer.Soc., 34, p. 841-848, 2014

[MOS15] : MOSHTAGHIOUN B.M., ORTIZ A.L., GOMEZ-GARCIA D., DOMINGUEZ-RODRIGUEZ A., "Densification of B4C nanopowder with nanograin retention by spark-plasma sintering", J.Eur.Cer.Soc., 35, p. 1991-1998, 2015

[MOS66] : MOSKOWITZ D., HUMENIK M., "Cemented titanium carbide cutting tools.", Mod. Develop. Powder Met., 3, 83, 1966

[NES93] : NESHPOR V.S., BRYKOV S.I., ZAKHAROV V.G., ZAITSEV G.P., NIKITINA T.P., PAVLOV S.M., PESIN V.A., FEHRETDINOV F.A., KTSAI A.A., "Structure and properties of boron and silcon carbide-base materials obtained by the method of reaction-activated microwave sintering in contact with aluminum nitride", Plenum Publishing Corporation, 1993

[NIU16] : NIU B., ZHANG F., ZHANG J., JI W., WANG W., FU Z., "Ultrafast densification of boron cabide by flash spark plasma sintering", Scripta Materialia, 1, [16], p. 127-130, 2016

[PRO77] : PROCHAZKA S., "Dense sintered boron carbide containing beryllium carbide", United States patent, 4.005.235, 1977

[RAD98] : RADEV D. D., ZAKHARIEV Z., "Structural and mechanical properties of activated sintered boron carbide-based materials", J. Solid Sate Chem., 137, p1-5, 1998

[REH15] : REHMAN S. S., JI W., KHAN A., FU Z., ZHANG F., "Microstrucuture and mechanical properties of B_4C densified by spark plasma sintering with Si as a sintering aid", Cer. Int., 41, p. 1903-1906, 2015

[SAH12] : SAHIN F.C., APAK B., AKIN I., KANBUR H.E., GENCKAN D.H., TURAN A., GOLLER G., YUCEL O., "Spark plasma sintering of B4C-SiC composite", Solid State Sciences, 14, p.1660-1663, 2012

[SAI14] : SAIRAM K., SONBER J.K, MURTHY T.S.R.Ch., SUBRAMANIAN C., FOTEDAR R.K., NANEKAR P., HUBLI R.C., "Influence of spark plasma sintering parameters on densification and mechanical properties of boron carbide", Int. Journal of refractory metal and hard materials, 42, p.185-192, 2014

[SCH96] : SCHWETZ K. A., SIG L., THALER H., "Process for producing bodies based on boron carbide by pressurless sintering", United state patent, 5.505.899, 1996

[SHA91] : SHAFFER P.T.B, "Engineered Materials Handbook", ASM International Handbook Committee, 4 Ceramics and Glasses, p804-806 1991

[SIG98] : SIGL L. S., "Processing and mecanical properties of boron carbide sintered with TiC", J.Eur. Cer. Soc, 6,[11], p.1521-1529, 1998

[SUN14] : SUN C., LI Y., ZHU L., JIANG Q., MIAO Y., CHEN X., "Effect of alumina addiition on the densifiaction of boron carbide cermics prepared by saprk plasma sintering technique", Cer. Int., 40, p. 12723-12728, 2014

[TAR04] : TARIOLLE S., THEVENOT F., AIZENSTEIN M., DARIEL M.P., FURMIN N., FRAGE N., "Boron carbide-copper infiltrated cermets", Journal of solid state chemistry, 177, p. 400-406, 2004

[TAR04t] : TARIOLLE S.,Thesis, "Carbure de bore monolithique poreux et composites lamellaires elaboration, proprietes, renforcement", E.N.S des Mines de Saint-Etienne, order n°328TD, 2004

[TEL87] : TELLE R., PETZOW G., "Mechanisms in the liquid phase sintering of boron carbide with silicon based melts." Mater. Sci. Monogr., 38A, 961, 1987

[TEL90] : TELLE R., "Structure and properties of Si-doped boron carbide",NATO ASI Ser., Ser.E, NATO ASI Series, Series E: Applied Sciences, 185, p. 249-267, 1990

[THE90] : THEVENOT F., "Boron carbide-A conprehensive review", J. Eur.Cer.Soc, 6 205-225(1990]

[THU13] : THUAULT A., MARINEL S., SAVARY E., HEUGUET R., SAUNIER S., GOEURIOT D., AGRAWAL D., "Processing of reaction-bonded B4C-SiC composites in a single-mode microwave cavity, Cer. Int., 39, [2], p. 1215-1219, 2013

[TUN11] : TUNCER N., TASDELEN B., ARSLAN G., "Effect of passivationand precipitation hardening on processing and mecahnical properties of B4C-Al composites", Cer. Int., 37, p. 2861-2867, 2011

[VAS16] : VASYLKIV O., DEMIRSKYI D., BADICA P., NISHIMURA T., TOK A.I.Y., SAKKA Y., BORODIANSKA H., "Room and high temperature flexural failure of spark plasma sintered boron carbide", Cer. Int., 42, p.7001-7013, 2016

[WAN14] : WANG J., LIN W., JIANG Z., DUAN L., YANG G., "The preparation and properties of SiCw/B4C composites infiltrated with molten silicon", Cer. Int., 40, p. 6793-6798, 2014

[WER94] : WERHEIT H., KUHLMANN U., LAUX M., TELLE R., "Solid solution of silicon in boron-carbide-type crystals", Journal of alloys and compounds, 209, p. 181-187, 1994

[WU12] : WU H., ZHANG S., GAO M., ZHU D., PAN Y., LIU Y., PAN H., OLIVEIRA F.J., VIEIRA J.M., "Microstructure and mechanical properties of multi-carbides/(Al,Si) composites derived from porous B4C preforms by reactive melt infiltration", Mat. Sci. Eng. A, 551, p. 200-208, 2012

[WU14] : WU H., ZENG F., YUAN T., ZHANG F., XIONG X., "Wettability of 2519 Al at 1000-1250°C and mechanical properties of infiltrated B4C-2519Al composites", Cer. Int., 40, p. 2073-2081, 2014

[YAM03] : YAMADA S., HIRAO K., YAMAUCHI Y., KANZAKI S., "High strength B4B-TiC composite fabricated by reaction hot-pressing, J.Eur.Cer.Soc, 23, [7], p. 1123-1130, 2003

[ZAK90] : ZAKHARIEV Z.,RADEV D., "Dense material obtained on the basis of boron carbide sintered without presiing", AIP conference Proceedings 231, boron-rich solids, Albuquerque, New Mexico, 1990

[ZHA14a] : ZHANG C., RU H., WANG W., YUE X., ZHAO J., "The role of infiltration in the reaction bonding of boron carbide by silicon infiltration", J. Am. Ceram. Soc., 97, [10], p. 3286-3293, 2014

[ZHA14b] : ZHANG Z., DU X., LI Z., WANG W., ZHANG J., FU Z., "Microstructures and mechanical properties of B4C-SiC intergranular/intragranular nanocomposite ceramics fabricated from B4C, Si, and graphite powders", J. Eur. Cer. Soc., 34, p. 2153-2161, 2014

Chapter II: Methodology

INTRODUCTION

This chapter presents the experimental methods used in this work. The first part deals with sample fabrication by conventional and microwave heating.
In the second part, the description of the sample characterization methods will be presented.

1 Fabrication of B_4C-SiC composites

1-1 Preform manufacture

Preforms were obtained by cold compaction of a B_4C commercial powder (Cf. figure I)1) (HC stark, grade HS). The characteristics of this powder are (information from seller):

-D50: 0.8 µm
-Specific surface area (BET): 15-20m^2/g
-B/C (ratio): 3.7-3.9
-wt% C: 21.8
-wt% O: 2.3-2.6

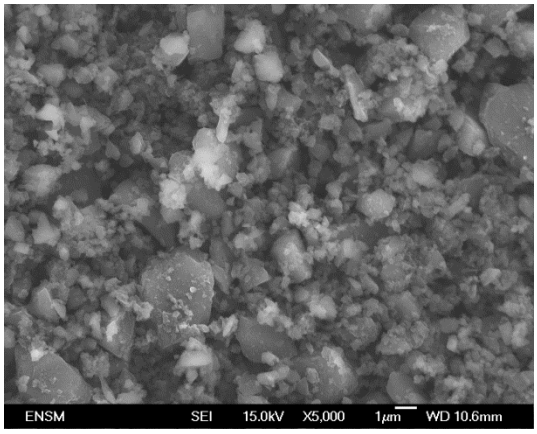

Figure II)1: SEM image of B_4C commercial powder

The powder is pressed without organic additives (plasticizer or binder).Teflon spray was used to protect the matrix and pistons, and to make the pressing process easier.
The pressing conditions depend on the sample diameters (see table II)1):

- The 20 mmm diameter samples (m= 4g) were obtained by uniaxial pressing under 180 MPa.
- The 35 mm diameter samples (m=10g) were obtained by uniaxial pressing under 100 MPa (maximum pressure for this device).
- Table II)1 presents the different forming conditions and the density of each green sample.

Table II)1: Pressing conditions and densities of green samples

Diameter (mm)	Uniaxial pressing (MPa)	Density (% TD)
20	160-180	62-63
35	100	59-61

If there is no sintering step a debinding stage is performed under argon atmosphere at a temperature of 600°C during 2h, with a heating rate of 1°C/min, in order to remove the Teflon. If a sintering step is occurred, the debinding is made during the heating (the thermal cycle is presented in the table II)2. Some of the pressed samples were sintered in a graphite crucible under argon (furnace VAS, France) following the thermal cycles described in the table II)2.

Table II)2: Sintering conditions of the preform and final densities

Initial diameter (mm)	Green Density (% TD)	Heating rate	dwell temperature and time	Cooling rate	Final density (% TD)	Final diameter (mm)
20	62-63	1°C/min->200°C (Vacuum) 5°C/min (Ar)	2150°C 30min	10°C/min	83-84	18
35	59-61	1°C/min->200°C (Vacuum) 1°C/min ->600°C (Ar) 5°C/min(Ar)	2050°C 30min	10°C/min	65-71	34
			2150°C 30min		73-75	32

The figureII)2 shows a typical microstructure and pores distribution in a sintered preform. a) sample edge and b) sample core. On the figure b) the porosity is not homogeneously distributed, there are clearly two very porous areas. Despite a few porous areas , this sample is homogeneous in terms of microstructure.

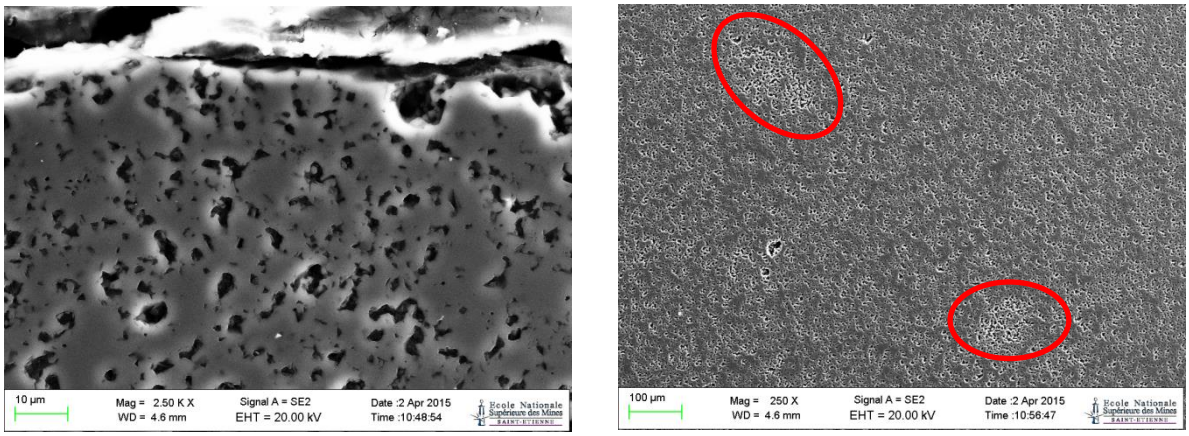

a)Sample's edge b)Sample's core

Figure II)2: Sintered sample (84% theoretical density)

Table II)3 presents the samples used during this PhD.

Table II)3: Presentation of the samples used for different tests

Test	Samples' porosity (%)	Diameter (mm)	Height (mm)
Parametric study	41-25	32-35	6-7
Preliminary study	16-17	18	7
Anisothermal study	38-41	35	5
Isothermal study	29-27	32	6.3
Conventional vacuum furnace	40-20	20	3.4-5.7

1-2 Nature and quantity of the silicon

- Nature

In order to compare our results with the previous works described by Hayun et al. [HAY09t, HAY09a, HAY09b, HAY09c, HAY06, HAY08, HAY10a, HAY10b, HAY10c] same silicon source was used: 98.4% purity in the form of lump furnished by Alfa Aesar the certificate of analysis mentions 0.45% of Fe, 0.08% of Al and 0.008% of Ca.

- Used quantity: the conventional heating method is processed under high vacuum ($1.3x10^{-2}$ Pa). In consequence, Hayun et al. [HAY06] take into account the evaporation of silicon, to calculate the used mass. As we will describe later, the microwave heating is performed under 140 kPa of Ar/H_2 (10%). Therefore, we decided to adjust the mass of silicon to the quantity that is sufficient to fill the preform porosity.

1-3 Heat treatments

The infiltration was performed in vacuum for conventional furnaces. The conventional furnace infiltration was carried out at Ben Gurion University of Negev (Israel). During this thesis, different microwave furnaces (Cf. chap. I 3) were used:

- At Mines Saint-Etienne: the 2.45GHz multimode furnace.
- At CRISMAT: the 915MHz single-mode furnace.

In order to lighten the notation, we named the method performed in the conventional vacuum furnace as CVF, that in the 2.45GHz multimode as 2.45, and that in the 915MHz single-mode as 915.

1-3-1 Heat treatments in microwave furnaces

1-3-1-1 Atmosphere selection

According to the literature survey, the conventional RBBC is fabricated usually at high vacuum ($1.3x10^{-2}$ – $1.3x10^{-3}$ Pa) (Cf. chap. I 2-4-2 table I)3). Unfortunately, this type of condition is incompatible with the microwave heating methods. Low pressure promotes plasma formation within the microwave furnace. Thus, it was necessary to find optimal atmospheric parameters (gas type, pressure and flow) (Cf. chap. III) part A. tab III)1) in order to solve this problem. Moreover, in order to avoid silicon and boron carbide oxidation, the only neutral gas was chosen in this study. These tests are described later (Cf. chap. III).
Before starting heating, a cleaning of the cavity by three vacuum steps was performed:

- First one: one hour under primary vacuum (≈10 Pa), followed by the filling of the cavity with Ar/H_2 (10%) gas to the atmospheric pressure.
- Second one: 30 minutes under primary vacuum (≈10 Pa), followed by the filling of the cavity in the same conditions.
- Third one: 1h30 under secondary vacuum (10^{-2} Pa), filling of the cavity with Ar/H_2 gas up to 0.4 bars (on the manometer) of overpressure. When the overpressure is reached, gas evacuation valve is opened slightly to maintain the pressure at the same level.

In the 915MHz single-mode cavity, the experiment was exclusively conducted in Ar/H_2 (10%) atmosphere, with a relative pressure of +0.2bar (on the manometer) compared to ambient pressure and a gas circulation.
Before starting heating, a cleaning of the cavity by three vacuum steps was performed:

- First one: Maximum obtained vacuum (5minutes) (≈600Pa), followed by the filling of the cavity with Ar/H_2 gas to the atmospheric pressure.
- Second one: maximum obtained vacuum (5minutes) (≈600Pa), followed by the filling of the cavity in the same conditions.

- Third one: maximum obtained vacuum (5minutes) (600 Pa), filling of the cavity with Ar/H_2 gas up to 0.2 bar of overpressure. When the overpressure is reached, gas evacuation valve is opened slightly to maintain the pressure at the same level.

1-3-1-2 Heating in 2.45GHz furnace

- Crucibles:

A porous/fibrous crucible made in aluminosilicate phases (quasi-transparent to microwaves) was used.

- Susceptor:

The heating process can be direct (Cf. chap. I)): without any susceptor. A mass of 10g of boron carbide makes it possible; this corresponds to the tests performed with a 35mm diameter preform. In the case of 20mm diameter samples the heating was hybrid: SiC plates played the role of susceptor. But to simplify and homogenize the heating a susceptor was used even in the case of 10g of boron carbide. This susceptor is composed of small SiC beads placed under the sample. (Cf. figure II)3).

- Maximum power:

The selected atmosphere limits the maximum incident power at 1700W. Consequently incident power of 1600W was applied. The heating rate was fixed to 10°C/min for all experiments.

- Temperature measurement:

The temperature was measured by two optical pyrometers, a mono-color to low temperature measurements (100-700 °C Raytek pyrometer or 250-1000°C Ircon Modline pyrometer) and a bicolor to high temperature measurements (700-1800°C Ircon Modline pyrometer). A switch is done from low to high temperature pyrometer as soon as the high temperature pyrometer measures a temperature of 800°C. The pyrometers are calibrated with the fusion of some elements (in this work: silicon, which melts at 1414°C. The piece of silicon is placed on the surface of the sample. The melting of the metal is detected with a camera; the pyrometer does not target the piece of metal but the sample. When the piece of metal melts, the program provided by the pyrometer constructor is used in order to calculate the emissivity, at the melting temperature. After that calibration, an error of ± 20°C can be considered. We used an emissivity of 0.5 and an E-slop of 1 (ratio of two emissivity values at wavelength of 1 and 1.1 µm in our case).

- CCD camera

A CCD camera (SVS-Vistek model SVS2050MTLGEC) permits to follow the process and to determine the temperature of melting and infiltration of the silicon lump.

- Thermal cycle:

The maximal temperature was between 1350°C and 1550°C (measured on B_4C). Indeed, from the microwaves heating, the two materials heat at a different speed: the silicon starts to melt when the boron carbide is at 1300°C. We will describe this phenomenon thoroughly later (Cf. chap. III). The dwell time was generally around 15min. The different thermal cycles are described in chapter III. A PID program was developed [ZYM11] to achieve thermal cycle

with a precision of ±30°C.

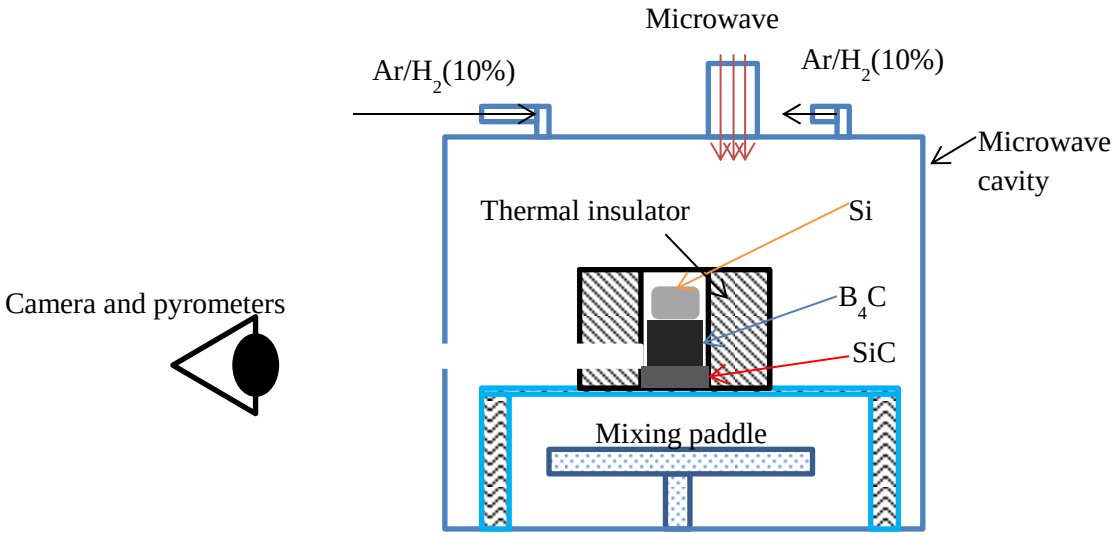

Figure II)3: scheme of the 2.45GHz microwaves cavity

All pictures of the manipulation presented in this work were taken from the camera in front of the cavity by a hole in the crucible made to see the sample during the heating.

1-3-1-3 Heating in 915MHz furnace

- Crucibles:

A homemade fibrous aluminosilicate crucible is used, cause of its microwave transparency.

- Susceptor:

SiC suceptor is used for the 915MHz heating. This susceptor is composed of two pieces of SiC placed under boron carbide preform.(Cf. figureII)4).

- Maximum power:

In a single-mode cavity the maximum needed power is lower than for a multimode cavity, however the plasma forming is easier in single-mode cavity than for multimode cavity because of the field intensity. A plasma formation was observed at a power between 900-1100 W of incident power.

- Temperature measurement:

The temperature was measured by one monocolor optical pyrometer, for the temperature range 350-2000°C. An emissivity of 0.5 was used for the temperature measurement without calibration. So the uncertainty on the temperature measurement is higher for 915MHz than the one in 2.45GHz (errors of 100-150°C).

- Thermal cycle:

In this cavity, the temperature was measured on the Si and by the top on the crucible. The maximum reached temperature was between 1550 and 1650°C, cause of the lack of time no calibration was done. So the temperature is not relevant. The thermal cycle was stopped after the melt of silicon and dwell time of 15min.

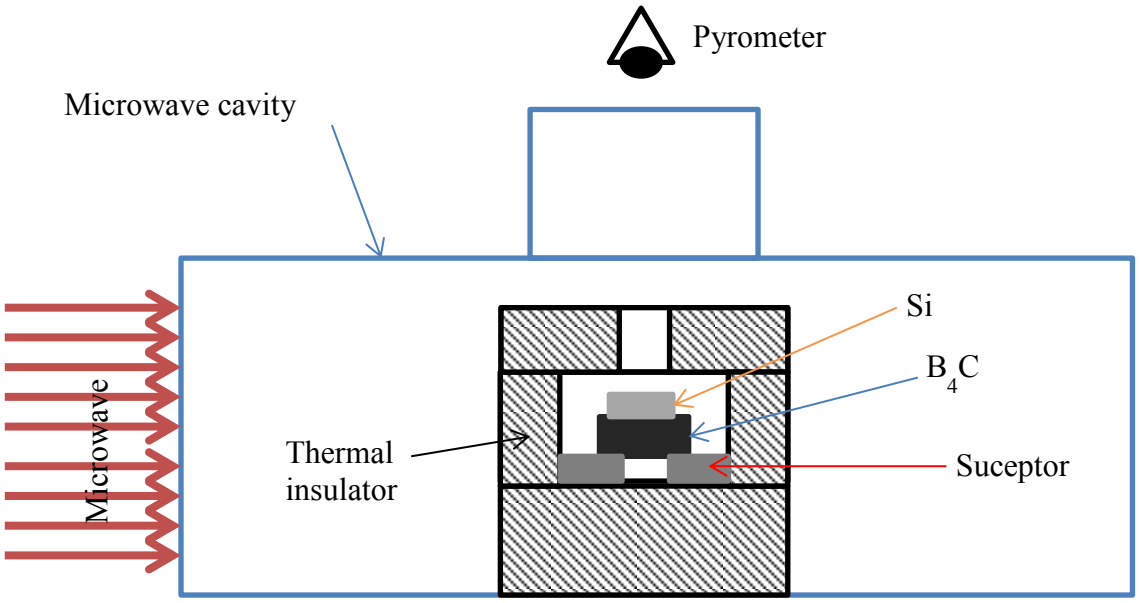

Figure II)4: Scheme of the 915MHz microwave cavity

1-3-2 Heat treatments in the conventional furnace

1-3-2-1 Atmosphere

In conventional furnace, the process was conducted under a vacuum of 1.3×10^{-2} Pa as it can be found in the bibliography (Cf. chap. I 2-4-2 table I)3). Two pumps, one for primary vacuum and another one for high vacuum, provide the vacuum: a diffusion pump. These two pumps work during all the infiltration process in order to eliminate the gas coming from the furnace and samples, and also the silicon evaporation at high temperature.

1-3-2-2 Heating method

Samples were placed in a SiC crucible on alumina plate to prevent the gluing of the sample on the SiC crucible. The crucible was closed and, then placed inside the furnace. The heating was assured by a carbon resistor; and the thermal insulation is ensured by carbon felt (Cf. figure II)5). The heating rate was fixed at 15°C/min, the dwell time at 20min and the dwell temperature at 1480°C to promote the complete infiltration of the silicon in the preform.

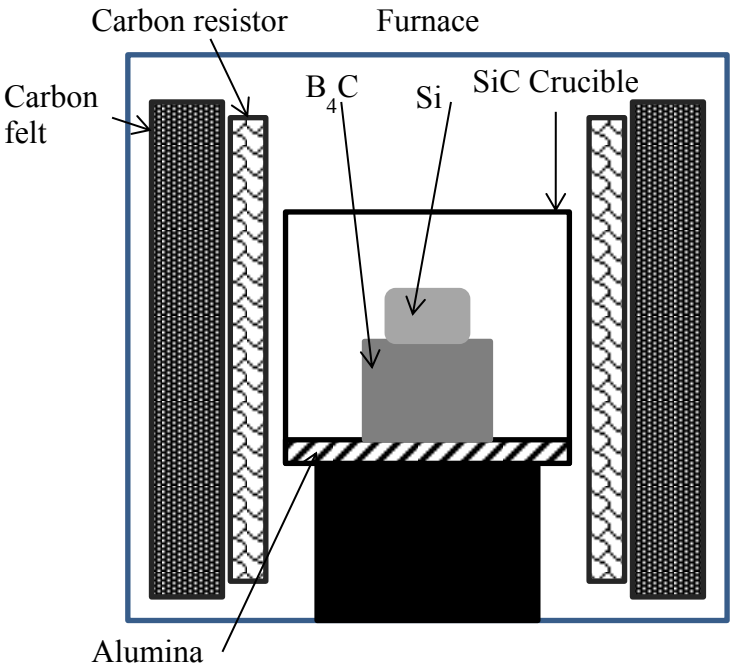

Figure II)5: Scheme of the conventional furnace used for the infiltration step

The furnace and crucible sizes permit the infiltration of 4 samples in the same treatment. This allowed us to do more different samples in conventional furnace than in micro-wave furnace in one experiment.

2 Characterizations

2-1 Densities

To determine the preforms and composites density before RB, we used a geometrical technique: measurement of both sample diameter and height with a caliper, then the sample was weighted. The mass was divided by the apparent volume of the sample to obtain the apparent density.

To determine the density of composite after RB, Archimedes method was applied. The weight of samples was taken in different conditions: dry, wet: see the explanation further, and immersed. The final density was calculated with the following equation:

$$D = \frac{dW * \rho l}{wW - sW} \qquad \text{Equ.7}$$

With: -D the density,
-dW the dry weight
- ρl the liquid density,
-wW the weight of the wet sample,
-sW the weight of the immersed sample.

At Saint-Etienne laboratory, absolute ethanol was used to fill up the open porosity and immersed samples.(Cf. figure II)6)

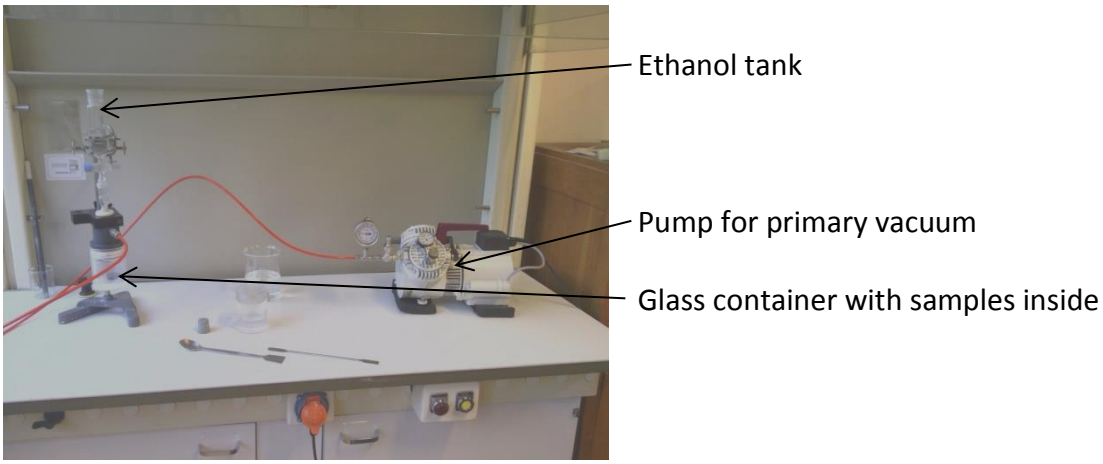

Figure II)6: Saint-Etienne device for Archimede's measurements

The measurements were preformed from the following protocol:
- The samples were put in a vacuum device in order to degas it.
- After 15min under vacuum, absolute ethanol was introduced into the vacuum chamber
- When the sample was totally submerged, the vacuum pump was stopped and the vacuum is broken
- After that the weight measurement was led.

At Beer Sheva water is used to fill up the open porosity and submerge samples.
The measurement was led following this protocol:
Samples were submerged in water contain in a beaker
- The beaker was put in a vacuum device in order to degas samples and permit the infiltration of water in the open porosity.
- After 15min under vacuum, the vacuum pump was stopped and the vacuum is broken
- After that the weight measurement was led.

We made some tests on different samples with the two methods and the difference between the values is ±0.03g/cm^3.

2-2 Samples preparation

Samples are extremely hard and brittle. Consequently, to cut (Buelher Isomet 4000) them, a special diamond disc was used (Struers Diamond Cut-off wheel M4D20). Samples were warm mounted (Buelher Simplimet 1000) with two types of resin powders. The amount of each powder was: one dose of Epomet F and two doses of green Bakelite powder. The samples were then polished (LAMPLAN M.M.8027A), following this procedure: 40µm diamond plate to start polishing and remove polymer on the samples surfaces. Then, we used 45, 30, 15, 9, 6, 3 and 1µm diamond suspension on different canvas. To perform the final polishing, we used a mix of colloidal silica and ferric oxide to remove a maximum of scratches.

Note: all samples were mounted with the same amount of powder to compare their hardness that was directly performed on mounted samples.

2-3 Microstructures observations and chemical analysis

2-3-1 SEM

The observations with a Scanning Electron Microscope SEM (MEB-FEG Zeiss supra 55 VP and JEOL J-SM 5600) were performed on mounted and polished samples. The SEM analysis allows the description of the composite microstructure.
At Ben Gurion University of Negev (JEOL J-SM 5600), these parameters and magnifications were used: 15kV, SEI (topographic contrast) and BES (chemical contrast) detectors were used, and samples were observed at 200, 3000, 5000, 5500 magnifications.
At Ecole des mines de Saint-Etienne (MEB-FEG Zeiss supra 55 VP), these parameters and magnifications were used: 7.5kV, SE2 (topographic contrast), ASB (chemical contrast) and InLens (finer topographic contrast) detectors were used; a small work distance (≈4mm) is needed for InLens detector, and samples were overserved at 200, 3000, 5000, 5500 magnifications.

2-3-2 EDX

Energy-Dispersive X-ray spectroscopy (EDX) (OXFORD X-MAX^N 80) was used to identify the elements in the composite, and their distribution in the different phases. The selected detector allows making reliable measurements on the light elements. Mapping function and local pointed analysis were used to see the distribution of Si, B, C and O. Oxygen was searched to verify if there was oxygen at high temperature during the infiltration: B_2O_3 presence or not. This method analyzes 1µm^3 of material average, and mapping and local analysis show just tendencies.
Analyses were led with a working distance of 8.5mm, with 7.5kV of current in order to obtain a dead time less than 40% (software data). The exposure time was variable, analyze was stopped when the data was enough (<3min).

2-3-3 XRD

X-Ray Diffraction is a method giving some information on crystalline phase like: phase composition, lattice parameter, and relative proportion of each phase. To see a phase in XRD analysis, it has to be a certain amount of this phase and crystallized structure. For XRD analyses, a Cu anode, monochromator (Hybrid monochromator 2xGE220 Cu asym(MPD) PW3149/63) a divergence slit (Pw3083/00) of 1/8 °, a maximum of 45 KV and 40mA, and a Pixel detector (PIXcel medipic 2 detector PW3018/00) were used. The scan range was from

20 to 92° (2θ), with a step size of 0.013° and with a time per step fixed at 500s.
To use correctly the possibilities of the method, is important to work on powder. However, in the case of reaction bonded boron carbide, it is impossible to grind samples cause of their high hardness. So the measurements were led on polished surface and the obtained data were used to compare samples between each other. In order to compare samples, the MAUD software was used to calculate the proportion of each phase.

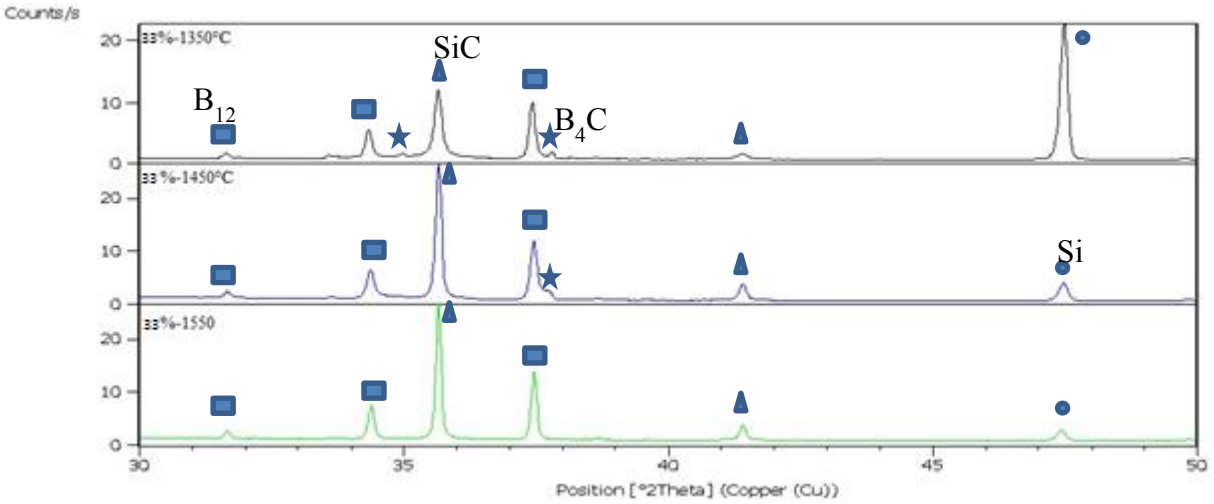

Figure II)7: XRD results for three samples with the same initial porosity

On figure II)7 diffractograms for 33%initial density samples can be seen. Stars represent residual boron carbide XRD peak, rectangles represent $B_{12}(B,C,Si)_3$, circle represent residual silicon and triangle represent silicon carbide peaks. The boron carbide XRD peak is still visible for sample infiltrated at 1350°C and 1450°C but it decreases between these two temperatures to finally completely disappear at 1550°C. The SiC XRD peaks increase between 1350°C and 1450°C and there is almost no evolution between 1450°C and 1550°C.

2-3-4 Composition derived from mix XRD and chemical silicon removing

After some experiments, the residual silicon in composite had large area structure which is incompatible with the calculation of the proportion of each phase. So to obtain valid data, the excluded regions function of MAUD software was used to ignore silicon XRD peaks. Others phases proportion were calculated normally. To obtain the proportion of residual silicon, a small part is removed, weighted and chemically etched in a 50/50 solution of HF (49%) and HNO_3 (69%).Etching is due to four chemical expected reactions:

1- $3Si_{(s)}+4HNO_{3(l)}+18HF_{(l)}=8H_2O_{(g)}+2H_2SiF_{6(l)}+4NO_{(g)}$
2- $3Si_{(s)}+4HNO_{3(l)}+12HF_{(l)}=8H_2O_{(g)}+4NO_{(g)}+3SiF_{4(g)}$
3- $4Si_{(s)}+2HNO_{3(l)}+6HF_{(l)}=(NH_4)_2SiF_{6(l)}+3SiO_{2(s)}$
$SiO_{2(s)}+4HF_{(l)}=SiF_{4(g)}+2H_2O_{(l)}$
4- $Si_{(s)}+4HNO_{3(l)}+6HF_{(l)}=4H_2O_{(g)}+H_2SiF_{6(l)}+4NO_{2(g)}$

A brown/orange gas was observed during the etching; that gas is probably NO_2. So the reaction 4 took place during this etching.
After etching, the sample was weighted: this allowed the calculation of the amount of residual silicon. Others phases amount are corrected with the amount of silicon following the equation:

$$\%A = \%a * \frac{100 - \%Si}{100} \qquad \text{Equ.8}$$

With: - % A, the real proportion of the phase A
- % a, the amount of phase A obtained by MAUD software without Silicon peaks
- % Si, the amount of Silicon obtained by chemical etching

This method induces hypotheses:
- all silicon is removed by the etching.
- silicon is equally distributed in the composite
- only silicon is removed, not the other phases (we check the stability of the SiC and B_4C to this solution but some small grains can move from the surface).

This way of calculation will be used for porous composites only.

2-3-5 TEM

Transmission Electron Microscopy (TEM) was used to perform fine observations of microstructures. It is a very local analysis, i.e. of 4*4µm^2 on few nanometers of thickness. Samples were prepared by Focus Ion Beam (FIB) methods following this protocol (Cf. figure II)8):

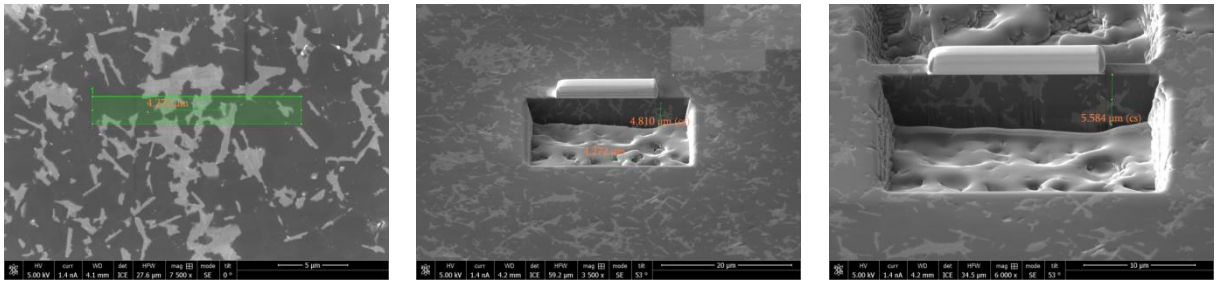

Step 1 Step 2 Step 3

Figure II)8: Sample preparation for TEM observation by FIB method

Step one: An area of 4µm length at least is chosen. A protective layer of platine is deposited on the surface.
Step two: Two areas from either side of the protective layer length is dug to 5µm of depth.
Step three: When the two areas has the good depth, FIB start separating the TEM sample for thin it.
A Philips CM 200 was used for TEM observation and a PGT system was used for EDX analysis in TEM.

2-4 Mechanical properties

2-4-1 Hardness

The hardness was measured on mounted and polished samples. Both Vickers and Knoop indenters were used in this study:
Vickers hardness (Matsuzawa MXT 70): at 300g with 10s of dwell time: 21 measurements on the surface divided in 3 zones (parallel to the direction of infiltration) of 7 points. The 300g load was selected in order to prevent cracks with the Vickers indenter (Cf. figure II)9).
The Vickers hardness was obtained from the measurement of two diagonals of the imprint done with a diamond square based pyramid with an angle of 136**°** between opposed face. The hardness was calculated as follows:

$$HV_{Pa} = \frac{2F * g * \sin(\frac{136}{2})}{d^2} \qquad \text{Equ.10}$$

With: HV_{Pa}: Vickers Hardness (Pa)
F: applied force to do the imprint (kg)
g: constant of the acceleration of average gravity on earth (N/kg)
d: average of the two diagonal length (m).

Knoop hardness (Buehler MMT7): at 2000g with 10s of dwell time: 12 measurements on the surface in random choice (Cf. figure II)10).

The Knoop hardness is obtained from measurement of the longest diagonal of the imprint done with a diamond lozenge based pyramid (angle of 172°30’ between opposed faces, and 130° between the two other faces). The hardness was calculated as follows:

$$HK_{Pa} = 14.229 * 10^6 * \frac{F_N}{{D_m}^2} \qquad \text{Equ.11}$$

With HK_{Pa}: Knoop Hardness (Pa)
F_N: applied force (N)
D_m: Imprint diagonal length(m)

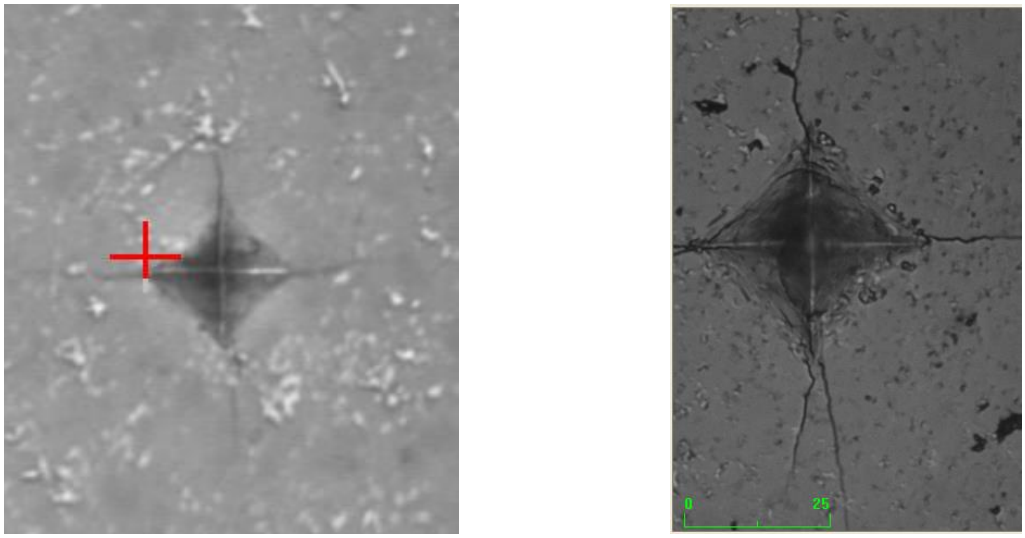

a)300g load b) 2000g load

Figure II)9: Vickers imprint with different charge loads

Figure II)10: Knoop imprint with 2kg load

The Knoop indenter allows doing the hardness measurement on larger imprint. The error on the measure is lower than for Vickers hardness. A comparison of Vickers hardness and Knoop ones is presented in table II)4.

As expected, the standard errors are less important for Knoop hardness than for Vickers ones.

The Knoop hardness values are lower than Vickers one, ≈3GPa. It's important to keep in mind this fact to compare with values reported in literature. Knoop hardness will be used as the reference values.

Table II)4: Comparison between Vickers hardness and Knoop hardness

Tests	HV_{300} (GPa)	HK_{2000} (GPa)
25%-1500°C	2337 (22.9)	1887±86 (19.24)
25%-1400°C	2312 (22.7)	1786± 158 (18.21)
33%-1550°C	1997 (19.6)	1678± 62 (17.10)
33%-1450°C	1901 (18.6)	1647±97 (16.79)
35%-1350°C	2016 (19.8)	1647± 83 (16.79)
40%-1500°C	1780 (17.5)	1398±67 (14.26)
40%-1400°C	1678 (16.46)	1488± 83 (15.17)

2-4-2 Fracture toughness

The fracture toughness was determined by the indentation method on polished specimens, as explained by Liang et al.[LIA90]. The equation below was used to calculate the fracture toughness, where Φ is a constant (equal to 3), H the hardness, E the Young's modulus, α a coefficient as a function of Poisson's ratio, a the diagonal of indent, and c the crack radius. The load was chosen in order to generate cracks at the imprint corners.

$$\left(\frac{K_{1C}.\Phi}{H.a^{1/2}}\right).\left(\frac{H}{E\Phi}\right)^{0.4}.\alpha = \left(\frac{c}{a}\right)^{(c/18a)-1.51} \qquad \text{Equ.12}$$

From the equation (12) K_{1C} may be calculated with the equation:

$$K_{1C} = \frac{\left(\frac{c}{a}\right)^{(c/18a)-1.51} * H^{0.6} * E^{0.4} * a^{0.5}}{\alpha * \Phi^{0.6}} \qquad \text{Equ.13}$$

To apply this method, the size of cracks formed around the indent was measured. Indentation experiments used loads of 1 kg during 10s (5 per sample), one measurement on each diagonal's imprints. The fracture toughness measurement was realized on the same device than the Vickers hardness one.

Fracture toughness and hardness were measured in dense area, where imprint are readable. The given values are for ideal material (no residual porosity and tougher enough to didn't explode under pressure).

2-4-3- Flexural bending strength

The bending test is a method used to determine the flexural strength of samples. The measurement was realized on crude cut parallelepipeds (1.5*2*(11) mm^3) by a three-point bending test. Generally, three tests are used for each sample.

$$FS = \frac{30 * F * L}{2 * w * h^2} \quad \text{Equ.14}$$

With: -FS flexural strength (Pa)
-F breaking load (N)
-L length between axes (m)
-w sample width (m)
-h sample height (m)

Measurements were conducted on Amateck Lloyd instruments LRX plus device. Crossbar displacement was fixed at 0.5mm/min.

2-4-4 Young modulus, shear modulus and Poisson coefficient

Young Modulus, shear modulus and Poisson coefficient were measured by using an ultrasonic pulse echo method. Times between two reflections of the sound in the longitudinal and transversal ways of the sample were measured. These measurements permit to determine both transversal and longitudinal ultrasonic wave speeds. Young's modulus was then calculated from the following equation:

$$E = \frac{3 * D * S(t)^2 * (S(l)^2 - \frac{4}{3}S(t)^2)}{S(l)^2 - S(t)^2} * 10^6 \quad \text{Equ.15}$$

With D the density of the sample measured by Archimedes method (g/cm^3).
S(t) the sound speed in transversal direction in mm/ns.
S(l) the sound speed in longitudinal direction in mm/ns.
E the Young Modulus in GPa.

Shear modulus was then calculated from the following equation:

$$G = D * S(t)^2 * 10^6 \quad \text{Equ.16}$$

With D the density of the sample measured by Archimedes method (g/cm^3)
S(t) the sound speed in transversal direction in mm/ns
G the shear modulus in GPa

Poisson coefficient was then calculated from the following equation:

$$\nu = \frac{1 - 2(\frac{S(t)}{S(l)})^2}{2 - 2(\frac{S(t)}{S(l)})^2} \qquad \text{Equ.17}$$

With D the density of the sample measured by Archimedes method (g/cm^3)
S(t) the sound speed in transversal direction in mm/ns
S(l) the sound speed in longitudinal direction in mm/ns
v the Poisson coefficient

Bibliography

[HAY06] : HYUN S., FRAGE N., DARIEL M.P., "The morphology of ceramic phases in BxC-SiC-Si infiltrated composites", Journal of solid state chemistry, 179, p. 2875-2879, 2006

[HAY08] : HAYUN S., RITTEL D., FRAGE N., DARIEL M.P., "Static and dynamic mechanical properties of infiltrated B4C-SiC composite", Mat. Sci. Eng. A, 487, p. 405-409, 2008

[HAY09a] : HAYUN S., WEIZMANN A., DARIEL M.P., FRAGE N., "The effect of particle size distribution on the microstructure and mecahnical properties of boron carbide-based reaction-bonded composites, Int. J. Appl. Ceram. Technol., 6, [4], p. 492-500, 2009

[HAY09b] : HAYUN S., DILMAN H., DARIEL M.P., FRAGE N., "The effect of aluminum on the microstructure an phase compositionof boron carbie infiltrated wit slicon", Materials chemistry and Physics, 118, p. 490-495, 2009

[HAY09c] : HAYUN S., WEIZMANN A., DARIEL M.P., FRAGE N., "Rim region growth and its composition in the raction bonded boron carbide composites with core-rim structure.", 16th International Symposium of Boron, Borides and Related materials, Journal of Physics: Conference Series, 176, 012009, 2009

[HAY09t] : HAYUN S., Thesis, "The Inter-relationships between the static and dynamic mechanical properties and microstructure of reaction bonded boron carbide composites", Ben Gurion University of Neguev, Septembre 2009

[HAY10a] : HAYUN S., DILMAN H., DARIEL M.P., FRAGE N., DUB S., "The effect of carbon source on the microstructure and the mechanical properties of reaction bonded boron carbide", Advances in sintering science and technology, Book series: Ceramic Transaction, 209, p. 29-39, 2010

[HAY10b] : HAYUN S., WEIZMANN A., DARIEL M.P., FRAGE N., "Microstructural evolution during the infiltration of boron carbide with molten silicon", J. Eur. Cer. Soc., 30, p. 1007-1014, 2010

[HAY10c] : HAYUN S., DARIEL M.P., FRAGE N., ZARETSKY E., "The high-strain-rate dynamic response of boron carbide-based composites: The effect of microstructure", Acta Materialia, 58, p.1721-1731, 2010

[LIA90] : LIANG K. M., ORANGE G., FANTOZZI G., "EVALUATION BY INDENTATION OF FRACTURE-TOUGHNESS OF CERAMIC MATERIALS", Journal of Materials Science, 25, [1A], p. 207-214, 1990

[ZYM11] : ZYMELKA D., SAUNIER S., MOLIMARD J., GOEURIOT D., “Contactless monitoring of shrinkage and temperature distribution during hybrid microwave sintering”, Advanced Engineering Materials, 13, [9], p. 901-905, 2011

Chapter III: Tests and results

INTRODUCTION

As shown in the bibliographic study, the research on the reaction bonded boron carbide synthesis by conventional heating method is well established. Contrarily, feasibility under microwave fields has been little explored. Microwave heating offer perhaps better heating rate, possible saving in energy use and a better heating homogeneity. This is the purpose of the study presented in this chapter.

First, the development of the RBBC synthesis procedure under a microwave field will be presented and its feasibility demonstrated.

Then, a parametric study will be carried out, to better identify the reactivity of the phases under microwave field, and develop composites with optimal mechanical properties. We will focus especially on hardness, which is a criterion for forecasting ballistic behavior.

Finally, a more specific study on the microwave effect will be made. We will focus on the reactivity, microstructure, and formal mechanical properties in comparison with a specific phenomenology in microwave heating infiltration.
All experimental results can be found in appendix IV.

Part A: Preliminary study: feasibility

A-1 Can microwave heat B_4C and Si?

The first part concerns the heating RBBC composites using microwaves for which the objective is to understand phase coupling. To accomplish this, we carried out temperature rise tests with constant incident power in two different configurations under a gaseous atmosphere of hydrogenated argon. FIG. III)1)a shows the arrangement of a sample for the first test: the boron carbide is in the form of pellets of mass 10 g, diameter 35 mm and height 7 mm (Cf. chap. II 1-1). The sample of B_4C is placed in a cylindrical crucible of refractory material. On the pellet, an irregularly shaped silicon chips is placed (mass = 5g), of which a plane face is in contact with the carbide. The size of the chips was adjusted in order the molten phase completely fill the porosity.
For the first run, direct microwave heating was tested on our configuration.
The test was carried out at a constant power of 1550W for about one hour (for the configuration of the 2.45GHz furnace, see chapter II)1-3-1-2). Figure III)2 shows that the incident energy was partially absorbed: the power absorbed, the difference between the incident power and that measured by the magnetron, was approximately 1000W throughout the test.

Considering that the crucible absorbs little of the microwaves, we can deduce some coupling of involved materials, which is also evidenced by the joint temperature rise: the temperature measured on the boron carbide pellet reached 550°C, which is far from the silicon melting point. Nota bene: the power absorbed by a material depends not only on its dielectric characteristics but also on its mass. It is therefore conceivable to reach the silicon's melting point using a larger mass. Another possibility is to use a susceptor (Cf. chap. I 3-2-3). For this purpose, in the second run, a layer of SiC beads under the surface of the silicon pellet of B_4C was selected, as shown figure III)3).

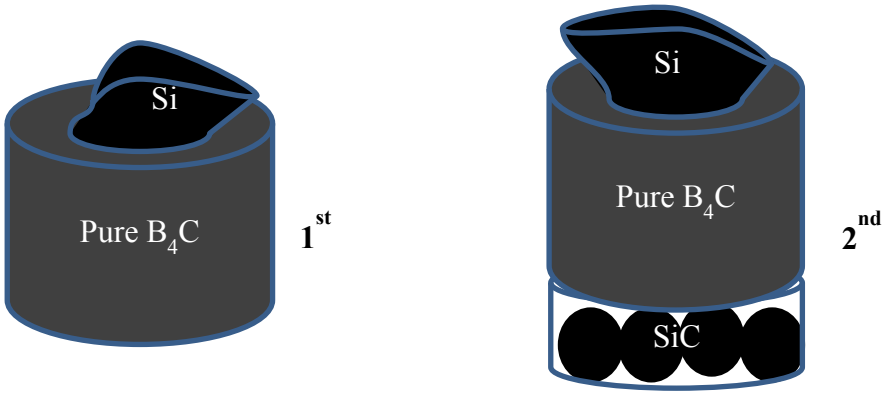

Figure III)1: Scheme of the two test rigs used for constant incident power tests

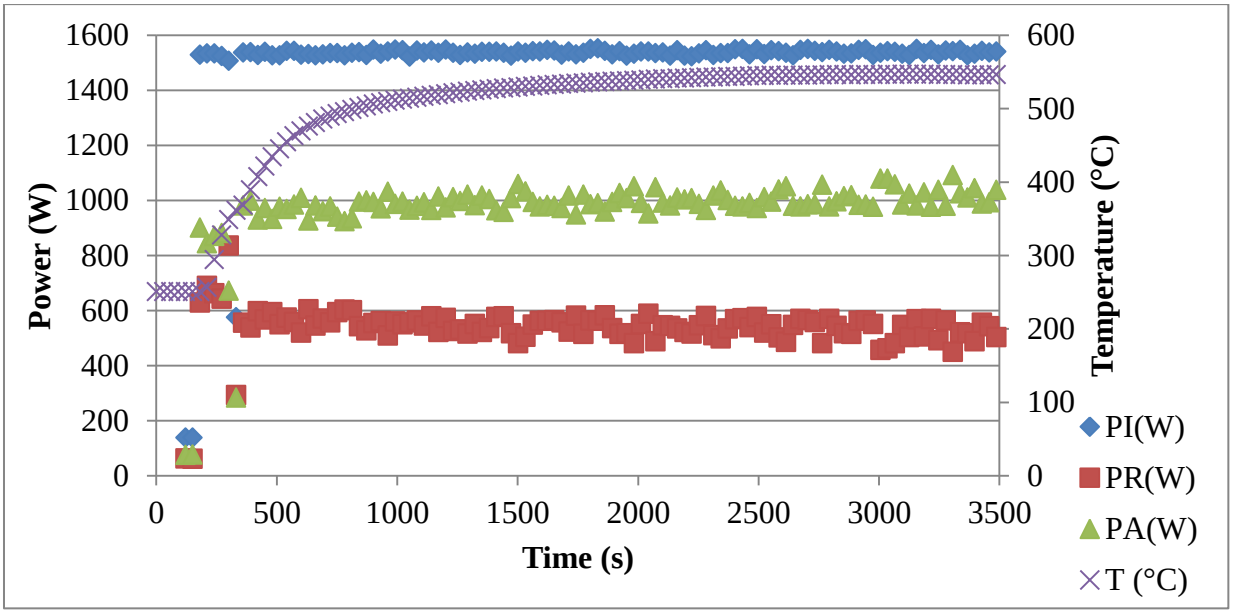

Figure III)2: Direct microwave heating test of sample

With : PI the incident power in W
PR the reflected power in W
PA the absorbed power in W
T the temperature in °C

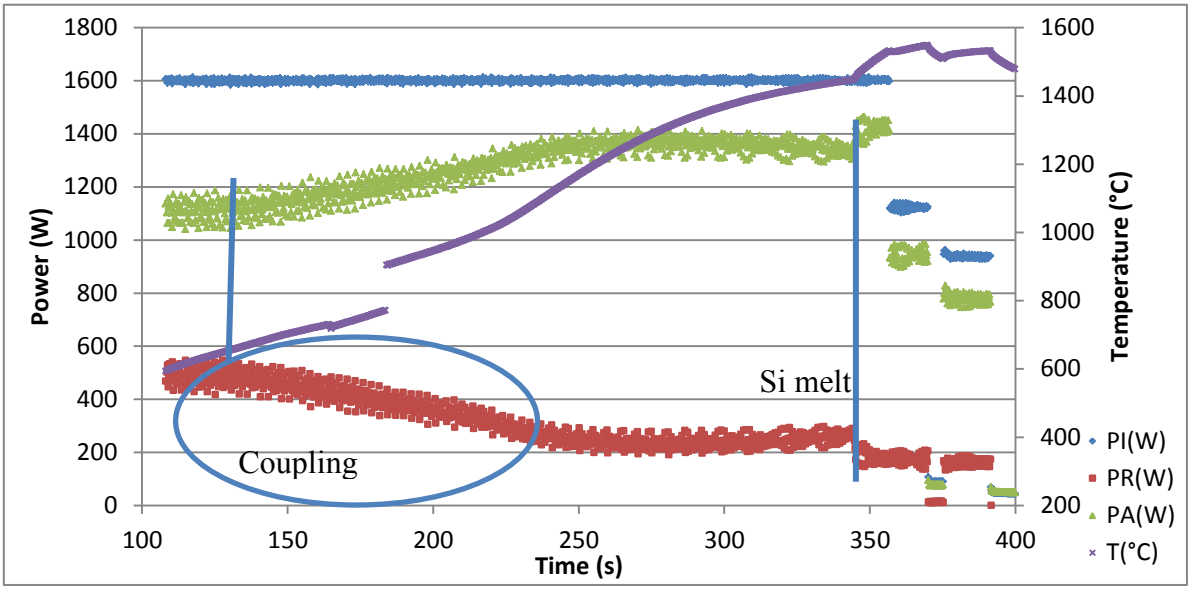

Figure III)3: microwave heating test of sample using a susceptor

For the same power as that used in the previous test, heating was more rapid and power absorbed by the system, was higher in this case, increased from 1150 to 1350W in two minutes, then remained constant, while the temperature reached 1400°C in 330 seconds. At this temperature, the silicon chip melted and infiltrated the preform. In parallel, an increase of both the absorbed power and the temperature up to approximately 1560°C was observed. Considering that the absorption of microwaves by SiC varies little in temperature, the increase in absorbed power observed at about 800°C would likely be linked to the coupling of B_4C and/or Si. The power jump observed at the moment of silicon melting is most probably related to the strong coupling of this phase in liquid form.

Considering that only with susceptors did heating reach the silicon's melting point, therefore the second configuration was mainly used in the thesis. Moreover, even if some samples could be permeated by direct heating, the addition of an external susceptor homogenizes the temperature field in the system, thus without hot spots, the crucible life time is increased. Indeed, in the case of direct heating, crucible never withstood more than two thermal cycles because of the plasma formation that causes hot spots and localized melting phenomena. However, with an external susceptor placed under the boron carbide sample, the crucible resists at least to six thermal cycles.

In conclusion, we showed that it is possible to heat such a material involved in the RBBC process, namely boron carbide and silicon, under microwave conditions. In addition, we know that the product of the reaction, SiC, couples very well with microwaves. Thus, during the reaction, the composite may be heated by microwaves. However, most of the tests, presented in this thesis, were carried out with a susceptor in the form of a one-layer bed in a crucible placed just under the boron carbide sample. Hence, this provides better control, easier reproducibility of the process, and extending the lifetime of the crucibles.

A-2 Development of RBBC process using microwave furnace

A-2-1 choice of the working atmosphere

According to the bibliography, RBBC is obtained under high vacuum (10^{-4} – 10^{-5} mbar) but this high level of vacuum is incompatible with heating by microwaves: indeed, low pressure promotes plasma in microwaves furnace. Different atmospheric conditions (gas, pressure and flow) were tried (table III)1) to solve this problem. An oxidizing atmosphere, such as air, is *a priori* eliminated, because of silicon and boron carbide oxidations.

Table III)1: Influence the different working atmospheres on maximal reached temperatures

Gas	Ionization Energy (eV)	Pressure (bar)	power before plasma (W)	Maximum reached temperature (°C)
Ar/H_2 (10%)	15.496	1.4	1700	1550
		10^{-1}	500	NA
CH_4	12.61	1.4	NA	1060
		0.5	NA	850
		10^{-1}	500	200
CO_2	13.773	1.4	NA	1100
N_2/H_2(10%)	15.334	1.4	3000 (High temperature)	1530
Ar/CO_2 (30%)/H_2 (10%)	14.899	1.4	2800 (Crucible melting)	1400

The parameter ionization energy was considered to choose the atmosphere: this probably influences the plasma potential of a gas as does the pressure, the lower its ionization energy the easier it is to form plasma. Nevertheless, plasma stability can change due to external contact with furnace walls where charges can be eliminated. This contact is diminished, if the plasma can easily propagate through the gas when the non-ionized gas can be ionized with low energy.

- Moreover, the low ionization energy leads to a large number of electric arcs but with low energy; so the thermal disturbance during heating does not occur.
- Finally, the electric arcs are weaker so their temperatures are lower, which is not favorable to hot plasma formation.

Indeed, it is easier to ionize around the gas particle, so the formed plasma dissipates easily its energy. It seems logical when looking at the gases usually used for plasma formation: N_2 (15.58ev), Ar (15.76ev), He (24.58ev). Another interesting point is the energy transmitted by electric arc when it occurs in the furnace. Certainly, if a gas resists ionization the formed electric arcs are very energetic. Consequently, heterogeneity between the bulk and the impact point occurs. But if the gas is easily ionized, the energy in the electric arc is relatively low. The ionization energy of the air is used as a reference (14.84ev), in order to compare

with the possible gases used, because there is no plasma forming in air at 1 atm. A rough approximation of the ionized energy calculated by mix law was made to compare gases used with normal air.

The mean value of ionization energy is calculated from the amount of each gas and its ionization energy, for example for air:

$$Air_{IE} = X * N_{2IE} + (1 - X) * O_{2IE} \qquad \text{Equ.16}$$

With X the amount of N_2 in the air (0.79 here). For the calculation, all the gas mixtures will be considered without pollution.

Methane (CH_4) was abandoned because it decomposes into hydrogen and carbon at temperatures higher than 1000°C. But no plasma was formed before that point even if the incident power reached 3000W.

Pure carbon dioxide (CO_2) was abandoned because of the formation of CO in the cavity and we noted that there were some difficulties to heat this molecule. But no plasma occurred even if the incident power reached 3550W.

N_2/H_2(10%) was not used any further because of the risk of silicon nitriding before infiltrating the preforms. However, the N_2/H_2 gas mix can heat with microwave more quickly (50°C/min) than Ar/H_2 (10°C/min), N_2/H_2 gas could be interesting for nitride sintering under microwave heating.

Ar/CO_2 (30%)/H_2 (10%) could not be used at high temperatures (>1400°C) simply because smoke or flames appeared. Thus, temperature control was lost and the crucible melted. These flames are probably due to CO_2 reduction into CO which produces O_2 reacting with H_2. This forms water and releases high thermal energy.

Those behaviors corroborate the hypothesis made above about ionization energies: indeed, there is no plasma formation for the different gases tried but we overestimated the stability of methane and carbon dioxide.

Among the different atmospheres, only one allows us to heat at the desired temperature: an overpressure of 0.4 bar flow of hydrogenated argon (Ar/H_2 (10%)). Before heating, the cavity was cleaned by three vacuum steps (Cf. chap. II 1-3-1).

A-2-2 Crucible

Different “homemade” crucibles were tested to find the best for the reaction bonded technique. These crucibles can be regrouping in three different families:

-With silicon carbide plate (hybrid heating sides and top).

-Without silicon carbide (direct heating).

-With silicon carbide beads (hybrid heating beneath).

A-2-2-1 Crucible with silicon carbide plate

The first crucible was a box in porous alumino-silicate with a rectangular hole inside (Cf. figure III)4). This type of crucible withstood two or three tests before melting.

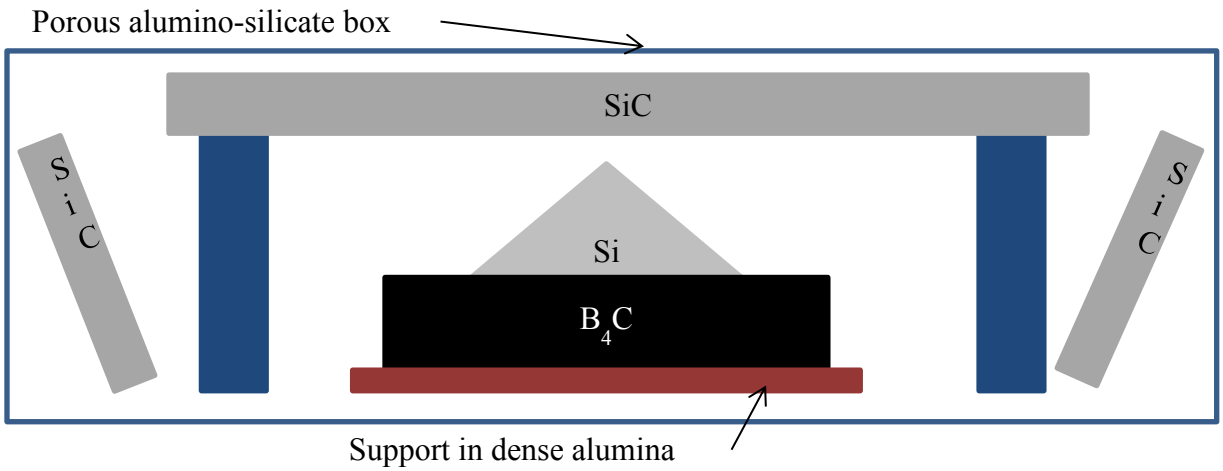

Figure III)4: Scheme of the first crucible

The preliminary studies and first parametric studies were done in this crucible. There were some troubles with this design: -Electric arcs between SiC and silicon

-Electric arcs between SiC top and side

These electric arcs caused some heterogeneous heating. Indeed, when an arc touched this silicon, it melted; so during all the tests, some parts of silicon were melted at 1000-1100°C and up (Cf. figure III)5).

The electric arcs (figure III)6) can have several causes:

- Thermal plasma, which locally overheats the gas via ionization.
- Potential difference between two pieces due to their exposure to the electromagnetic field. Certainly, each material absorbs microwaves differently so it appears as surface charges. Subsequently, dielectric breakdown can occur and an electric arc is produced.
- Peak effect, which concentrates the electric field in a small area and, consequently, provokes electric arcs between different parts of the same material.

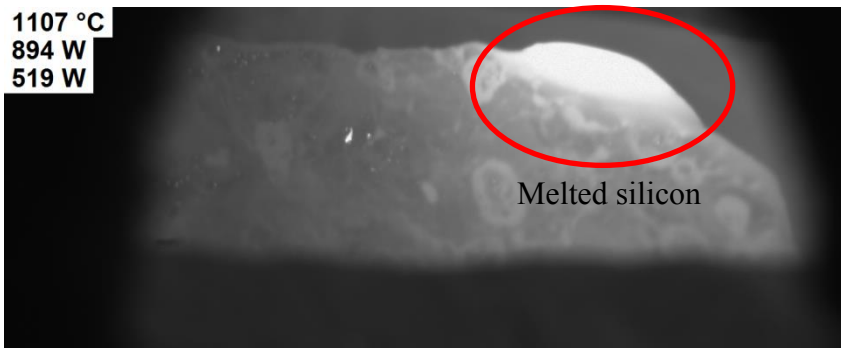

Figure III)5: Heterogeneous heating caused by the electric arc in the microwave furnace

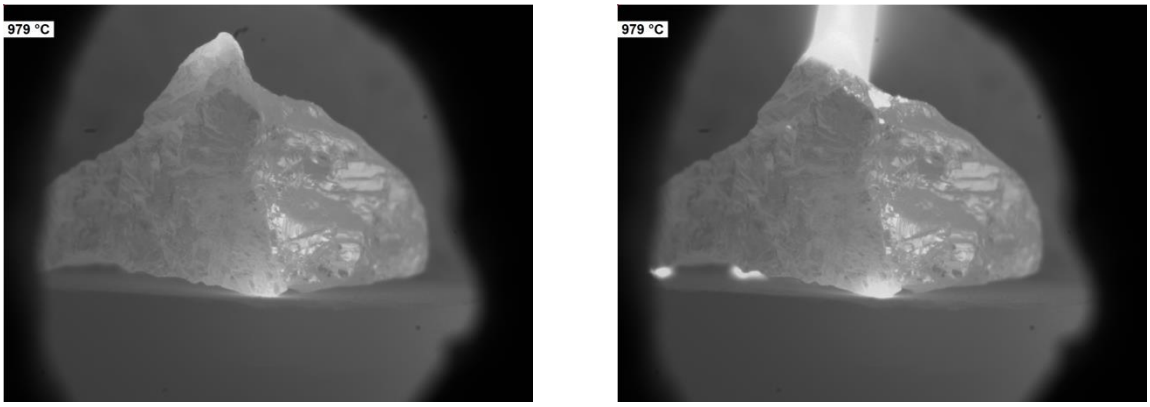

a) Sample before electric arc between Si and SiC

b) Sample during electric arc between Si and SiC

Figure III)6: Electric arc between SiC and silicon lump with local overheating

Figure III) shows the same sample at few seconds intervals: the white parts are hotter areas. Since the silicon lump hasn't a regular shape, an overheating effect can occur locally: if we stop the test before melting, it is possible to see the impact of the electric arc and the contact point of silicon on the boron carbide where a local melting is visible.

We also tried without the side silicon carbide plate but the electric arc between top SiC and silicon remained.

Consequently, we decided to remove all the silicon carbide from the crucible. In this case, the crucible was smaller to ensure good thermal insulation of the sample.

A-2-2-2 Crucible without silicon carbide

The majority of the parametric studies were made in this type of crucibles, which can be summarized as "a sample's size hole in a porous alumino-silicate box" (Cf. figure III)7). These crucibles last one or two tests before melting. As aforementioned, this type of crucible was designed to avoid the formation of electric arcs but also to limit the consummation of the porous alumino-silicate refractory material. To limit at the maximum, the thermal loss, the target hole was shrunk.

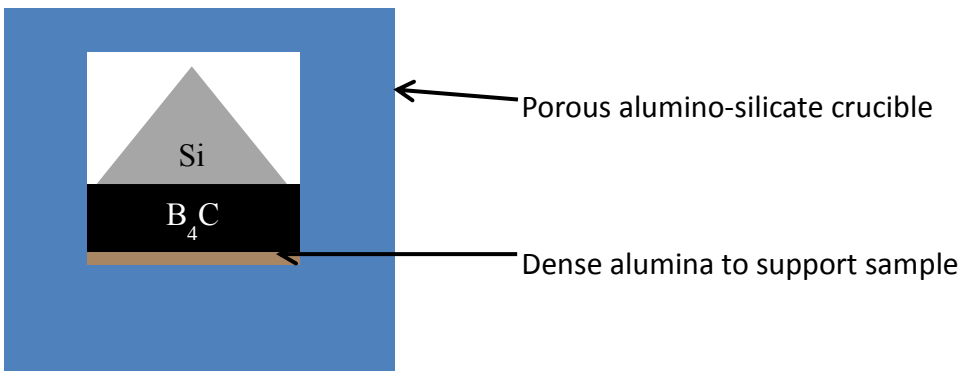

Figure III)7: Scheme of the second type crucible

A-2-2-3 Crucible with silicon carbide beads

The last type of crucible developed during this thesis was a combination of the two previous ones (Cf. figure III)8): -SiC suceptor to facilitate the heating.
-Small space to limit thermal loss.
This type of crucible lasted successfully five or six tests before melting. The susceptor was placed under the boron carbide preform to allow direct contact between each heated part of the crucible. This contact decreases the electric arc energy so it is less disturbing when heating. To prevent the SiC degradation by the accidental contact with liquid silicon, the SiC beads are coated by a boron nitride spray.

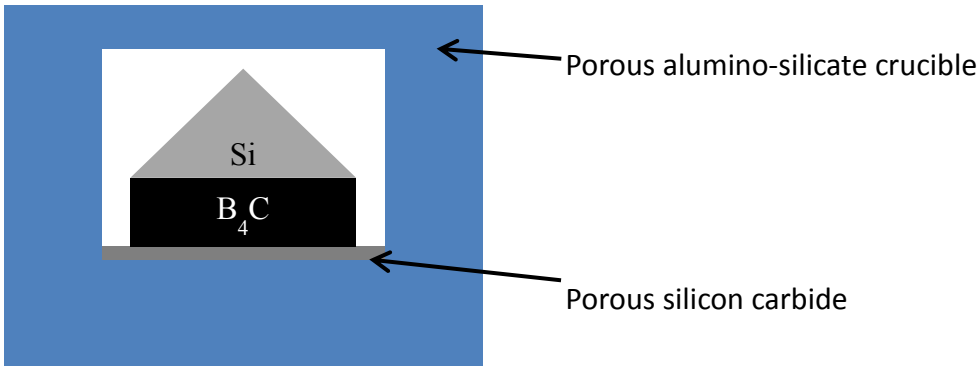

Figure III)8: Scheme of the third type crucible used

To conclude our remarks on the crucible design, some parameters are important to mention:
-The weight of the sample determines the type of crucible that can or should be used.
-The position of the susceptor is essential in the case of multi-material heating because of the electric arcs formation.
-The shape of heated pieces can also provoke electric arc formation because of the peak effect.
The development of a micro-wave crucible has to take account of all these points to be efficient.

Conclusion: By the adjustments we have just described, as to the atmosphere and the configuration of the crucible, we got a procedure that significantly better than at the beginning! In the following part, we illustrate the feasibility of obtaining a RBBC under a microwave field in a 2.45 GHz multimode furnace.

A-3 Feasibility of RBBC process under microwave (preliminary study)

A-3-1 experiments

For these first tests we used 20mm diameter pellets with an open porosity of 13% (Cf. chap II 1-1). Some samples were provided by Ben Gurion University before the beginning of this thesis. These tests were performed under a flow (pressure: 1.4 bar) of Ar/H_2 (10%). This atmosphere provides a heating rate of 10°C/min; the infiltration temperature and dwell time at high temperature and the different observations are described in table 2.
Our tests showed that at high temperature, a certain time is necessary to achieve infiltration (silicon covering the composite was no longer visible, 8 min at 1350°C, as shown chapter III part A-3-1). For those 20mm pellets, this time was 8 minutes: from Si melting to the cooling period or the total infiltration, determined by video analysis. A temperature difference (≈100°C) between the B_4C preform (on which we measured the temperature) and the silicon was observed. Actually, silicon started to melt (1414°C) when boron carbide was at significantly lower temperature, i.e. 1280°C. This difference explains the infiltration of boron carbide observed at "low" temperature: for example, when the preform was at 1330°C. These tests defined basic conditions for permeation in Ar/H_2 atmosphere under microwave heating.

Table III)2 : preliminary study of the RBBC process under microwave

Try	I	II	III
Sample height (mm)	4	7	7
temperature (°C)	1330	1450	1450
Dwell time (min)	0	15	0
Total porosity (%)	18	16	16
Open porosity (%)	-	13	13
from	BGU	EMSE	EMSE
Infiltration	incomplete	complete	incomplete
Temperature on B_4C when Si begins to melt (°C)	1250	1300	1350
Temperature on B_4C when Si melting is achieved (°C)	1309	1375	1410
Electric arcs localization	Between Si and B_4C SiC and SiC	Between Si and SiC Si and B_4C SiC and SiC	Between Si and B_4C SiC and SiC
Infiltration time	2 min	8 min	4 min

The placement of the preform and Si lump is shown in figure III)9 (view across the target hole in the crucible).

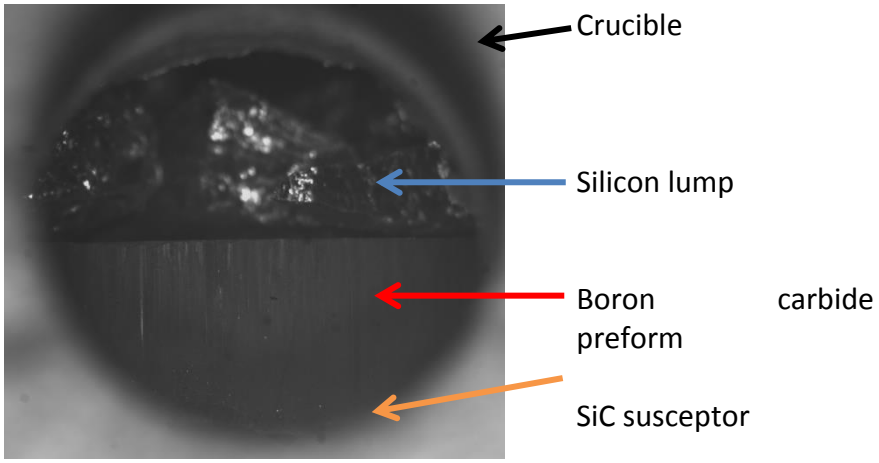

Figure III)9: Crucible disposition

When the infiltration is complete, the final sample is surrounded by a layer of solidified silicon containing precipitates (dark in the figure III)10) probably B12 phase. It is also possible to see a layer (about 50 micrometers) probably of SiC (according to bibliography) on the upper side of the sample which was in direct contact with the silicon during the rise in temperature (Cf. figure III)9).

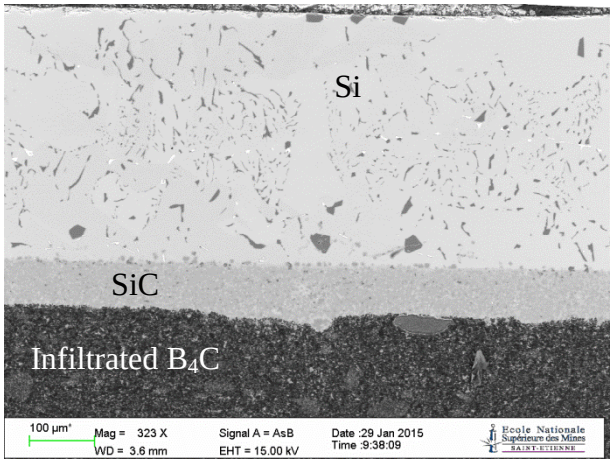

Figure III)10: SEM observation of a partially infiltrated sample I

In figure III)11, it can be seen that the infiltration was not only vertical (combined effect of the gravity and the capillarity) but also horizontal (only capillarity): this horizontal infiltration indicates an excellent affinity between B_4C and the melted silicon. This can also be deduced from the observation in figure III)12: it shows a crack passing through the interfaces rather than along them (delamination), which means that the adhesion of the different phases to one another is extremely strong.

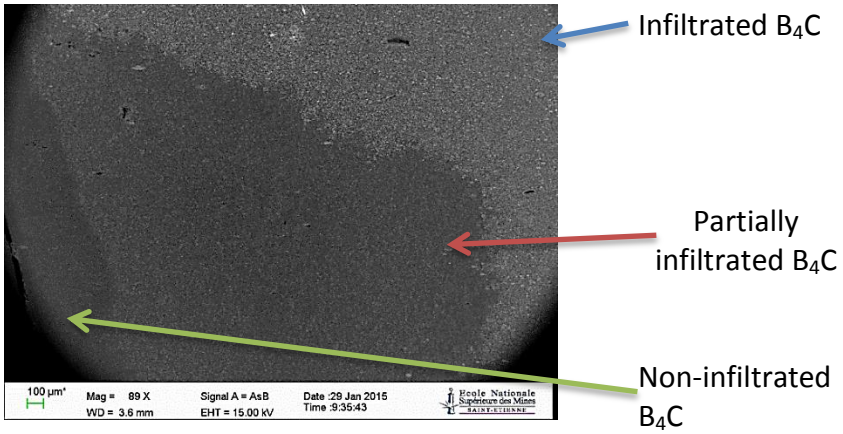

Figure III)11: SEM image (backscattered electron) on the upper right side of the sample I (low magnification)

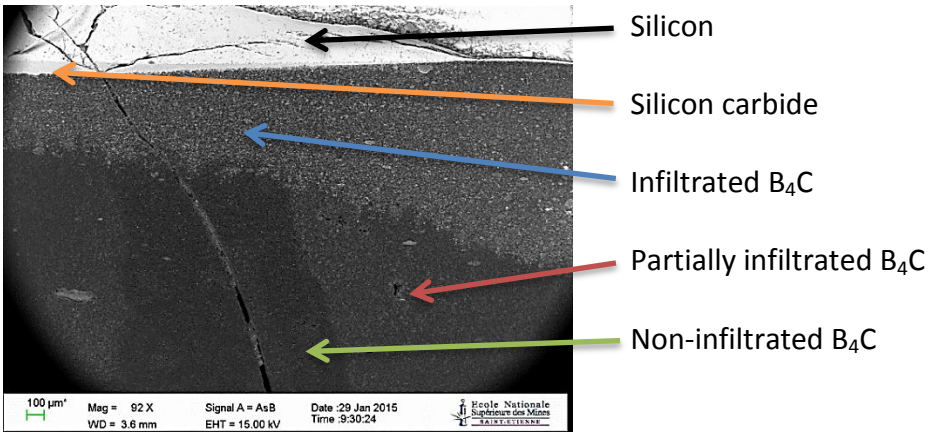

Figure III)12: SEM image (backscattered electron) on the upper side of the sample I (low magnification)

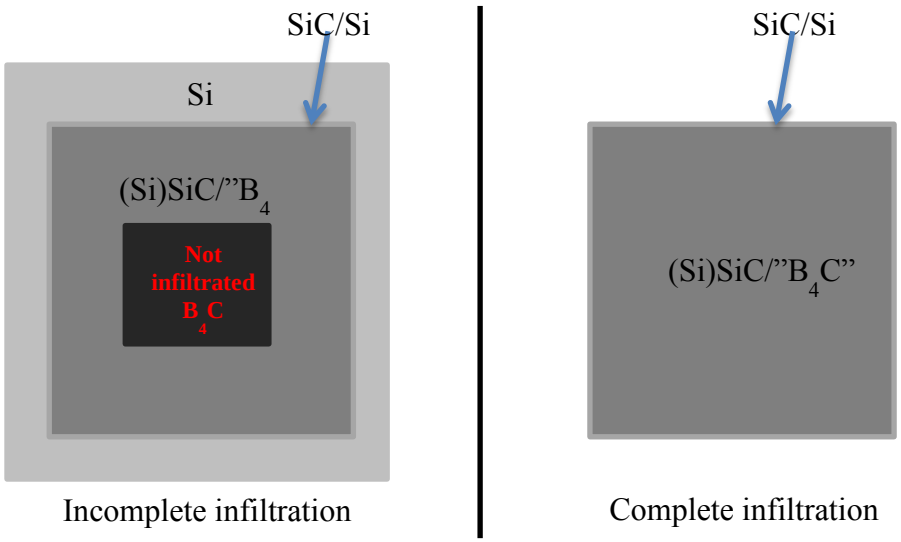

The complete infiltration (figure III)13) can be defined by the preliminary observation. It took 8 min at 1350°C to silicon to fully infiltrate

Figure III)13: Scheme of the difference between complete and incomplete infiltration.

A-3-2 Microstructure

The microstructure of RBBC after MW is shown in figure III)14 and figure III)15. This microstructure is similar to the ones obtained for the conventional RBBC [HAY09t], which consists in four phases, each with different color: black: boron carbide, light black: $B_{12}(B,C,Si)_3$, dark grey: silicon carbide and light grey almost white: residual silicon. Phases identification will be confirmed further in part B by XRD analysis.
Moreover, the microstructure seems to be different after a thermal treatment in microwaves furnace than in conventional furnace, as described above (Cf. chap I 2-6). Indeed, silicon carbide seems to be smaller after a microwave treatment. SiC particles are some hundreds nanometers of length. At this stage the reasons of this divergence is not understood yet, and has to be investigated further.

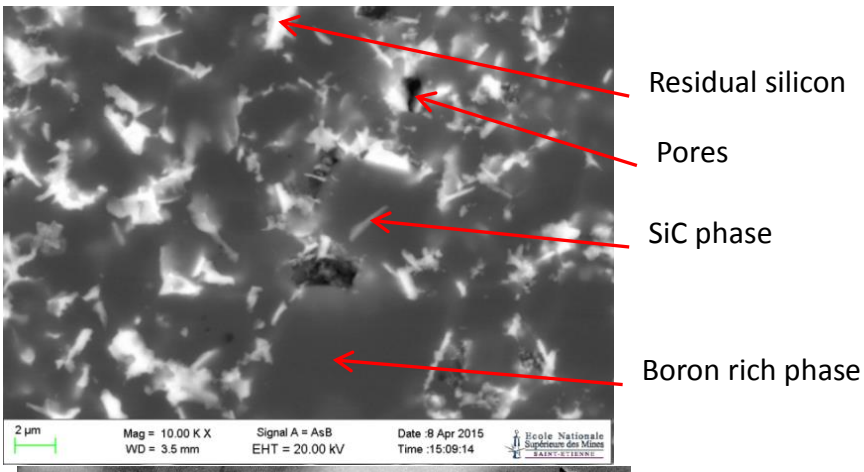

Figure III)14: Microstructure (SEM image) of the composite II. (Backscattered electron detector).

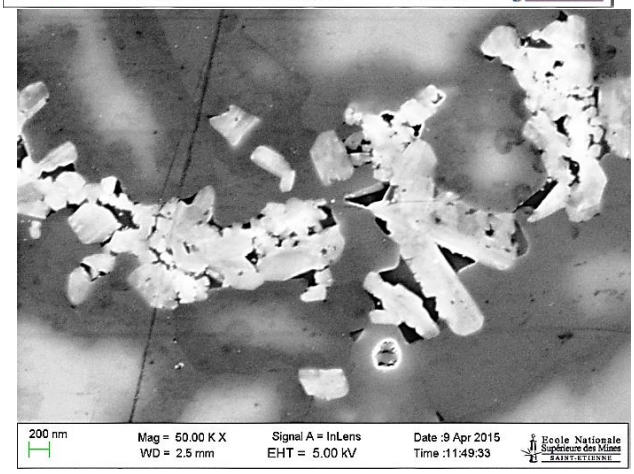

Figure III)15: Microstructure (SEM image) of the composite II Inlens detector (Secondary electron detector).

Energy-dispersive X-ray spectroscopy (EDS) analysis was done by Matthieu Lenci and Sergio Sao-Jao on the Focus Ion-Bean (FIB) device for the first test (Cf. figure III)16). Their results proved that residual silicon can be close to boron rich phase and SiC. Silicon carbide precipitates in the liquid and its growth follows several directions.

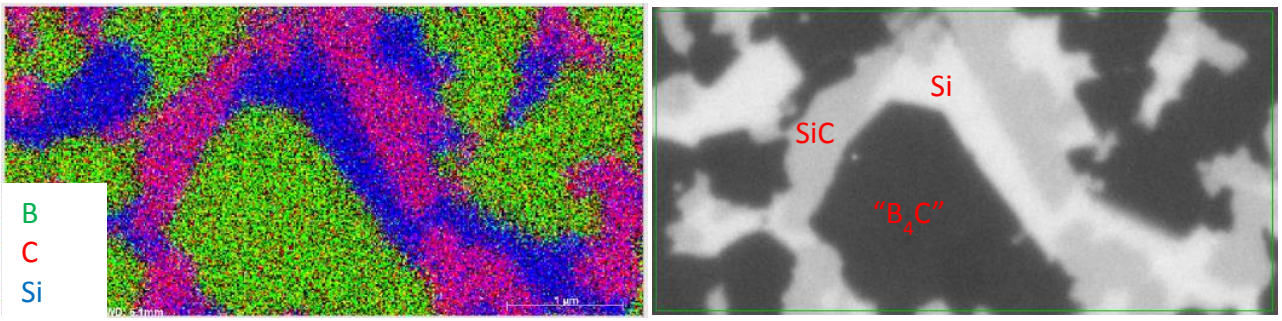

Figure III)16: EDX analysis and SEM picture of the composite II

Conclusion Part A

The microwave technique was challenging to adapt to this way of composite preparation because of the atmosphere, multi-material heating, and high temperature heat treatment. Nevertheless, in despite of these difficulties, these preliminary tests demonstrate that it is possible to synthesize RBBC under a microwave field. Our next step is to study the influence of the process parameters to optimize the reaction and the mechanical properties of the final product.

Part B: Parametric study

After the adjustment of the technological parameters (crucible, susceptor and atmosphere) and showing the possibility of obtaining RBBC by microwave heating, we will explored the influence of the process parameters on the reactivity of the system and the mechanical properties of the final composite.
First infiltration tests and literature showed us some influential parameters. We can divide them in three families of parameters:

- ✓ Preforms:

- With and without addition of free carbon in the preform. The influence of the free carbon additives was studied in some publications [HAY06, THU13, WAN14, HAY10a, WU12, HAY10b, ZHA14a, BAR13, ZHA14b] and authors showed that the direct reaction of silicon and boron carbide in absence of free carbon provides to the best mechanical properties. So to obtain adequate hardness, no free carbon was used for the parametric study. Some additions of SiC are also possible: specifically micro-wave heating (Cf. Chap. III part.A) the usefulness of this phase as susceptor was shown. It is possible that an adding of SiC in the initial powder could play the same role, in situ, in the composite during the process.
- Porosity: in the range 15-45% was chosen, to compare our results with those, previously, obtained in BGU.
- Sintering: depending on the intended porosity samples were pre-sintered or not, that may have an influence on the properties of the final composite

- ✓ Silicon:

-The quantity of silicon was adjusted to fill the porosity preforms (plus an excess of 10wt% for the first tests, then an excess of 20wt%). The silicon physical form (lump) and purity (98.5%) were set, in order to compare with composites obtained in BGU.

- ✓ Heating process:

- Heating methods: microwaves versus conventional furnaces: to compare between them to elaborate RBBC will be presented in the next section. Here few tests with a 915 MHz generator are described. As mentioned in the bibliographic review, the generator's frequency modulates the wave's penetration depth. This type of generator is also interesting for the heat treatment of large pieces.
- Atmosphere (Ar/H_2): we previously described the technical limitation linked to the interaction between atmosphere and microwave field (plasma, sparks…). Therefore, this parameter was selected.
-Cycle (temperature, heating rate, dwell time): the influence of the temperature and dwell time was studied. The heating rate is fixed at 10°C/min, to limit the maximum incident power lower than 1700W, due to the plasmogenic effect of the gas; the cooling rate could influence internal stresses, but was not within the scope of this research.

First, we will show the influence of some parameters linked with the preform, as the pre-sintering step. Second, the respective influence of the temperature and dwell time will be described; there exists probably some interactions between preform porosity parameters and heat treatment temperature; we will discuss of this two parameters together with one of the adapted experimental designs. Finally, the feasibility of this process in microwave furnace heating at a frequency of 915MHz will be demonstrated. We focus on the phase analysis, microstructure, mechanical properties as the hardness, Young modulus, flexural strength (three point bending test), and the toughness characterized by the critical stress intensity factor in mode I. All characterization methods was described in chapter II.

B-1 Theoretical composition of the composite

In this parametric study, the used preforms are of different pores. Therefore, it will be difficult to compare phase composition by considering the final composition because the carbon content available is different. Moreover, in most case, this content does not offer a complete reaction. Consequently, we suggest determining the theoretical composition for each type of preform.

This theoretical maximum composition is calculated taking into account the chemical formula of the B_{12} phase: $B_{12}C_{1.99}Si_{0.037,}$ determined by Hayun in his PhD thesis [HAY09t].

From this formula, one can calculate the carbon released by the transformation of B_4C to B_{12}:

$$3B_4C_{(s)}+0.037Si_{(l)}\rightarrow B_{12}C_{1.99}Si_{0.037(s)}+1.01C_{(s)}$$

From our calculation, we stipulated the amount of carbon that limits the reaction.

To simplify: 3 moles of boron carbide release 1 mole of carbon. Most of samples had an initial mass of 10g of boron carbide. We used this value to calculate the carbon released by solid solution formation. So, the maximum freed carbon can be calculated, if we postulate that all boron carbide is transformed into B_{12}: 0.06 moles. In the initial powder there is still carbon remaining (4 wt.% value from the supplier), corresponding to 0.03mole of free carbon in the preform. Note: the maximum available carbon is 0.09 moles and, the maximum amount of SiC is 0.09 moles which corresponds to $1.12cm^3$.

Subsequently from these values, the theoretical chemical composition can be calculated (Table III)3).

Table III)3: Theoretical chemical composition of composites from preforms with different initial porosity amounts

Initial density (%TD)	Initial porosity (Vol.%)	Vol.% SiC	Vol.% $B_{12}(B,C,Si)_3$	Vol.% Si
56	44	15,84	55,68	28,48
60	40	16,96	59,64	23,40
61	39	17,24	60,63	22,13
62	38	17,53	61,61	20,86
65	35	18,37	64,57	17,06
66	34	18,65	65,56	15,79
67	33	18,93	66,55	14,52
70	30	19,77	69,51	10,72
71	29	20,05	70,49	9,46
72	28	20,33	71,48	8,19
73	27	20,61	72,46	6,92
74	26	20,89	73,45	5,66
76	24	21,45	75,42	3,13
77	23	21,73	76,40	1,86
79	21	22,29	78,37	-0,66

Comment on the Figure III)17

As explained above, in the system, the amount of carbon released by B_4C, or present as impurity, is limited. Thus, there is a threshold of porosity (hence proportion of silicon relative to the boron carbide at the beginning of the reaction) beyond which silicon will remain in the composite at the end of the reaction. The threshold is 21.5 vol.%, which is lower than the selected pores quantities. The final composites will therefore contain silicon, the proportion of which increases with the initial porosity. If the reaction is complete, the percentage of silicon carbide is about 20 vol.%, and varies little with the initial porosity. All the results will be discussed in function of their corresponding theoretical composition.

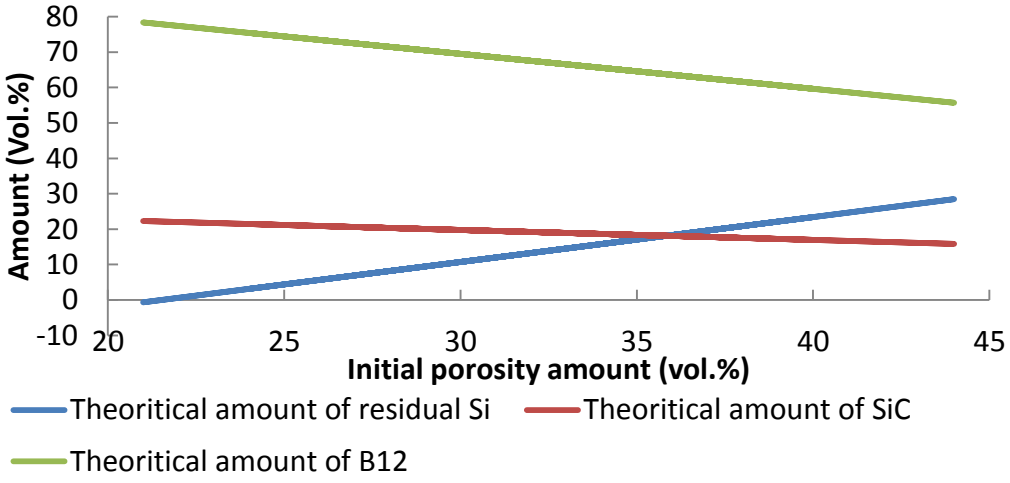

Figure III)17: The changes of final composition with increasing of the initial porosity

The degrees of transformation were calculated for three phases:

- SiC formation:

$$\alpha_{SiC} = \frac{SiC_{real}}{SiC_{th}} \qquad \text{Equ.17}$$

-transformation of B_4C into $B_{12}(B, C, Si)_3$:

$$\alpha_{B12} = \frac{B_{12real}}{B_{12th}} \qquad \text{Equ.18}$$

- disappearance of Si:

$$\alpha_{Si} = \frac{Si_{real} - P_{ini}}{Si_{th} - P_{ini}} \qquad \text{Equ.19}$$

With -X_{real} the amount of the X phase determined by XRD and etching technique

-X_{th} the amount of the X phase if the reaction reached the maximum and limiting by the amount of carbon

-P_{ini} the porosity percentage of the preform

For this, we will use the amount of B_{12} obtained by combining XRD results with chemical removing of silicon (chap II)2-3-4).

B-2 Parametric studies: preform parameters

Influence of sintering of initial preform.

Samples pressed from powder with a monomodal particle distribution (Cf. chapter II 1-1) were used for RBBC process. Their behavior is compared to that of non-sintered preforms with the same density: about 30%. To obtain this density with any densification by sintering, Hayun et al. used a mixture of powders, chosen in order to obtain a multimodal particle distribution: they were composed of 42w% of B_4C powder with mean size of 130µm, 32w% of 70µm and 26w% of 1µm [HAY09a]. In that case, the silicon excess was about 20w%. The multimodal and monomodal samples will be noted as Mm & mm, respectively.

Table III)4: XRD combined with chemical etching results for multimodal and monomodal composites (error : ±2 vol.%)

Samples	B_4C (vol%)	Si (vol%)	SiC (vol%)	B_{12} (vol%)
MW-1450°C-30%-15min-Mm	13	15	4.7	67
MW-1450°C-33%-15min-mm	11	26	12	50
MW-1400°C-27%-60min-mm	3	12	12	73
MW-1400°C-28%-5min-mm	2	14	12	72

The composition (Table III)4)) given by the XRD analysis associated with chemical etching for Mm sample doesn't correspond with the other microwave heated samples. This is probably due to residual porosity of the sample. Undeniably, if it remains porous there has to be less silicon than expected in the sample.

The figure III)18 shows microstructure for multimodal sample and one monomodal pre-sintered sample. As expected, monomodal samples have a finer microstructure than multimodal sample. The microstructure of the monomodal sample is more homogeneous as well. The monomodal sample presented here was infiltrated with low silicon over-weight (10wt.%), whereas the multimodal sample was permeated with a silicon over-weight of 20wt.% compared to the calculated amount of silicon necessary to complete infiltration. The higher porosity observed here, probably, came from two distinct causes:

-For the multimodal, higher porosity is probably due to a particles displacement during the infiltration step.

-For the monomodal, increased porosity is probably due to a lack of silicon from evaporation or oxidation during infiltration step, because later permeated samples with 20wt% of silicon surplus are fully infiltrated without residual porosity.

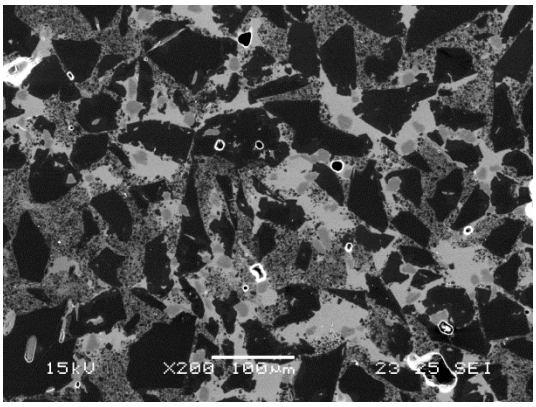

a) MW-1450°C-30%-15min-Mm

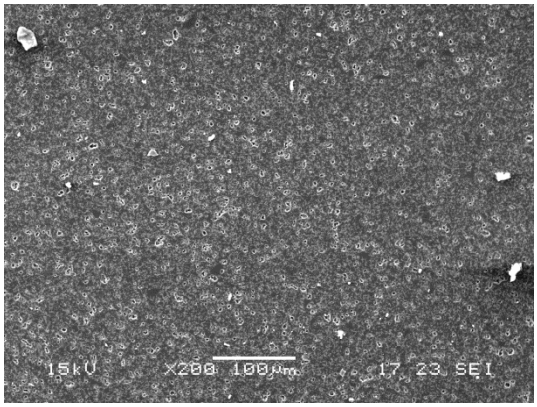

b) MW-1450°C-33%-15min-mm

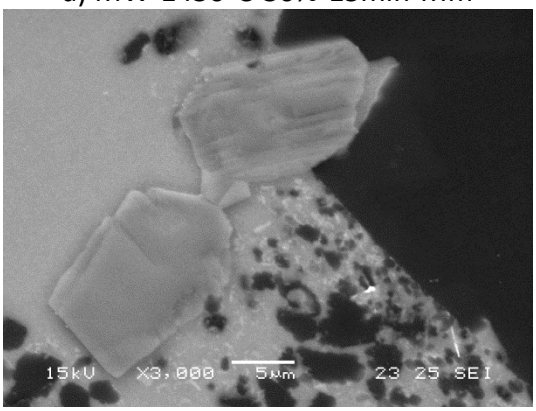

c) MW-1450°C-30%-15min-Mm

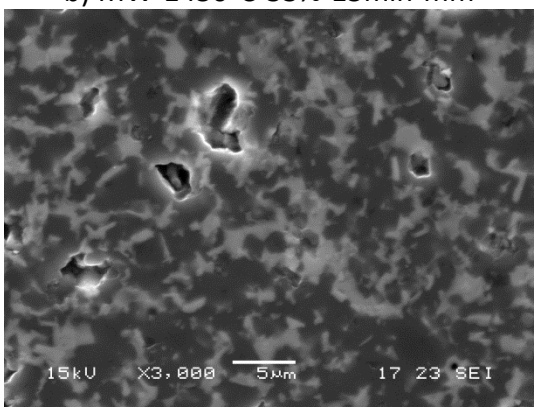

d) MW-1450°C-33%-15min-mm

Figure III)18: Microstructure comparison between multimodal sample and monomodal sample obtained with similar MW conditions

The reaction products are influenced by the size of the initial powder grains (and probably the sample heterogeneity).

Indeed, in the case of multimodal sample, some large (32µm) SiC structure are present, whereas for monomodal finer initial grains the obtained silicon carbide grain is about 1µm.

Table III)5: Properties of monomodal pre-sintered samples and a multimodal sample

Sample	Density (g/cm3)	Hardness (GPa)	Shear modulus (±3GPa)	Young Modulus (±5GPa)	Poisson coefficient
MW-1450°C-30%-15min-Mm	2.43	15.9±3	142.5	322	0.13
MW-1400°C-27%-60min-mm	2.59	17.9±0.4	166.25	396	0.18
MW-1400°C-28%-5min-mm	2.56	18.1±0.4	152	364	0.19

The properties (Table III)5) for the multimodal sample are slightly lower than pre-sintered samples. This is probably owing to the fact there are no bonds between boron carbide particles so they can spread out.

Conclusion: In our case, the pre-sintering step seems imperative because composite obtained without a pre-sintering step have lower mechanical properties than those obtained with a pre-sintering step. Furthermore, density is lower with multimodal powder than for monomodal because of the grains' reorganization during the infiltration. Nonetheless, Hayun [HAY09t] shown that pre-sintering step is not so crucial; this difference probably came from residual porosity in our case. In all cases, multimodal samples are less homogenous than monomodal. That is unfavorable to the final properties.

B-3 Parametric study: Thermal cycle parameters

B-3-1 Dwell temperature

Our aim was to see the influence of the temperature, with no dwell duration, on the final microstructure, composition and mechanical properties.

Samples (diameter 35mm, height 5mm, porosity 38-39%) were heated between 1300°C-1500°C

- 1300°C: the silicon didn't start to melt so the preform was not infiltrated.
- 1350°C: some silicon covered preform, so silicon partially melted and preform was partially infiltrated. There are some infiltrated areas and some non-infiltrated areas distributed in the piece (figure III)19).
- 1400°C and 1500°C: permeation was complete (total melting of silicon and no more silicon visible outside of the preform). Figure III)19 a) shows also that silicon didn't follow a simple path form the top to bottom to infiltrate the preform. Melted silicon starts to enter into the piece by smallest pores then it fills a larger one.

In the sample treated at 1400°C (figure III)19 b) there is a large residual silicon area probably due to initial microstructure heterogeneity.

The sample treated at 1500°C figure III)19 c) presents some residual porosity.

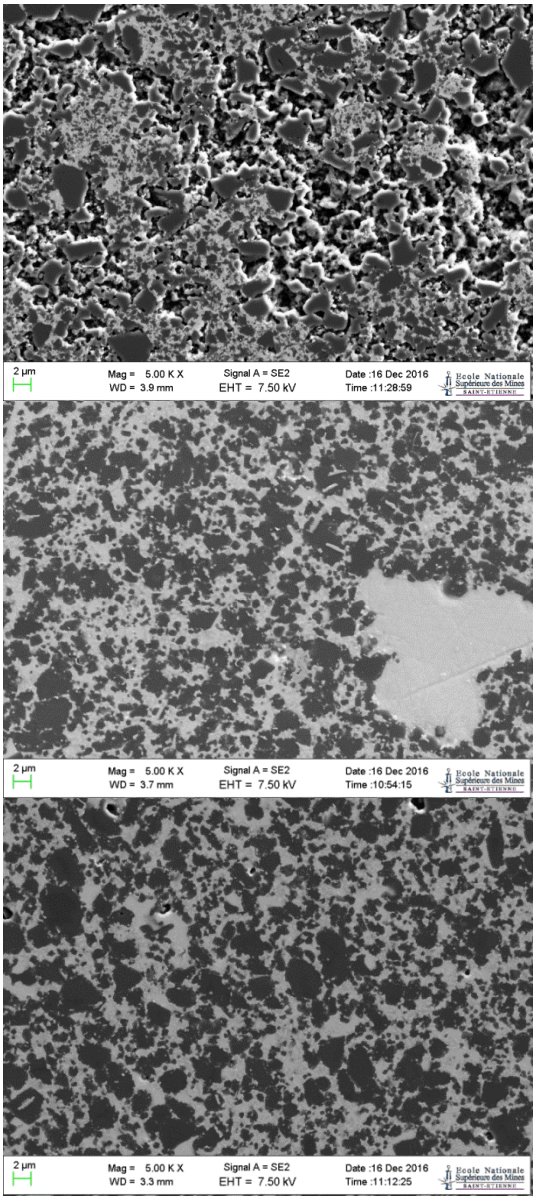

a)1350°C

b)1400°C

c)1500°C

Figure III)19: Microstructure of samples treated at different temperatures (no dwell time).

Comparing each microstructure of the samples and corresponding procedure suggests that a dwell period is needed for a temperature lower than 1400°C to obtain a full infiltrated composite.

Table III)6: XRD analysis of composites obtained at different temperatures (no dwell time)

Error: ±2 vol.%

Samples	B_4C (vol%)	Si (vol%)	SiC (vol%)	B12 (vol%)	B_4C+B12(vol%)
1350°C-38%	5	22	11	62	66
1400°C-39%	3	30	10	56	59
1500°C-38%	6	28	10	55	61

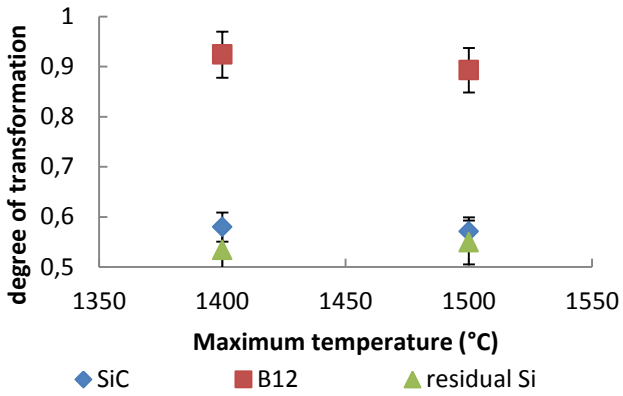

Figure III)20: the evolution of the degree of transformation for two maximum temperatures for each phase

In the table III)6 and the fig III)20, the evolution of the composite's composition with the maximum temperature can be observed. For the 1350°C-40% sample the quantitative results can't be discussed because of the incomplete infiltration but even at this low temperature some reaction occurs, leading to SiC and B_{12} formation. The samples heated at 1400°C and 1500°C present almost the same composition, a maximum of 6 vol.% is observed for residual B_4C. This suggests that as soon as the infiltration is possible, the formation of the B_4C/SiC solid solution as well as the precipitation of the silicon carbide in the melted silicon, are carried out rapidly. It has to be noted that it takes only 10min to increase from 1400 up to 1500°C; this may not be enough time to see any real difference.

The mechanical properties of only fully infiltrated samples (1400°C and 1500°C) were studied (Table III)7).

Table III)7: Properties of samples treated without dwell time

Samples	Density (±0.01g/cm$_3$)	Hardness (GPa)	Young modulus (±5GPa)	Poisson coefficient (±0.02)	Shear modulus (±3GPa)	Toughness (MPa.m^{½})
1400°C-38.2%	2.56	14.8±0.4	344	0.19	143.5	2.16±0.22
1500°C-38%	2.56	13.8±3	334	0.2	139	2.62±0.11

Except for toughness, there are no differences between samples heated at 1400°C and 1500°C. Both hardness properties are modest, linked to the high amount of residual silicon.

Conclusion

From these tests, the precise temperature (measured on boron carbide) for which silicon starts to melt is 1350°C. Without dwell time, a minimum of 1400°C has to be reached to obtain a complete infiltration. For lower temperatures, a dwell time is necessary to obtain complete infiltration. However, the reaction between silicon and boron carbide starts at low temperature: even when boron carbide is at 1350°C, silicon carbide and B_{12} appear.

Under these conditions, the temperature (with no dwell time) has a poor influence on the final composite composition, microstructure, and mechanical properties (except toughness).

B-3-2 Isothermal study: influence of the dwell time.

As seen in the previous paragraph, the reaction of SiC formation starts since silicon melts and infiltrates in the preforms. Now the study of the influence of dwell time on the composite development will be demonstrated.

The heating rate of 10°C/min (to avoid plasma formation), was again selected. All samples were fully infiltrated.

Except for some heterogeneous zones in samples, the microstructures seem to be independent of the dwell time. In figure III)21 a) there are two large boron rich heaps (>10µm, left middle and a smaller bottom right Figure III)21 a) with some non-infiltrated residual porosity inside, this type of cluster was probably obtained during the sintering step by heterogeneous densification. Remember, the color of the four phases: black for boron carbide, light black for $B_{12}(B,C,Si)_3$, dark grey for silicon carbide and light grey almost white for residual silicon.

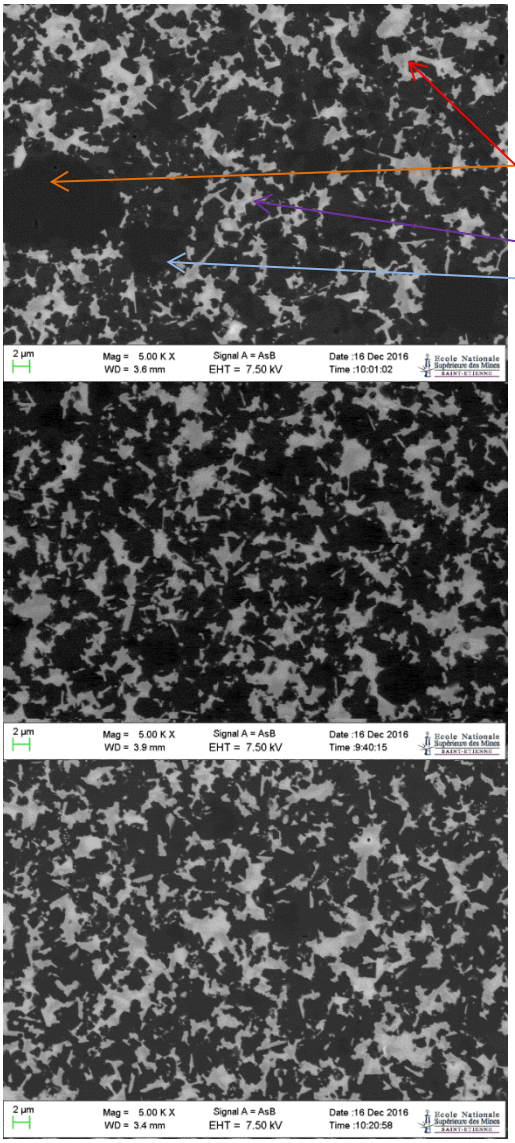

Figure III)21: Microstructure of isothermal samples with differing dwell times at 1400-1450°C

Table III)8 shows the three composites' compositions obtained, and fig III)22 the degree of transformations. It appears that boron carbide transformation in $B_{12}(B,C,Si)_3$ solid solution is fast, because the B_4C residual amount is low in all cases. However, the amount of silicon decreases and that of SiC slightly increases with time. The reaction is very fast at the beginning of the infiltration then very slow, and it is function of the available carbon in the system:

- The first step is the consumption of the free carbon and that provided by the transformation of the boron carbide into the solid solution $B_{12}(B, C, Si)_3$ [HAY09b],
- After these reactions the carbon intake is probably due to its diffusion through the B_{12} solid solution, a slow and limited phenomenon.

Table III)8: Influence of dwell time on the composite composition (XRD)

Error: ±2 vol.%

Samples	B_4C (vol%)	Si (vol%)	SiC (vol%)	B12 (vol%)	B_4C+B12(vol%)
5min-29%	2	14	12	72	74
60min-27%	3	12	12	73	76
120min-29%	2	9	13	75	77

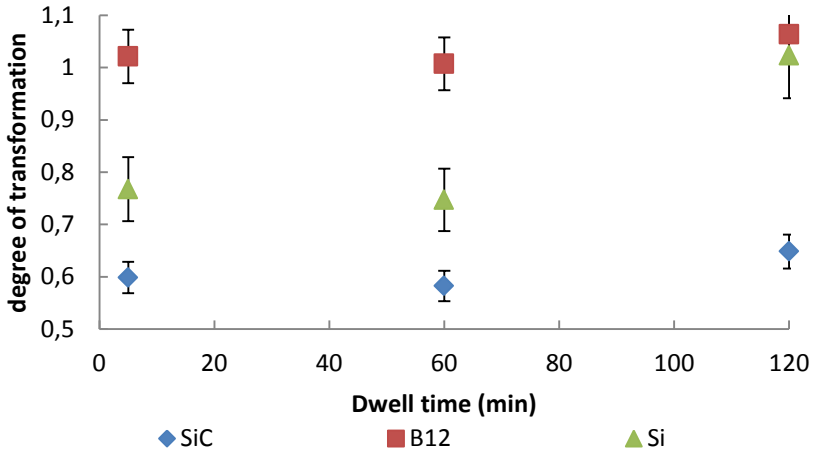

Figure III)22: Evolution of the degree of transformations with the dwell time

In figure III)22 degree of transformation of B12 formation is considered equal to 1 taking into account the measurement errors.

Table III)9: Influence of dwell time on the composite properties

Samples	Density (±0.01g/cm3)	Young modulus (±5 GPa)	Hardness (GPa)	Poisson coefficient (±0.02)	Shear modulus (±3GPa)	Toughness ($MPa.m^{1/2}$)
5min-29%	2.56	364	18.1±0.4	0.19	152	2.69±0.25
60min-27%	2.59	396	17.9±0.4	0.18	166.25	2.68±0.25
120min-29%	2.57	382	18.2±0.7	0.19	160	3.1±0.58

Conclusion

The SiC formation reaction reaches quickly a quasi-steady state, and then the diffusion of needed carbon is very slow. So, from the two previous studies (anisothermal and isothermal) it can be concluded that reaction is weakly influenced by dwell time or maximum temperature when infiltration is complete for small (1µm) boron carbide initial particles.
Next, dwell time will be fixed at 15min, to have enough time for the infiltration step.

We study further two possible dependent parameters: temperature and initial porosity. Indeed, if the reaction quickly reached a maximum, then this could depend on the quantity of silicon (the preforms initial porosity percentage).

B-4 Parametric study: porosity of the preform and temperature of microwave treatment

The effect of two major parameters (initial porosity and dwell temperature,) on final mechanical properties and microstructures were investigated. First the experimental design will be presented. Second results will be exposed and modeled.

B-4-1 Presentation

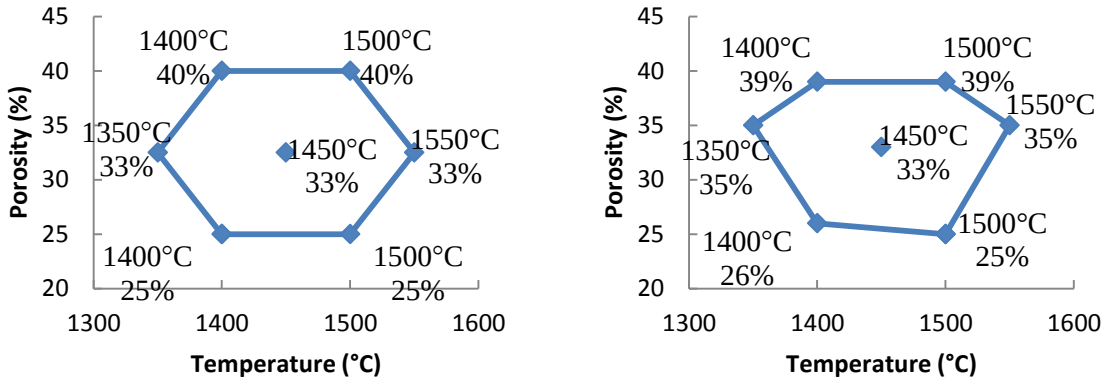

a) Theoretical design of experiment b) Actual design of experiment

Fig III)23 : Influence of both porosity and temperature : experimental design

Based on previous results, we designed a two dimensional parametric study, to model hardness values, with a second-degree polynomial equation, on the two dimensions: dwell temperature and initial porosity experimental domain. This modeling allows, knowing optimum experimental conditions, to obtain a high hardness. The Doehlert experimental design (Cf. figure III)23) consists in the combination of three initial porosities and five dwell temperatures. Figure III)23 a) shows the theoretical design of experiment proposed by Doehlert. Figure III)23 b) shows the current design of experiment. Naturally, the modeling calculations will be made with the actual values. This type of design needs 7 points and two parameters. The limits of the studied field were chosen after the preliminary tests (low limit: 1350°C) and not upper than the studied temperature in conventional furnaces (upper limit: 1600°C). Indeed, in [ZHA14a] authors show that a too high temperature is deleterious for mechanical properties, so the temperature of 1550°C was selected. Porosity values were 25, 33/35 and 39%. The elaboration of the sample was described in chap. II.

Nota bene: samples containing 39% porosity were not sintered. Samples were infiltrated with a slight overload of silicon (10wt.%).

B-4-2 Results

Our first observation was that even at low temperature (1350°C), samples were completely infiltrated when dwell time was reached. This remark confirms previous results: since as silicon melts it quickly infiltrates the preform.

B-4-2-1 Composite Volume Variation

The volume variations (VV), (figure III)24), are in general relatively low, except for one sample with an initial porosity of 25%. Such result was curious! For the high porous no-sintered preforms the volume variation is also high (ΔV/V≈5%), which is normal. These high porosity samples (the highest two points) were observed at low magnification and presented a large heterogeneity (Cf. figure III)25) between infiltrated areas and no-infiltrated areas. All samples were pressed from fine powder. Therefore, it is possible that the preforms were already heterogeneous. During the RBBC process, no-sintered preform has weaker cohesion than pre-sintered samples; they can swell or shrink that explains the observed volume variation. That confirms the benefit of the preforms sintering. Despite of the observation of some aberrances, these samples were able to be characterized: XRD and hardness (indentations were made in infiltrated area). Evidently, the results for those composites have to be taken with a grain of salt.

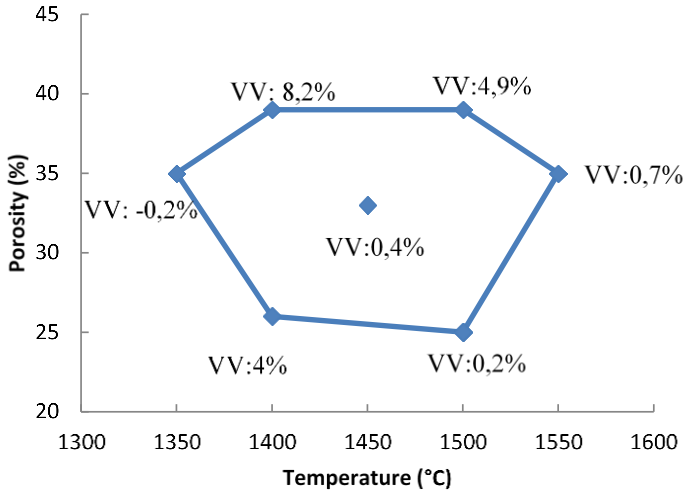

Figure III)24: Volume variation reported on the experimental graph

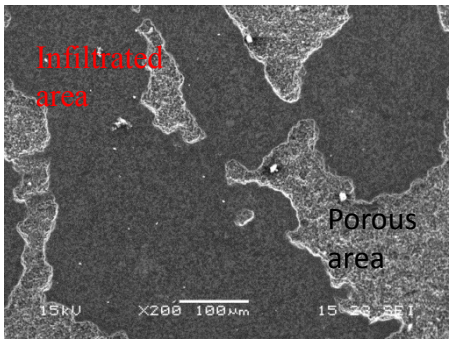

Figure III)25: Low magnification SEM picture (Secondary electron detector) of sample obtained from preform with about 40% porosity (non-pre-sintered)

B-4-2-2 Microstructure

Pre-sintered samples microstructure is homogenous but some residual porosity remains (Cf. figure III)26, that shows the microstructure for extremum temperatures for each initial porosity samples).

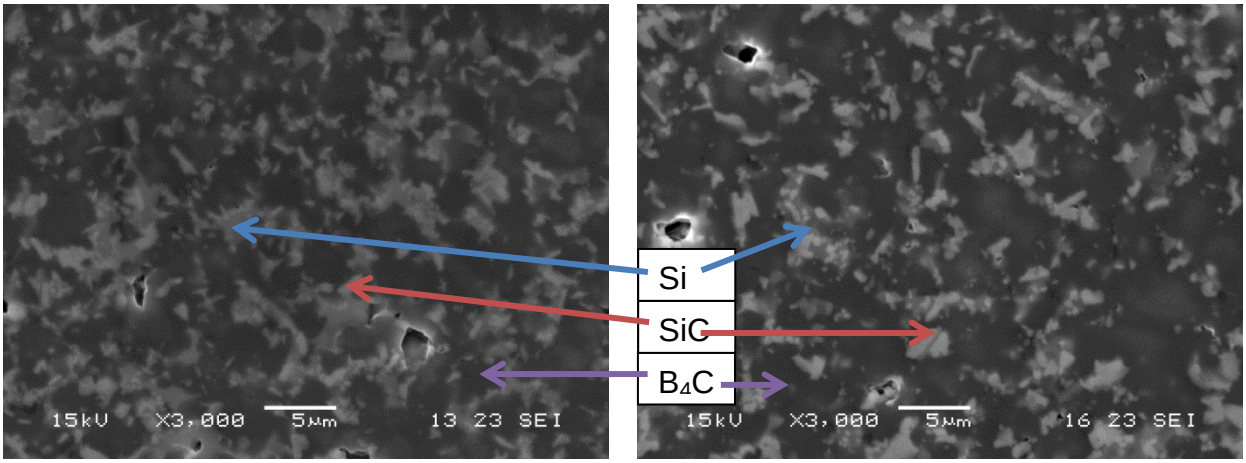

a)MW-26%-1400°C b)MW-25%-1500°C

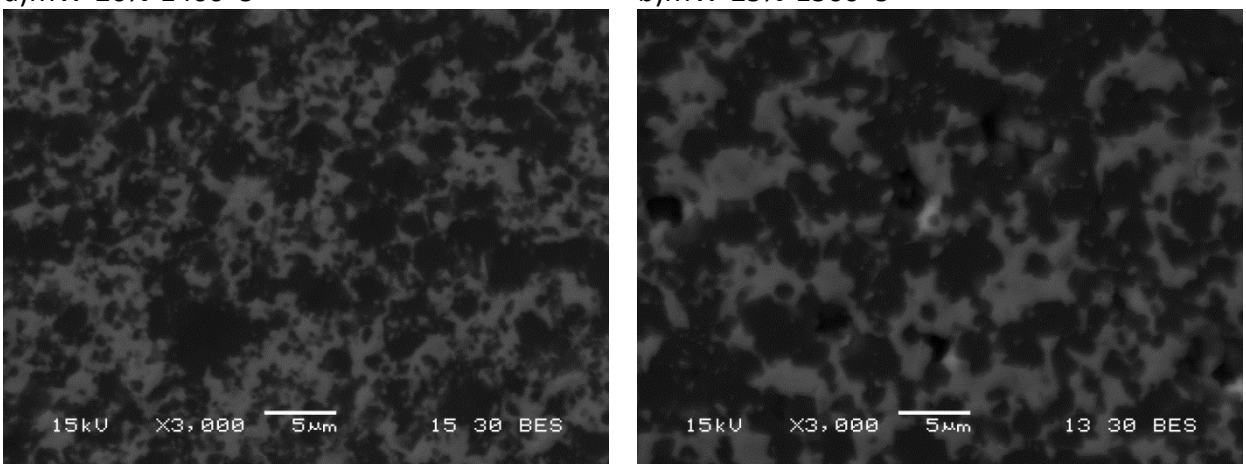

c)MW-35%-1350°C d)MW-35%-1550°C

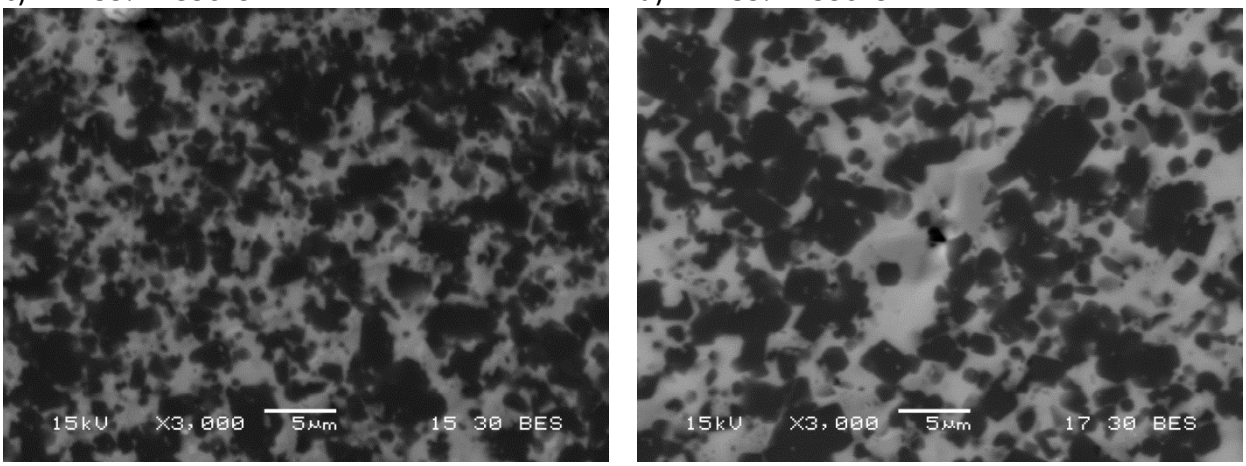

e)MW-39%-1400°C f)MW-39%-1500°C

Figure III)26: Microstructure observation by SEM
of composites prepared via microwave process

Porosity was systematically present in these samples; this could be due to slight silicon evaporation and/or a silicon oxidation. We used the combined method (XRD analysis and acid bath to remove silicon) to determine the composite composition (Cf. chap. II 2-3-4).

All samples present phases: "B_4C" areas in black, the residual silicon sectors in dark grey and the small needles of previously observed SiC in light grey. Silicon carbide is less visible on the 40% samples' micrograph, because they are probably drowned in residual silicon.

B-4-2-3 Composition of the samples

Table III)10 shows the volume composition of different samples, and figure III)27 the degree of transformations.

Table III)10: Composite compositions for different initial porosity and maximum temperature; error : ±2 vol.%

Sample	Si (vol. %)	B_4C (vol. %)	SiC (vol. %)	B_{12} (vol. %)
25%-1500°C	5	5	14	76
26%-1400°C	7	14	11	68
35%-1550°C	23	0	12	64
33%-1450°C	26	11	12	50
35%-1350°C	24	9	11	55
39%-1500°C	27	2	10	59
39%-1400°C	25	4	12	57

For all samples, the SiC formation reaction is partial, the degree of transformation (Cf. figure III)27) of SiC formation varies from 0.5 to 0.7. There remains some untransformed silicon throughout, but the disappearance rate is high for the composites derived from preform with the lowest porosity. The $B_{12}(B,C,Si)_3$ solid solution is generated in the same time in great quantities and it replaces almost completely the boron carbide. It is somewhat surprising to obtain a degree of transformation of SiC formation so low, when the proportion of silicon and B_4C decrease greatly. We believe that the theoretical level of SiC that can be obtained is distorted by several uncertainties on the:

- determination of the chemical composition,
- composition of the solid solution, silicon consumption was ignored in the theoretical calculation. If the B_{12} formula is different, then the silicon is consumed by a reaction other than silicon carbide formation,
- carbon content in the initial powder,
- volume variation and density of the B12 phase.

All these possibilities could explain why the maximum amount of obtained SiC in the final composite is not as high as that provided in our calculations. Despite this uncertainty, it is evident and verified that a low initial porosity achieves the best transformation rate.

If those samples from very porous and non-sintered preforms are not taken into account, it can be noticed that temperature does have slight positive effect on the progress of the reaction.

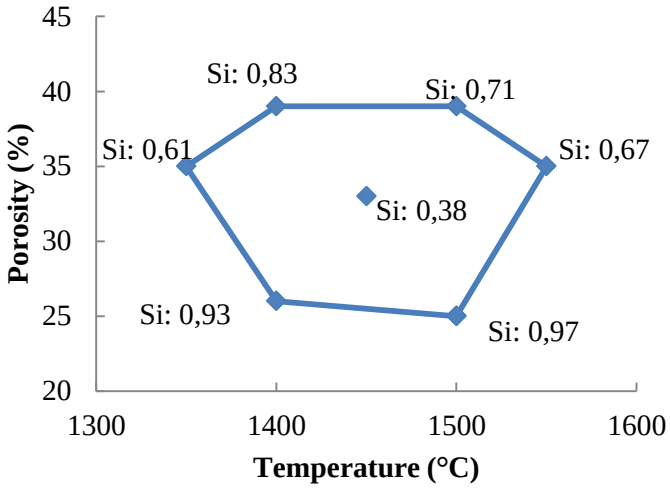

a) disappearance of silicon rate

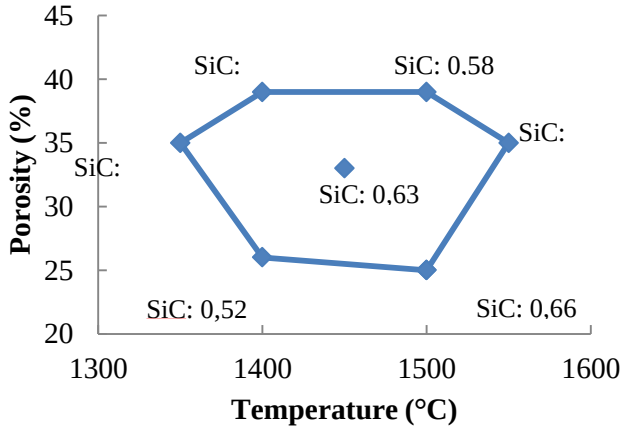

b) silicon carbide formation rate

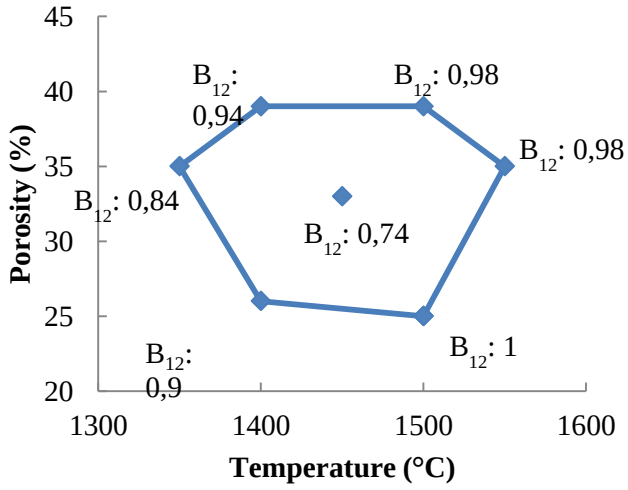

c) $B_{12}(B,C,Si)_3$ formation rate

Figure III)27: Degree of transformation of each phase:
appearance or disappearance from the reaction between Si and B_4C.

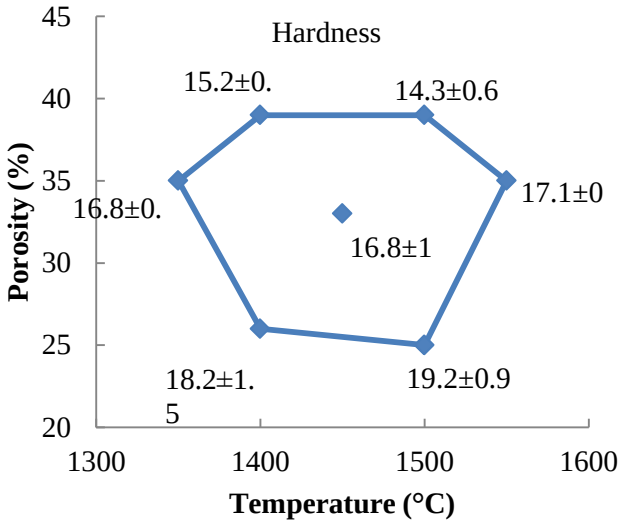

Table III)28: Composite hardness plotted on the experimental domain

The figure III)28 groups the hardness results. The dwell temperature for a given initial density weakly influences these results. Measured hardness was high and in accordance with literature data (2300 Hv for low porosity samples). Nemrodw software was used for modeling the influence of dwell temperature and initial density on the composite hardness. Figure III)29 shows the result with a) the two dimensional representation in blue the iso-hardness lines and b) the three dimensional representation in red the highest hardness values and in purple the lowest. These illustrations confirm the low influence of the maximum temperature on the hardness as compared to the impact of the initial porosity. The 2D representation shows that the influence of the initial porosity increases when initial porosity decreases. This is explained by the decrease in the distance between iso-hardness lines for low porosity.

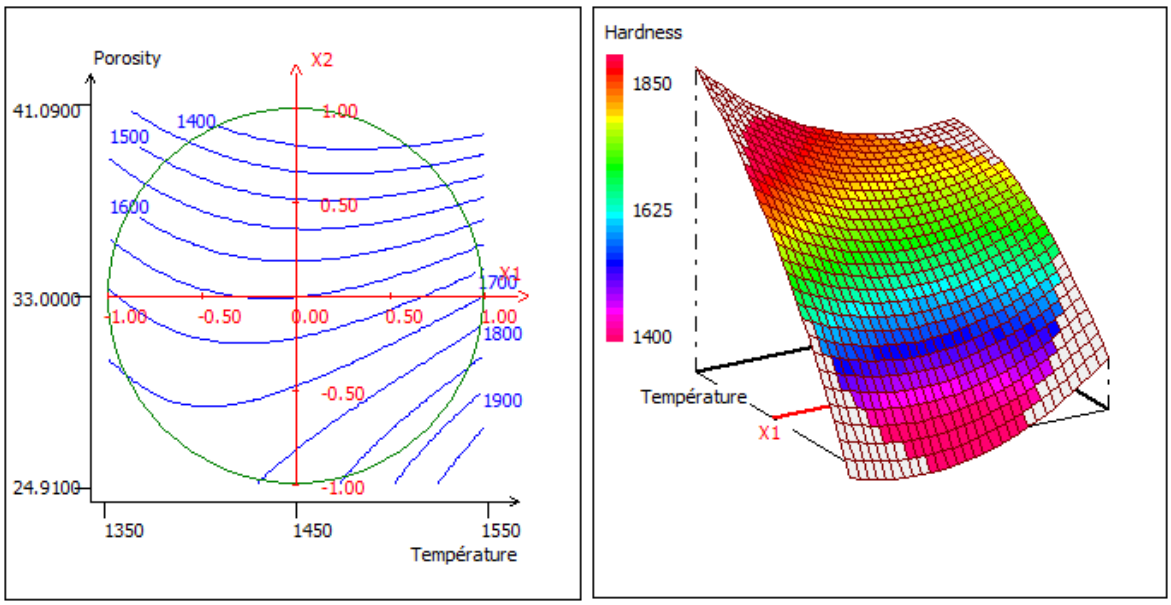

a) Two dimensional representation b) Three dimensional representation

Figure III)29: Answer surface modeling by the experiment plan

Nemrodw software furnished a second-degree equation for modeling the effect of dwell temperature and initial density on the final hardness:

$$H_{k2000} = 79.8t^2 - 77.2p^2 - 248.4p + 22.2t - 91.3pt + 1649.2 \qquad \text{Eq.20}$$

With $t = \frac{T-1450}{100}$

$p = \frac{P-33}{8}$

T the temperature in °C

P the porosity in %

H_{k2000} the Knoop hardness

This equation shows the low influence of the temperature on the final composite hardness. For low porosity samples, the temperature has a strong effect on the final hardness, but this effect decreases with increasing porosity.

If we postulate that all composites have the same density and, that the size of the boron carbide matrix and formed SiC didn't change, which is a possible hypothesis, the chemical composition can be related to hardness. As seen previously, microstructure is low affected by the temperature. This is logical with a low progression of the hardness poorly linked to temperature.

However, the microstructures obtained are very different from ones expected from the bibliography (Cf. chap. I 2-6). These incongruous results will be discussed in part C.

Summary: This experimental plan makes it possible to confirm the modest influence of temperature on the SiC formation reaction in the composite. Among the initial porosity conditions tested in this work, we found that the reaction is most advanced in the samples prepared from the preforms containing about 25% of porosity. Hardness can be modeled experimentally, confirming these results, and showing high values throughout. The highest values are obtained for composite prepared from preforms containing of 25% porosity.

B-5 2.45GHz multimode vs 915MHz single-mode

For the infiltration in 915MHz cavity, 35mm pellet was used with two level of porosity: 40% (cold compaction) and 45% (multimodal mix of small powder Dmax: 1µm). The amount of silicon was chosen to fill the pores with a slight (10-20%) excess of silicon just to be sure there is enough. There are not a lot of tests in single-mode furnace. Indeed, the temperature is not clearly defined because no calibration test could be made because of limited samples. However as seen in the part A, the infiltration temperature has little effect on the final composite composition, microstructure and properties. These tests are not a formal comparison but we can verify if there are large differences between 2.45GHz multimode furnace and 915MHz single-mode furnace.

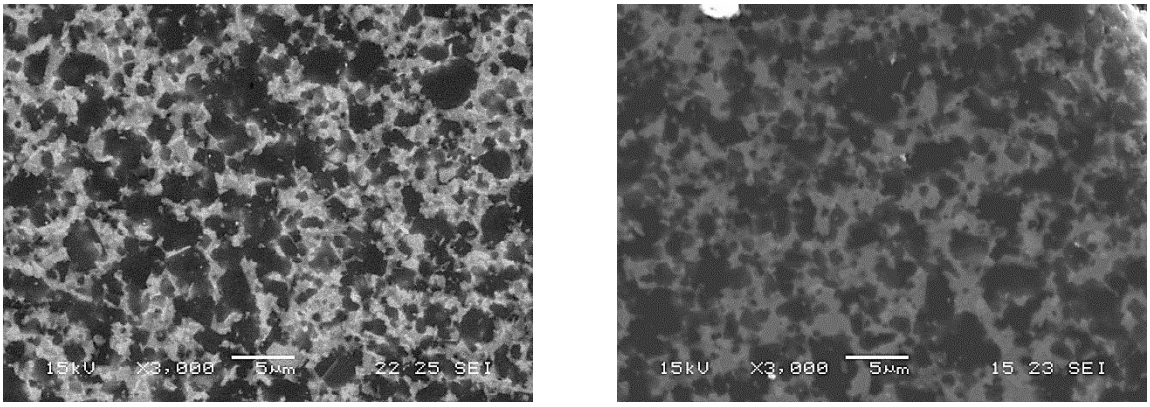

a) monomode heated sample b) multimode heated sample

Figure III)30: Microstructure of a) monomode heated sample (40% Dth) and b) multimode sample (40% Dth)

Figure III)30 shows microstructures obtained with both heating modes. No visible difference appears between these microstructures. Therefore, the frequency doesn't influence the microstructure.

Table III)11: Mechanical properties for monomode 915MHz furnace sample and multimode 2.45GHz furnace sample

Samples	Hardness (GPa)	Young Modulus (GPa)	Toughness (MPa. $m^{1/2}$)	Flexural strength (MPa)
915 MHz single-mode	15±0.7	340±5	2.24±0.2	129±22
2.45GHz multimode	15.1±0.5	340±5	2.25±0.3	100±30

Table III)11 shows the mechanical properties. The only difference between single-mode infiltrated samples and multimode infiltrated samples seem to be the flexural strength but when we took into account the errors, the two values overlap each other's. Samples can be made indifferently by 915monode or by 2.45multimode furnace, which did not influenced composition, microstructure, nor properties. For larger pieces, it would be preferable to work in multimode furnace working at 915MHz because of the cavity size.

B-6 Towards ballistic test pieces

One test was carried out on large piece (60mm of diameter and 10mm of height) in order to evaluate an upscale factor using microwave technology. The heating used type was direct because the weight of the samples made it possible to reach high temperature without a susceptor. The initial porosity percentage was 30%. As standard, heating rate was limited to 10°C/min the maximum achieved temperature was 1450°C and a dwell time of 15min was employed. This was just a feasibility test. Figure III)31 shows a picture of the final composite.

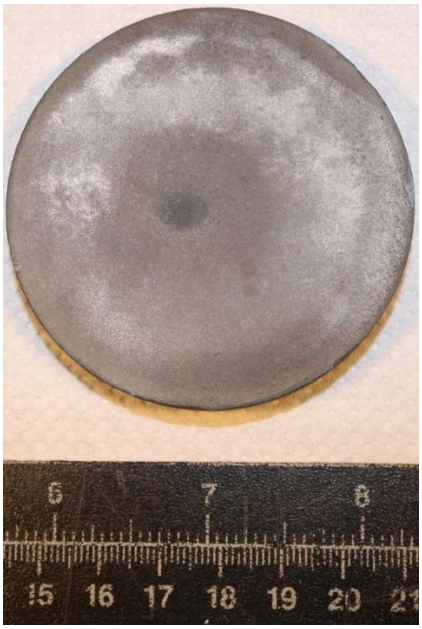

Figure III)31: Sample sized for ballistic test

Test was a success because a fully infiltrated composite was obtained with a standard thermal cycle. Moreover, heating was easier with the Φ 66 mm sample because of the sample's weight. The final product showed no sign of embrittlement. This is a promising result for the rest of the project.

Conclusion part B:

In part B, the influence of some parameters on the mechanical properties, the microstructure and the chemical composition were examined.

These tests defined a minimum surplus of silicon is needed to avoid residual porosity in the final composite. First tests were carried out with an overflow of 10wt% compared to the exact amount of silicon needed to fully infiltrate the preform porosity. In these composites, some residual porosity was observed for pre-sintered sample and heterogeneous structure was observed for non-pre-sintered samples. For the last tests, an excess of 20wt% of Si was utilized and the preform didn't have residual porosity whether preform was sintering or not. It is noteworthy that when no more silicon can be found outside of the preform then this indicates that the amount of silicon is sufficient to infiltrate the preform but it not too much to be considered as waste material.

The initial porosity is the major parameter to modify the final mechanical properties. It is linked with a low amount of residual silicon (the weakest phase).

The dwell time at high temperature hasn't an effect for small (1µm) boron carbide initial grains. Others parameters didn't have a strong effects neither on the mechanical properties nor on the microstructure.

Part C: Relationship between properties, composition and microstructure of RBBC composites: influence of microwave heating

After showing the feasibility of the RBBC by microwaves heating (part A) and, then having optimized some parameters to achieve high hardness (part B), we explore the microwaves process specificities: what do the microwaves bring to the process, to the microstructure of the composites and to their final properties.
This demonstration follows several steps:
Firstly, we compare the system reactivity during the different modes of heating: For this study, a comparison of the reaction process during the resistive and microwave heating of the composites will be carried out; in addition, according to these two heating techniques, a comparison of the transformation thicknesses of coarse grains of B_4C in solid solution will be made.
Secondly, the microstructure of composites obtained by the same techniques are compared, and the specific microstructure of the composites obtained by the microwave heating technique will be explained.
In the previous paragraph, some mechanical characterizations have been presented; these whole measurements will be associated with ones obtained by conventional heating. So finally, from global point of view, relation between microstructure and mechanical properties will be established.
Throughout this analysis, we will identify the consequences of microwave heating on the development of the RBBC.

C-1 Do microwaves have an influence on the composite reactivity?

C-1-1 Comparison of the system reactivity during the conventional or microwave heating

C-1-1-1 Preform elaboration for conventional vacuum tests:

For the infiltration in Conventional Vacuum Furnace (CVF) we used 20mm pellet with different levels of porosity. In order to compare with the microwave infiltration (MW) the porosity was chosen to be the nearest possible with the samples infiltrated in the microwave furnace. A porosity between 21 and 37% (in microwave we used preforms with porosity between 25 and 37%). We also used compacted preforms with 37-39% of initial porosity (in microwave 39%).
In order to have enough silicon to fulfill the infiltration, almost twice the amount of silicon required was used, to take into account its evaporation. Indeed, at high temperature under vacuum, silicon easily evaporates.
The thermal cycle for infiltration is a heating rate of 15°C/min until 1480°C and 20min of

dwell time then the cooling is not controlled (the resistive heating is cut off).

C-1-1-2 Results

As initial porosity of the samples was different, the degree of transformations are useful to compare the reactivity of system during heating (Cf. figure III)32). Red squares (full or empty) represent the silicon degree of transformation. Purple triangles (full or empty) represent the SiC degree of transformation. Blue circles (full or empty) represent the B12 degree of transformation.

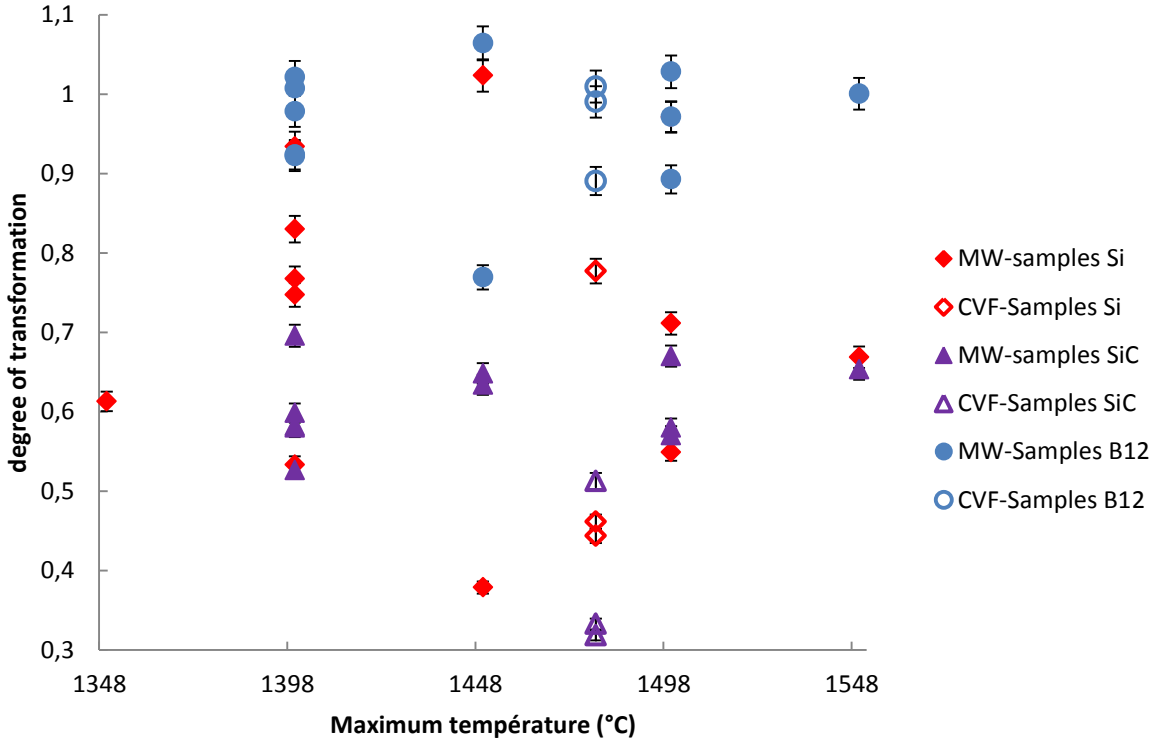

Figure III)32: Degree of transformation in function of the maximum temperature: composites RBBC heated by conventional or microwaves techniques

B_{12} degree of transformation is similar between both heating methods whatever the permeating temperature. This suggests that the amount of carbon available for silicon carbide formation is the same in both cases. Nevertheless, the silicon carbide degree of transformation is lower in the conventional furnace. This, in agreement with a less advancement of the disappearance of the silicon, makes it possible to conclude that the reaction is less advanced in conventional furnace than in MW furnace for close measured temperature. This difference causes will be discussed later.

Another experiment can be carried out to confirm this difference in reactivity: infiltrating preforms containing large size boron carbide grains. Indeed, Hayun et al.[HAY09b] had demonstrated the core-rim effect: the transformation of the B_4C grains into the $B_{12}(B, C, Si)_3$ solid solution takes place at the periphery of the carbide grains. By following the solid solution thickness, we can thus compare the degree of transformation for the two heating

techniques.

C-1-2 Reactive thickness in B_4C grains

To observe the transformed thickness of boron carbide grains, preforms made with coarse B_4C (130µm) were used. The dwell time varies between 0 and 240min. The infiltration temperature of 1400°C was chosen to compare with literature data [HAY09t]. Samples weren't completely infiltrated because of a lack of silicon.

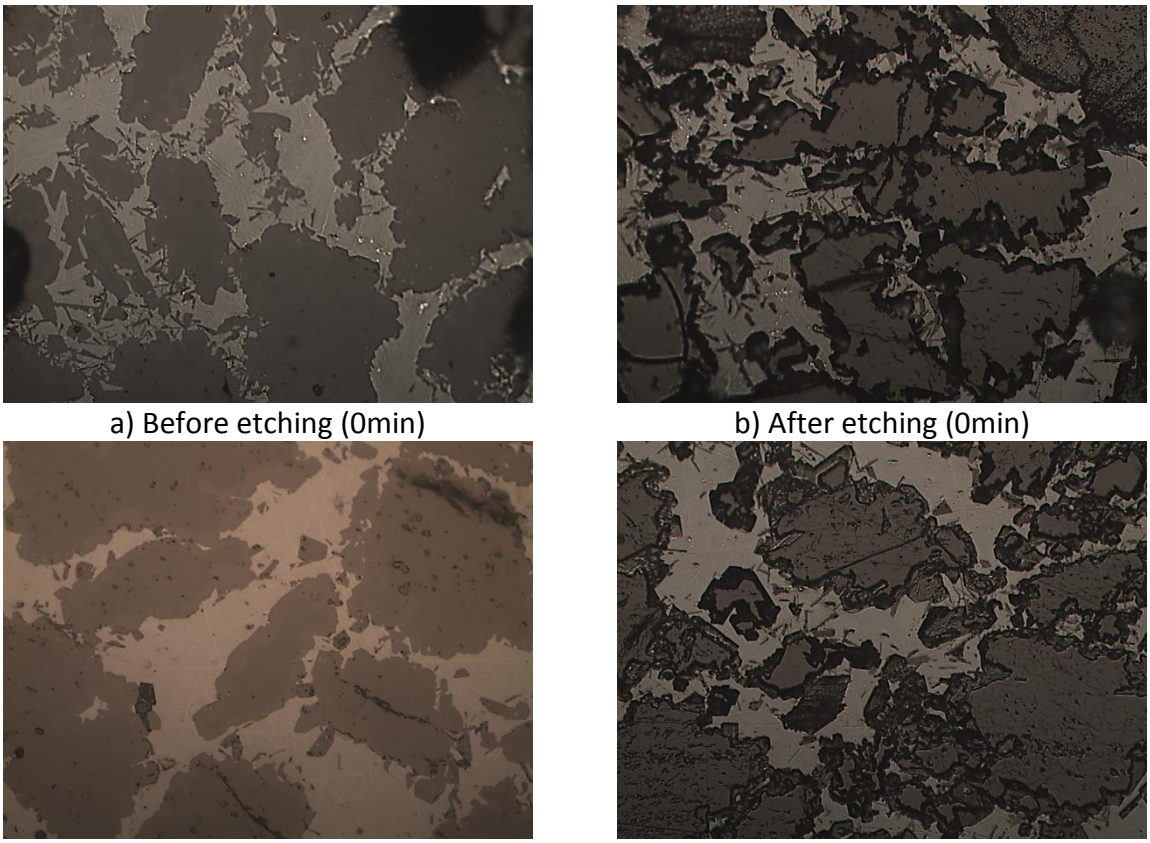

a) Before etching (0min) b) After etching (0min)

c) Before etching (60min) d) After etching (60min)

Figure III)33: Composites obtained by microwave heating at 1400°C: Microstructure before (a,c) and after (b,d) electro-etching to remove $B_{12}(B, C, Si)_3$.

Figure III)33 and figure III)34 show the difference between before and after electro-etching in KOH solution. This method was used by Hayun to reveal the core-rim effect. The size of reaction layer was determined by SEM image analysis.

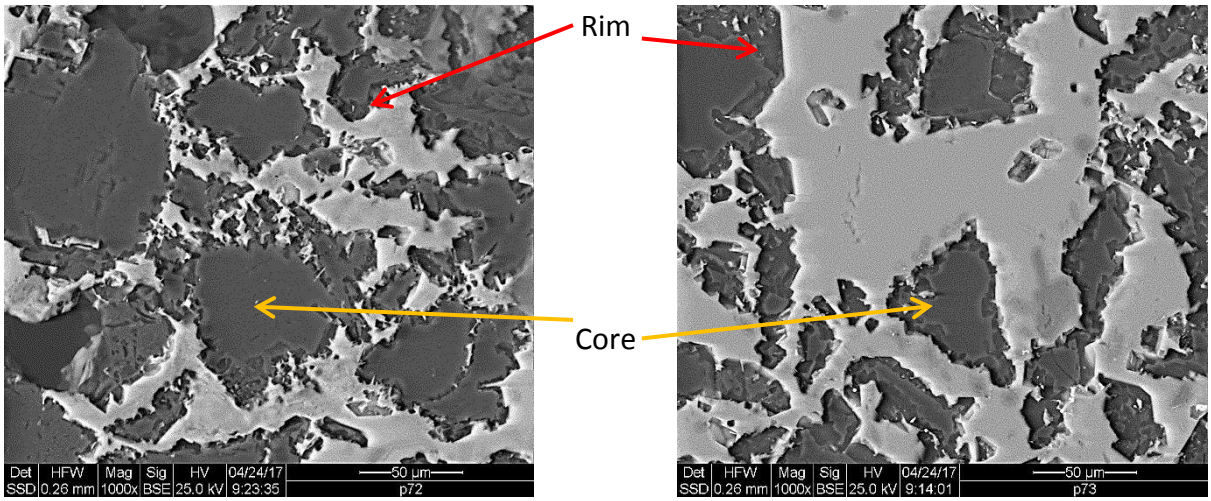

a) 0min sample after etching b) 60min sample after etching

Figure III)34: Composites obtained by microwave heating at 1400°C: SEM picture of coarse composite to measure the reaction thickness in B_4C grains.

The rim layer size was measured on SEM picture by direct measurement and conversion with the picture scale. The measurements were achieved on, at least, eleven interfaces. The same experiments were done for longer dwell times: 120 and 240 min. The figure III)35 resumes our results, in comparison with those obtained by Hayun [HAY09t]. Between the two used techniques, the temperature is not measured in the same manner. That can introduce a probable difference in temperature of samples treated in the two heating modes. Nevertheless, we have seen above that the dwell temperature has a low influence on the reaction progress. We can therefore consider here that the difference on the curve of figure III)35 allows a comment.

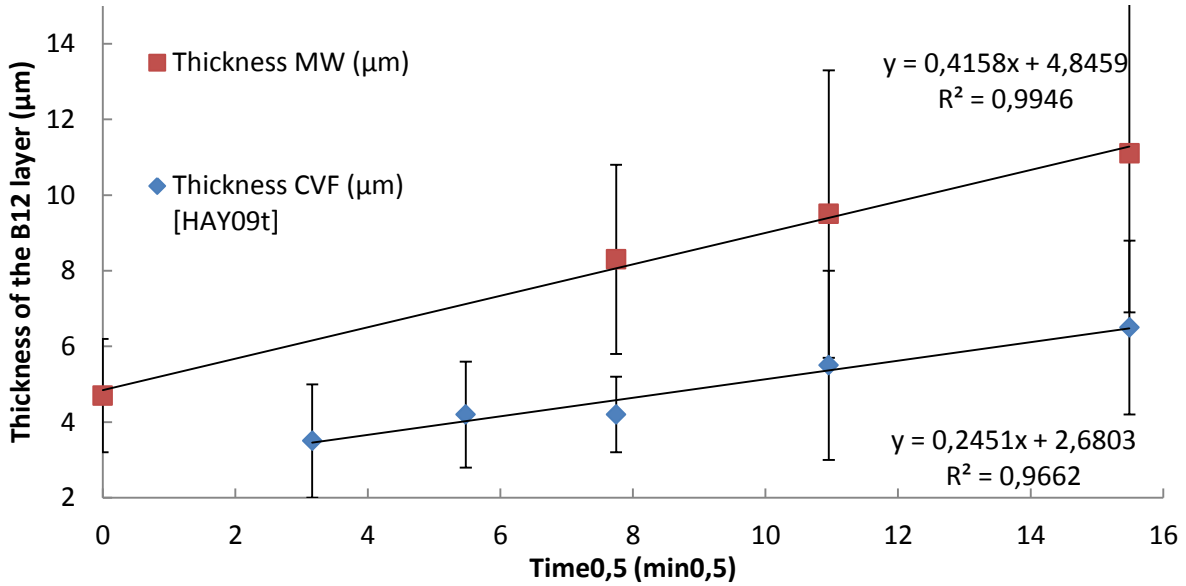

Figure III)35: Evolution of the Rim thickness with the square root of time

The observation of the figure III)35 allows two observations:
- Firstly, regardless of the heating methods, the points obtained are aligned: the formation of the solid solution is therefore a diffusional process. This leads to the conclusion that the reaction mechanism is similar in the two heating modes.
- Secondly, the thicknesses obtained in the microwave heating case are much higher than those obtained from conventional heating. This is further proof that the reaction is faster if the heating takes place in microwave condition with a possible effect of the electromagnetic field or of the atmosphere, it will be discussed later.

These experiments also explain that during the parametric study we found that boron carbide was almost completely transformed into the B12 solid solution. In fact, the thickness of the transformed grain is here in the order of 4-5 µm at the beginning of the dwell time. This thickness is greater than the grain size of B_4C used for the previous study. It is therefore logical that the conversion rate of the boron carbide into the solid solution $B_{12}(B, C, Si)_3$ is very high in the composite obtained from fine-grained preforms.

Conclusion:

Those two series of experiments show that the reaction of RBBC formation is accelerated in the microwave furnace. But we must keep in mind that there are differences in operating conditions between microwave and conventional heating techniques:

-The electromagnetic field of the microwave furnace can obviously influence the reaction by its action on diffusion, which has been demonstrated in the case of sintering for example [ZUO13a, ZUO13b].

-But the atmosphere is not the same in both techniques; it is possible that the presence of H_2 in Ar atmosphere influences the reaction mechanism.

At this stage, it is difficult to conclude on the influence of these two factors. This point will be discussed later, after observation of the composite microstructures resulting from the two heating modes.

C-2 Do microwaves affect the final microstructure of composites?

C-2-1 Scanning Electronic Microscopy observations of RBBC after heating by CV or MW.

Figure III)36 shows the microstructure of CVF and MW samples for the nearest conditions (porosity and maximum temperature). For all pictures: boron rich phases appear in black, SiC appears in light grey and residual silicon appears in dark grey. Silicon carbide does not present the same morphology when the heating way changes, it is smaller and more number for MW samples than for CVF samples. At the contrary, the other phases the way of heating seems have no effect.

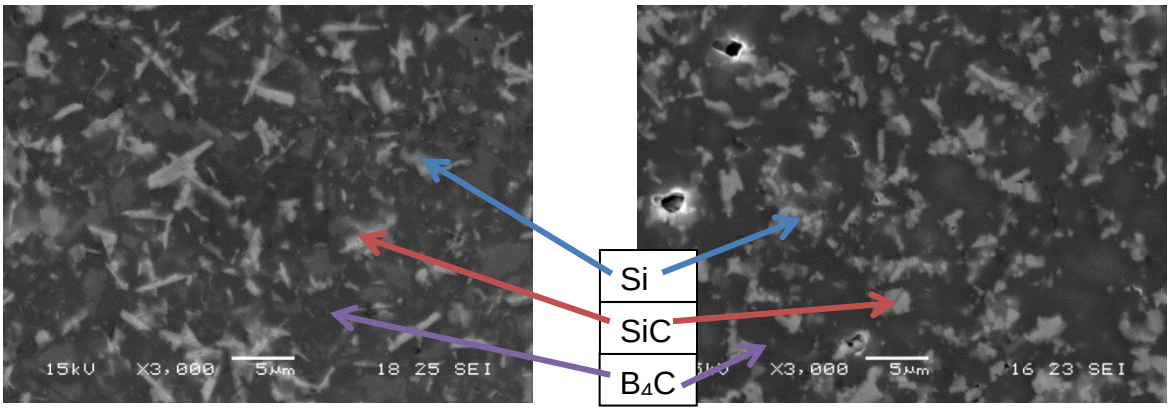

a)CF-21%-1480°C b)MW-25%-1500°C

Figure III)36: Comparison of the microstructure of CVF and MW samples. SEM picture for secondary electron mode (SEI topography).

Different assumptions can be made to explain the difference in terms of microstructures between the conventionally processed samples and those produced in the microwave furnace:

-*(i) Temperature gradient*, between molten silicon (minimum 1414°C) and boron carbide (≈1300°C) at the first step of the infiltration. The molten silicon temperature decreases while it infiltrates the cooler boron carbide preform. This can modify the carbon solubility in the molten silicon, which causes the precipitation of many SiC clusters. Then, all these clusters grow but remain smaller than those formed in conventional furnace.

-*(ii) Microwave field*, i.e. the electric field and/or the magnetic field could change the precipitation mechanism of SiC, in slightly changing the diffusion process linked or not by a preferential heating process. It could be also assumed that when SiC reaches a critical size, it starts to couple strongly with microwave so it increases locally the temperature which modifies significantly the grain growth.

-*(iii) Atmosphere condition*, the presence of gas can remove the oxide layer from silicon and boron carbide which increases the reactivity. It could also change the heat transfer compared to vacuum furnace. Hydrogen could also react with some of the formed SiC ($SiC+2H_2 \rightarrow Si+CH_4$) and changes its growing mechanism.

To check if the last hypothesis is plausible, one sample was made in conventional furnace in atmosphere used in microwave furnace.

C-2-2 Conventional atmosphere infiltration

In order to emancipate from the atmosphere influence, an infiltration was carried out in conventional tubular furnace (CTF) in Ar/H_2(10%) atmosphere. The composition of the composite and its microstructure were compared with the conventional vacuum furnace (CVF) and microwave furnace heating (MW) (Cf. figure III)37).

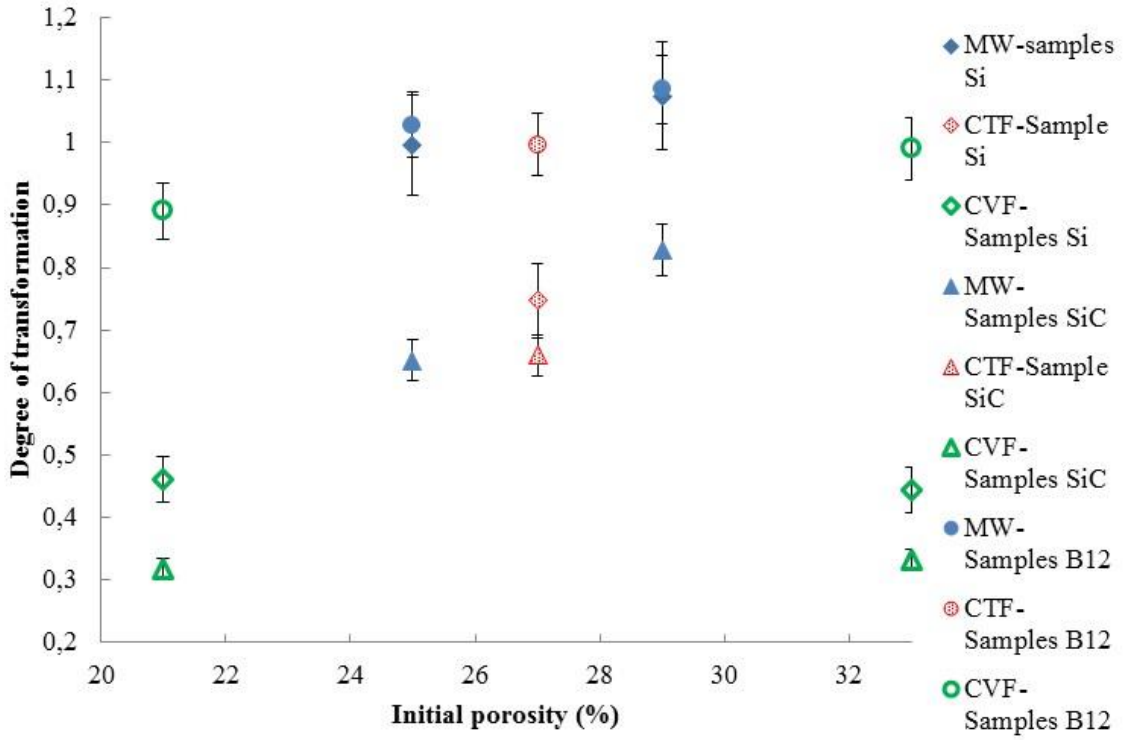

Figure III)37: Degree of transformation in function of the initial porosity (error on the porosity ±3%)

Figure III)37 shows the degree of transformation linked to the RBBC synthesis: it appears that the atmosphere facilitates the reaction. Under atmosphere, the reactions, whatever the heating method, are more close to the equilibrium than one under vacuum. The values higher than one came from the calculation approximation (Cf. chap. III part B) and from the lattice parameter increasing in the case of the B_{12}. Nota bene : the volume variation linked to the boron carbide transformation was not taken into account for the degree of transformation calculations.

Figure III)38 shows three different microstructures including one obtained by microwave heating infiltration (a), one obtained by conventional heating under vacuum (c) and one obtained by conventional heating in Ar/H_2 atmosphere (b). As it can be seen, when the infiltration is carried out in conventional furnace in atmosphere, the obtained microstructure looks like to the microstructure obtained by microwave heating. That implies the SiC morphology could be more dependent on the atmosphere than on the application of microwaves.

One explanation could be given. The H_2 gas is used in boron carbide sintering to remove from the boron carbide surface the B_2O_3 native oxide [TAR04t]:

$$H_2(g)+B_2O_3(l)\rightarrow H_2O(g)+B_2O_2(g)$$

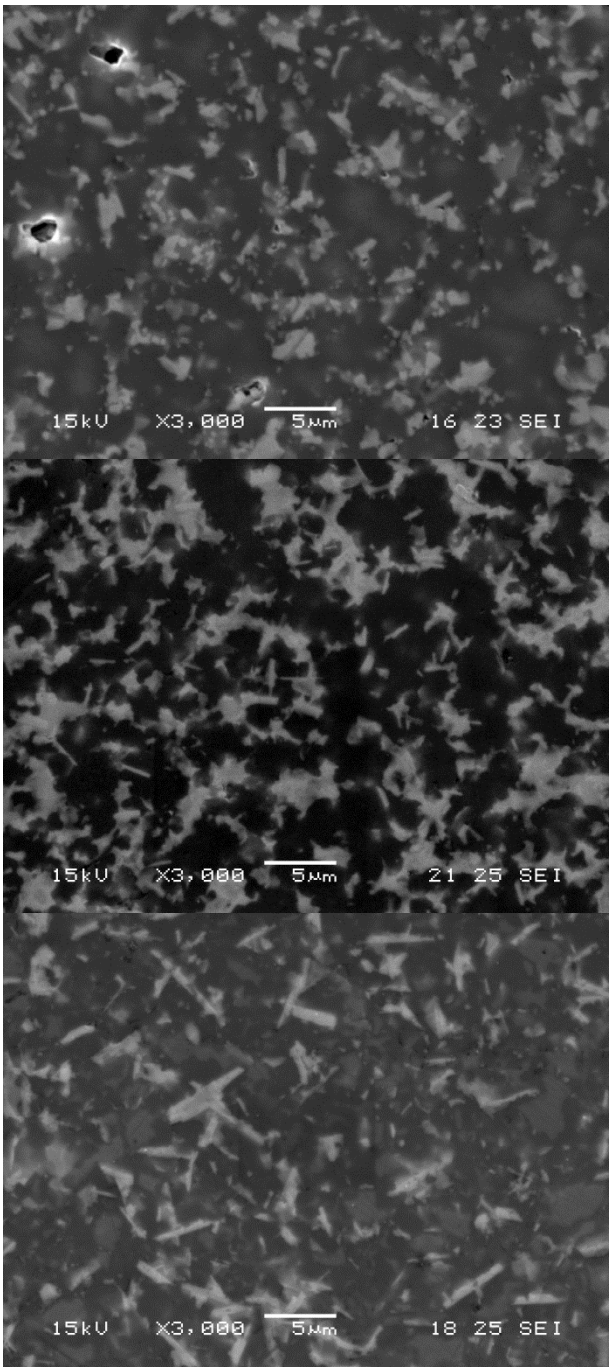

a)MW-25%-1500°C

b)CTF-27%-1450°C

c)CVF-21%-1480°C

Figure III)38: Gas effect on the composite microstructure

We think in the case of heating under Ar/H_2 atmosphere, the B_2O_3 is removed from the surface, nothing "protects" boron carbide from melted silicon. Consequently, silicon reacts quickly and attacks boron carbide everywhere. More carbon is dissolved in the early steps of the reaction, so more crystallites precipitation appears. These crystallites grow all together but remain relatively small because of the SiC quantity. This could explain the difference of SiC grains shape observed for composites obtained by CVF or MW heating techniques.

Partial conclusion:

These experiments lead us to moderate the previous conclusion on the influence of microwaves on the formation of RBBC: although it is sure that microwaves have a significant influence on the species diffusion and favors the reaction. However, it must be noted that the influence of the atmosphere is paramount on the reaction: it favors the formation of silicon carbide, and, moreover, it leads to SiC grains with rather polygonal or small plates shapes.

To go further in the microstructure analysis, two samples were observed by TEM.

C-2-3 Microstructure analysis by TEM

C-2-3-1 Transmission Kikuchi Diffraction (TKD)

The TKD analysis can be compared to EBSD map on the TEM lamella sample. While in EBSD the Kikuchi band analysis came from the backscattered electron at the surface layer of the samples, in TKD the Kikuchi band came from the slightly diffracted ray which can pass through the sample. The volume analysis is lower in TKD than in EBSD. The spatial resolution is higher.

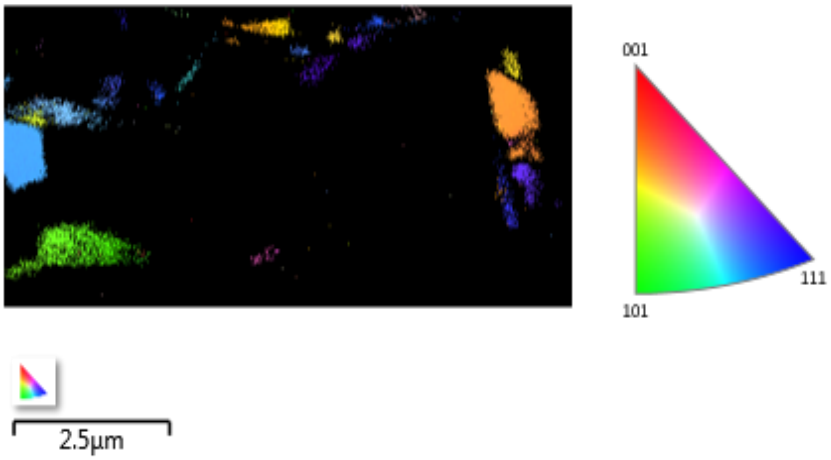

a) CVF-21%-1480°C-20min (orientation contrast)

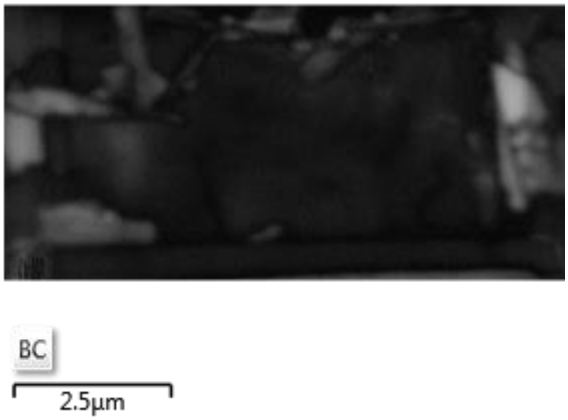

b) CVF-21%-1480°C-20min (diffraction contrast)

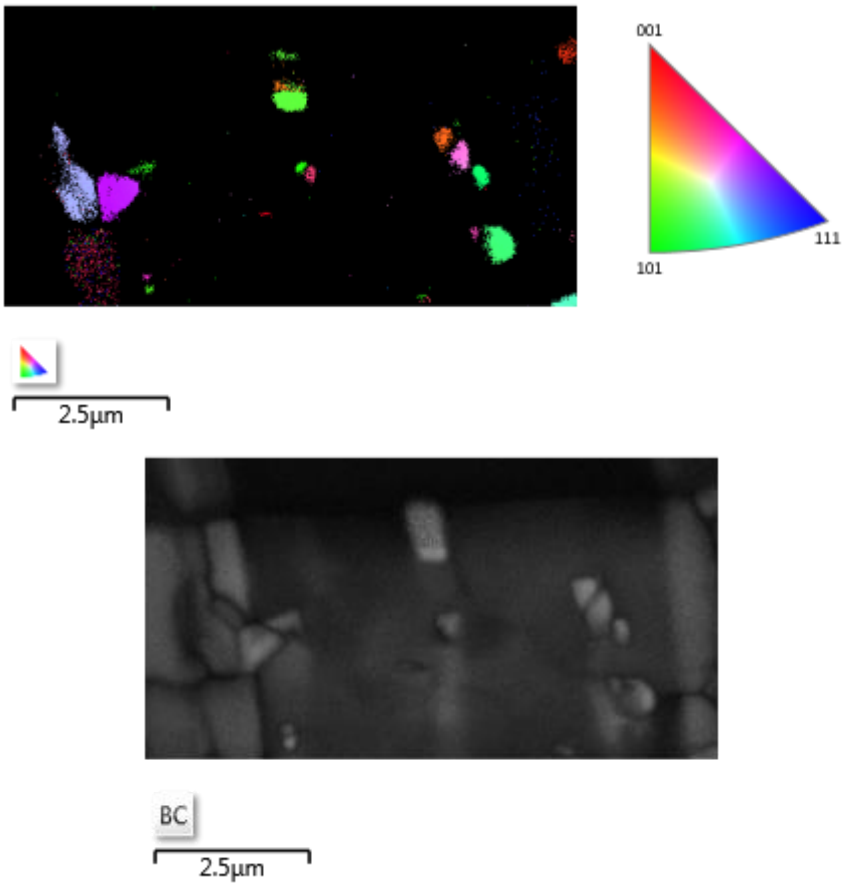

c) MW-25%-1500-15min (orientation contrast)

d) MW-25%-1500-15min (diffraction contrast)

Figure III)39: TKD results gave with the orientation color

TKD results (Cf. figure III)39) show that obtained SiC in CVF are composed by one grain orientation while ones obtained in MW are composed by many grain orientations. The picture figure III) b) and d) reflect the quality of the diffraction of each point, more a point is white more the kikuchi diffraction pattern presents a high contrast. This type of picture reveals the lattice default and very fine microstructure otherwise invisible. Pictures a) and c) show the orientation, Aztec software attributed a color for each grain orientation.

C-2-3-2 Transmission electronic microscopy

TEM analyses were carried out by Sergio Sao-Joao.

a) Conventional Vacuum Furnace sample

This sample had an initial porosity of 21%, it was infiltrated at 1480°C during 20min. The XRD coupled with the chemical etching give the following composition: 7Vol.% of Si, 19Vol.% of B_4C, 9Vol.% of SiC, 65Vol.% of B12 with an error of ±2%. The TEM observations are presented in figure III)40.

TEM observations confirm the needle shape of SiC grains, few tens nanometers width, and few micrometers length. As Hayun [HAY09t] showed, SiC needles have twins inside of their structure. EDX analyses confirm the presence of silicon grains close to B12 and SiC grains. B12 grains present some lattice default but we cannot define them. The initial B_4C grains are fine (≈1µm), so the core-rim effect is not observed in this case.

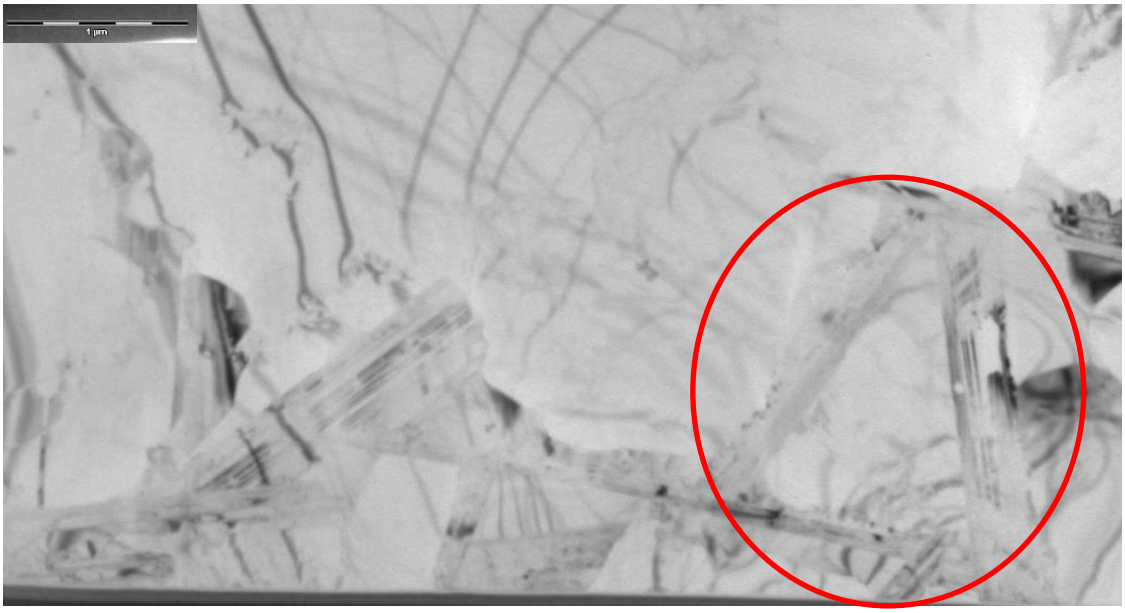

a) General view of the CVF samples

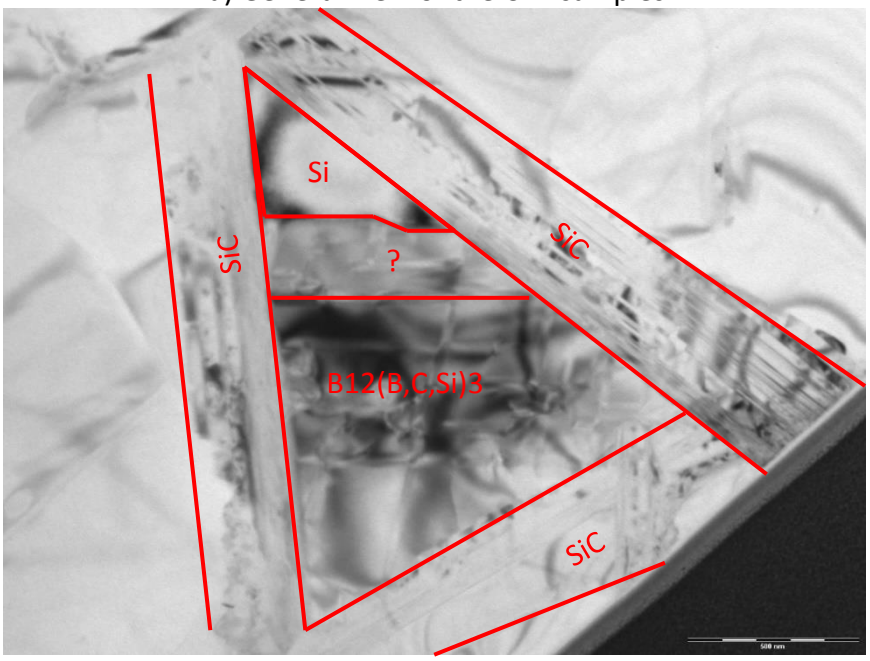

b) High magnification of an area with three phases

III)40: TEM microstructure of CVF sample

b) Microwave sample

This sample had an initial porosity of 25%, it was infiltrated at 1500°C during 15min. The XRD coupled with the chemical etching give the following composition: 5vol.% of Si, 5vol.% of B_4C, 14vol.% of SiC, 76vol.% of B12 with an error of ±2%.

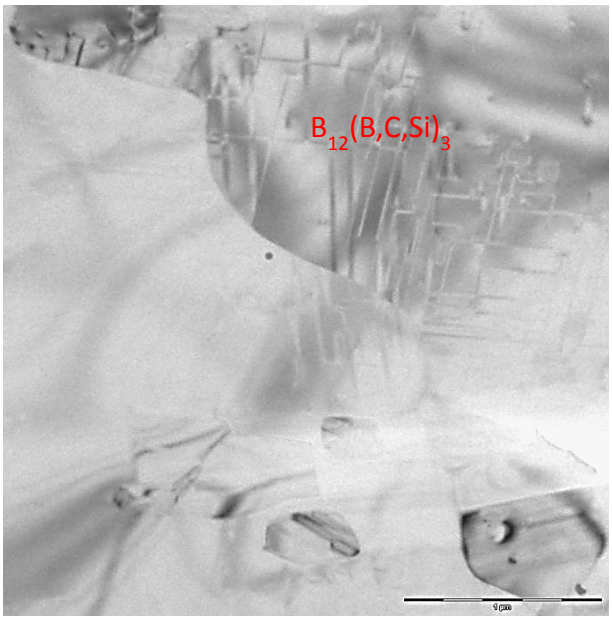

a) B12 grain with crystalline defect

As previously B12 grains present some defects (Cf. figure III)41 a and b).

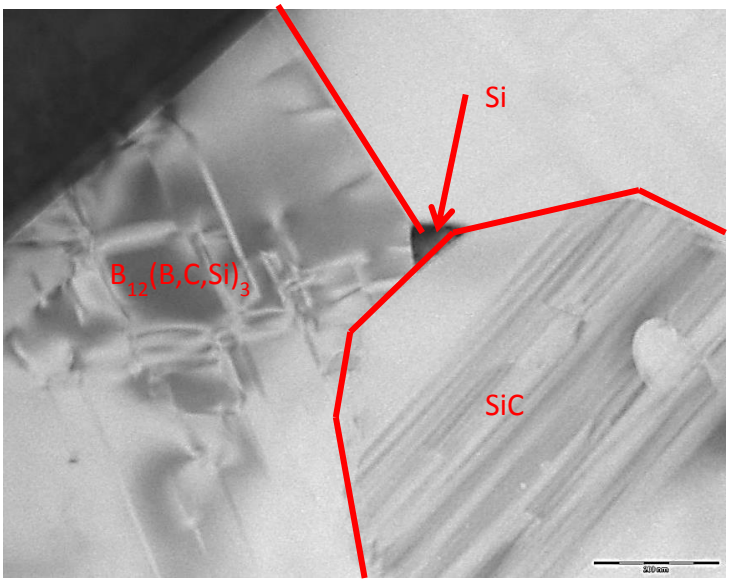

b) Area with three phases, in center (black) the residual silicon, in left the B12 with crystalline defect, and lower right SiC with twins

The silicon grains (Cf. figure III)41 b) black area) are rare, crystalized and close to the SiC.

Figure III)41: TEM microstructure of MW sample

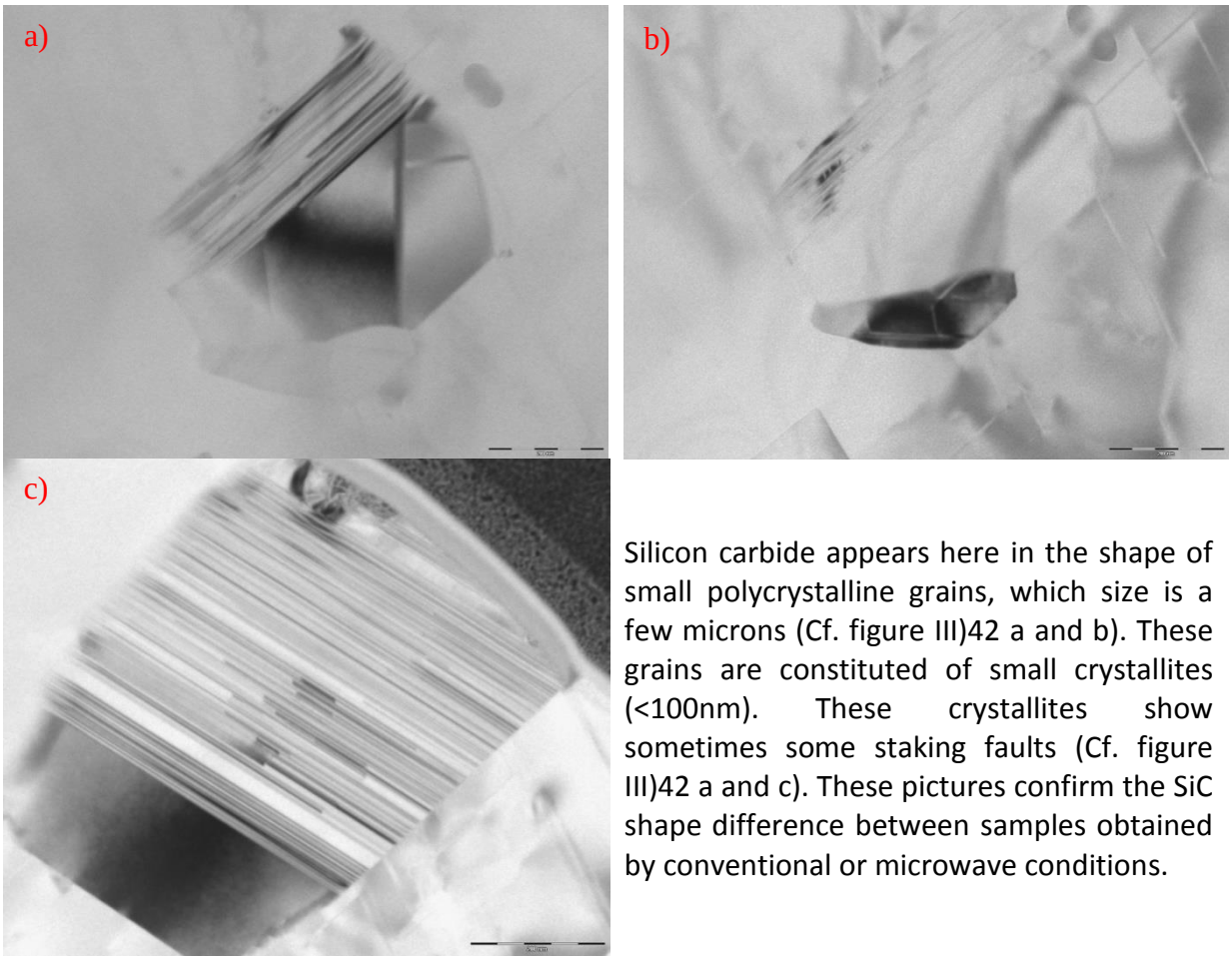

Silicon carbide appears here in the shape of small polycrystalline grains, which size is a few microns (Cf. figure III)42 a and b). These grains are constituted of small crystallites (<100nm). These crystallites show sometimes some staking faults (Cf. figure III)42 a and c). These pictures confirm the SiC shape difference between samples obtained by conventional or microwave conditions.

Figure III)42: TEM observations of SiC grains

C-3 Synthesis: Proposed Phenomenology

In this study, we showed that the formed phases are similar after conventional heating or under electromagnetic field: the core-rim effect of transformation of boron carbide is present in both heating modes, residual silicon is always present and, the silicon carbide is formed. Thus, overall, the system evolves in the same way in the two heating modes. However, two points are remarkable: the reaction is favored under an electromagnetic field and / or under argon atmosphere containing H_2. Moreover, the morphology of silicon is rather polygonal or in small platelets by treatment under microwave condition. However, the treatment atmosphere appears to be decisive. By testing in hydrogenous argon atmosphere in conventional furnace, we were able to doubt of a significant effect of the microwave effect on the silicon carbide morphology. Indeed, the obtained microstructure looks like to the one obtained in microwave furnace in the same atmosphere. We concluded that the microstructure differences came from the atmosphere not from the way of heating. This microstructure evolution is shown on figure III)43: as explained before, in the case of Ar/H_2 atmosphere, the SiC precipitates are more numerous than under vacuum, but their growth is lower.

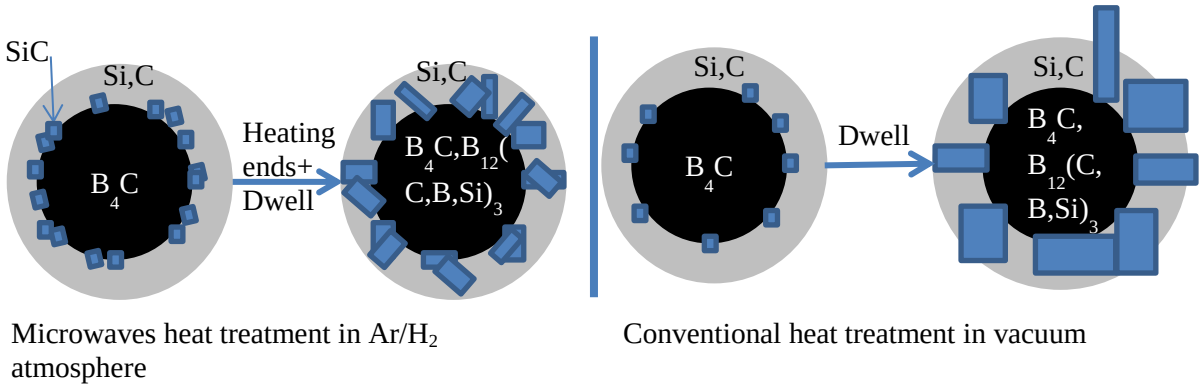

Figure III)43: Scheme of the silicon carbide precipitation

It is possible to explain the difference of SiC morphology and the slightly improved reactivity by microwave heating method and the use of Ar/H_2 atmosphere during the infiltration step.

C-4 Do microwaves lead to highest mechanical properties than conventional furnace? Relation microstructure properties

In this paragraph, we made a synthesis to put in evidence the influence of microstructure on the mechanical properties.

To establish microstructure-mechanical properties relationships, we considered all experiments performed in the thesis; it is evident to choose parameters that vary on the experimental plan. Consequently, some parameters were not studied because of their lack of change, as the final density (2.5-2.6 g/cm^3) and the amount of SiC (10-14 Vol.%). We concentrated on the influence of the residual silicon and the B12 amounts on the mechanical properties.

C-4-1 Choice of a relevant microstructure parameter: residual silicon amount or B12 amount?

Figure III)44 shows that the hardness decreases with the decrease of the B12 amount and with increase of the Si. Each representation is almost a mirror of the other one. So the two representations are relevant. We chose to work with the amount of residual silicon but same logic could be used with B12 amount.

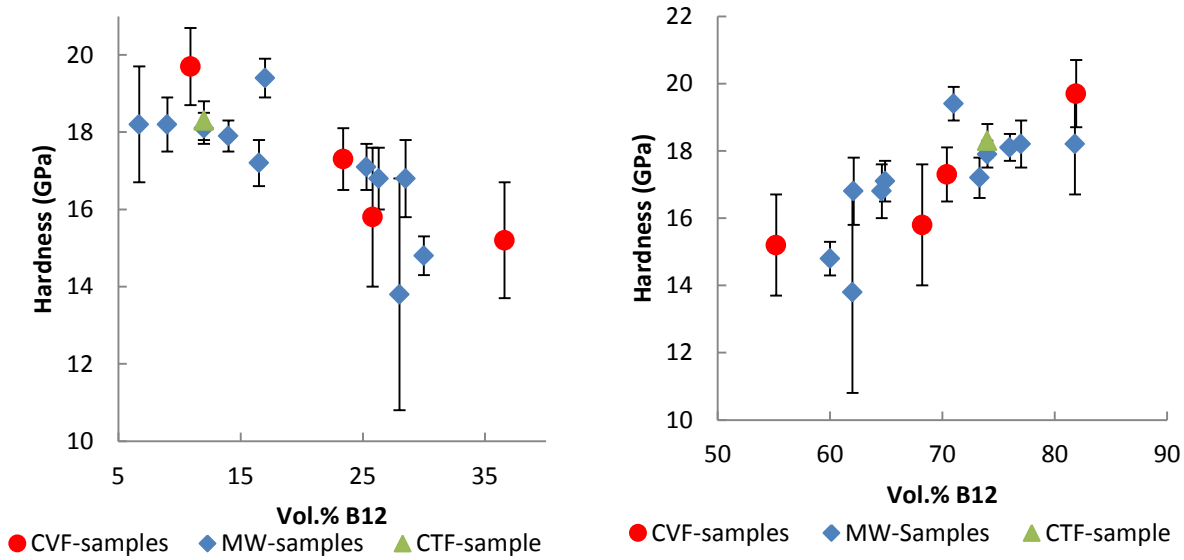

a) Residual silicon amount

b) B12 amount

Figure III)44: Hardness versus residual silicon and B12(B, C, Si)$_3$ contents in final RBBC composites.

C-4-2 Relation between residual silicon amount and the mechanical properties

Figure III)45 to Figure III)49 show the influence of the residual silicon amount on mechanical properties. They often show that microwave heated samples, conventional vacuum furnace samples and conventional tubular furnace have similar properties: this point will be detailed further.

Figure III)45 and figure III)46 show that the increasing of the residual silicon (the only non-ceramic phase) in the composite drastically decreases the hardness (from 19.5GPa to 13.8GPa) and the Young modulus (from 405 GPa to 335 GPa).

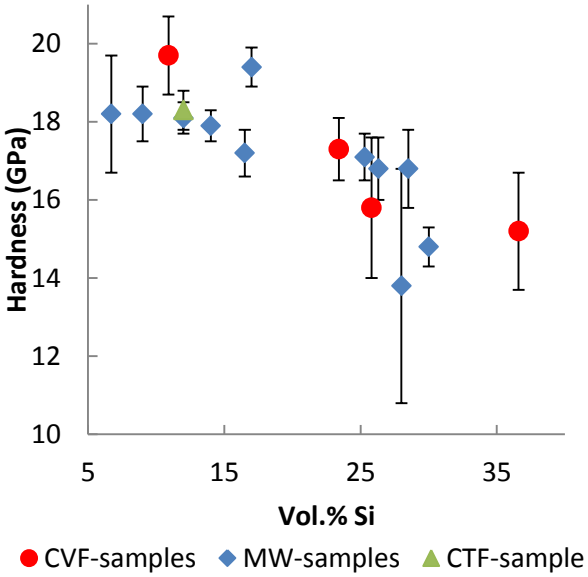

Figure III)45: Influence of the residual silicon amount on the hardness

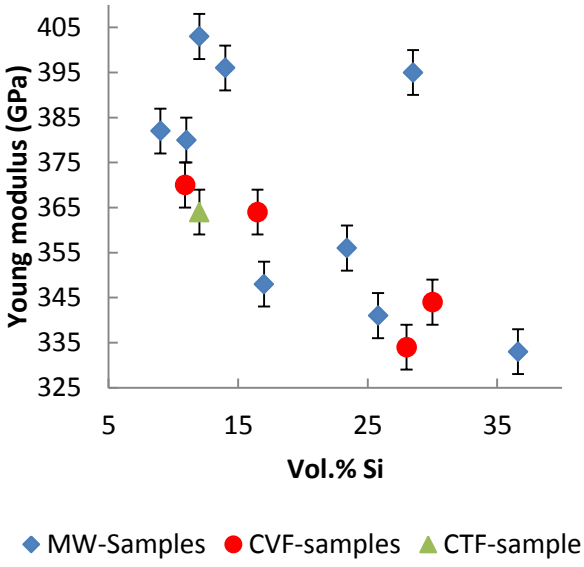

Figure III)46: Influence of the residual silicon amount on the Young modulus

Indeed, Knoop hardness is similar for microwave heating infiltration and conventional heating infiltration. The final hardness seems to be more influenced by the residual silicon, so by the initial density, than by the way of heating during the infiltration step. The SiC shape plays no role on the local plastic deformation or fracture during the indentation. The amount of the softer phase is the main factor that influences the hardness. This confirms the advantage to start from preforms with low porosity (20-25vol.%), in order to limit the content of residual silicon in the final composite.

The way of heating and the dwell temperature seem haven't influence on the composite Young modulus (Cf. figure III)46). Moreover, the initial density has low effect on the Young's modulus 333GPa for the highest initial porosity amount and 380GPa for the lowest initial porosity amount. These values are near to the pure dense boron carbide value which is a good point for the composite: for inferior lower cost and almost the same density (light

material) the same Young modulus can be obtained. Again, this property is not related to the SiC microstructure.

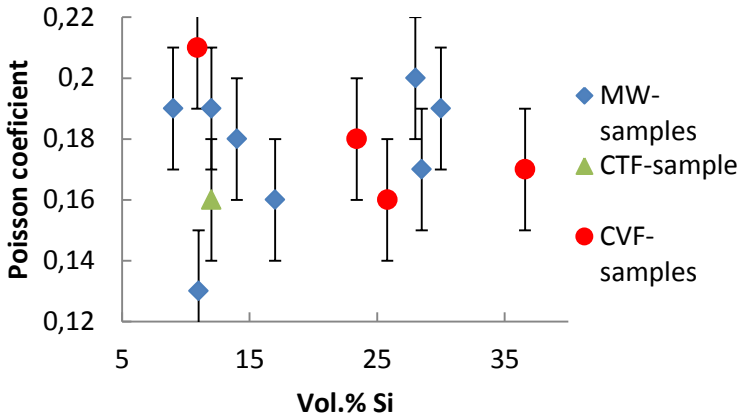

Figure III)47: Influence of the residual silicon amount on the Poisson coefficient

The Poisson coefficient (Cf. figure III)47) seems independent of the residual silicon amount for the microwave heated samples.

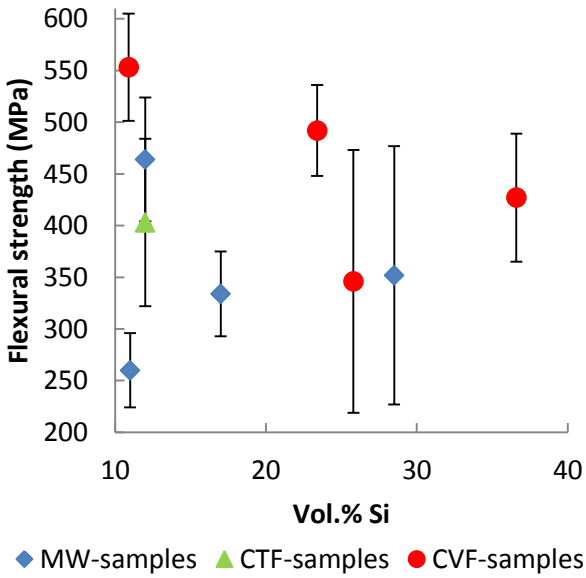

Figure III)48: Influence of the residual silicon amount on the flexural strength

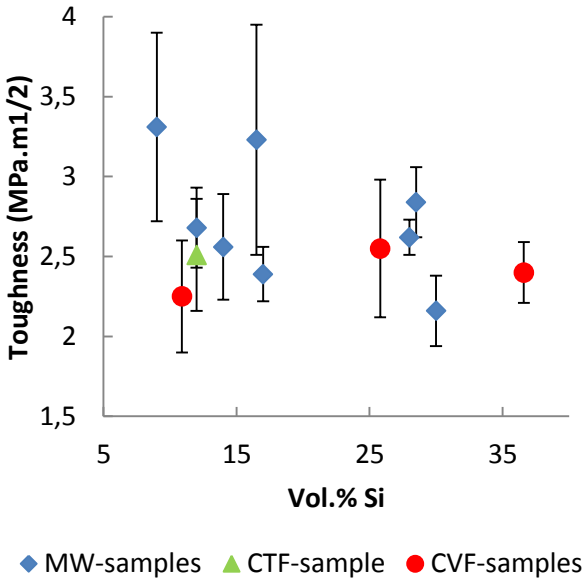

Figure III)49: Influence of the residual silicon amount on the toughness

The toughness and flexural strength (Cf. figure III)48 and 49) values are too dispersed to establish a real tendency but it seems to decrease with the amount of silicon, which is a brittle phase. They are poorly influenced by the way of heating: it seems that the flexural strength is lower in the case of microwave heating, perhaps in relation with residual porosity. On the contrary, the toughness is a slightly higher for RBBC obtained by this technique.

Indeed, fracture toughness is related to the way of cracks propagation (Figure III)50). This propagation depends more on the microstructure and, basically, on the phase distribution and morphology, than on the composition. A good way to study the origin of the fracture toughness similarity or difference is a crack propagation observation. We observed the crack propagation from Vickers indentation (1kg) made for fracture toughness measurement.

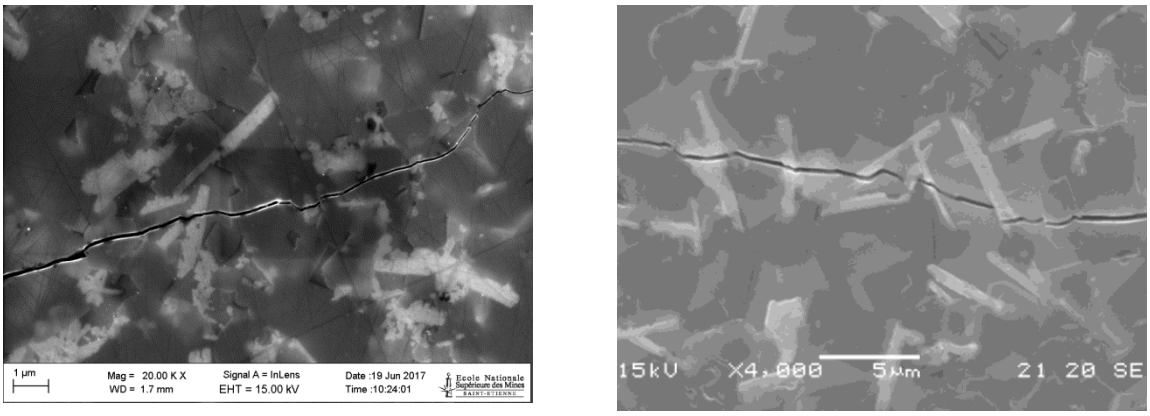

a) Microwave sample

b) Conventional vacuum sample from bibliography[HAY10c]

Figure III)50: Crack path in a) microwave sample and b) in conventionally made sample according to the bibliography

There is some cracks deflection in conventional vacuum samples but in the majority of cases the cracks cross the silicon carbide particles without being deflected. In microwave sample, it is the same: some silicon carbide grains deflect cracks but generally the cracks cross SiC without any deflection. In our case the cracks deflection is not efficient enough to have an effect on the toughness. This fact could explain the lack of mechanical difference despite the microstructure difference.

According to the literature [THE90], for pure boron carbide, the boron carbide grain size is crucial for high mechanical properties. When the grain size increases the mechanical properties tend to decrease. The same effect can be observed for residual porosity amount. For RBBC [HAY10c, HAY09t, DAR12], the role of silicon carbide microstructure (shape) seems to be more significant. The morphology of silicon carbide influences toughness and flexural strength. When slenderness factor (ratio between length and width of needles) increased, toughness and flexural strength increased too.

Conclusion part C:

In the part C, we saw the differences between conventional ways of fabrication of RBBC and micro-wave heating way. Although the microstructure differences, smaller SiC in micro-wave heated samples and in Ar/H_2 atmosphere than in conventional vacuum heated samples, the mechanical properties are similar (Cf. figure III)51). In the graph presented in figure III)51, we decided to express the hardness in function of the initial porosity because in the chapter III

part B, we saw that dwell temperature has low effect on the final hardness. This confirms the optimal porosity of preform is 20-25 vol.%. For upper values, the decrease is caused by the amount of residual silicon.

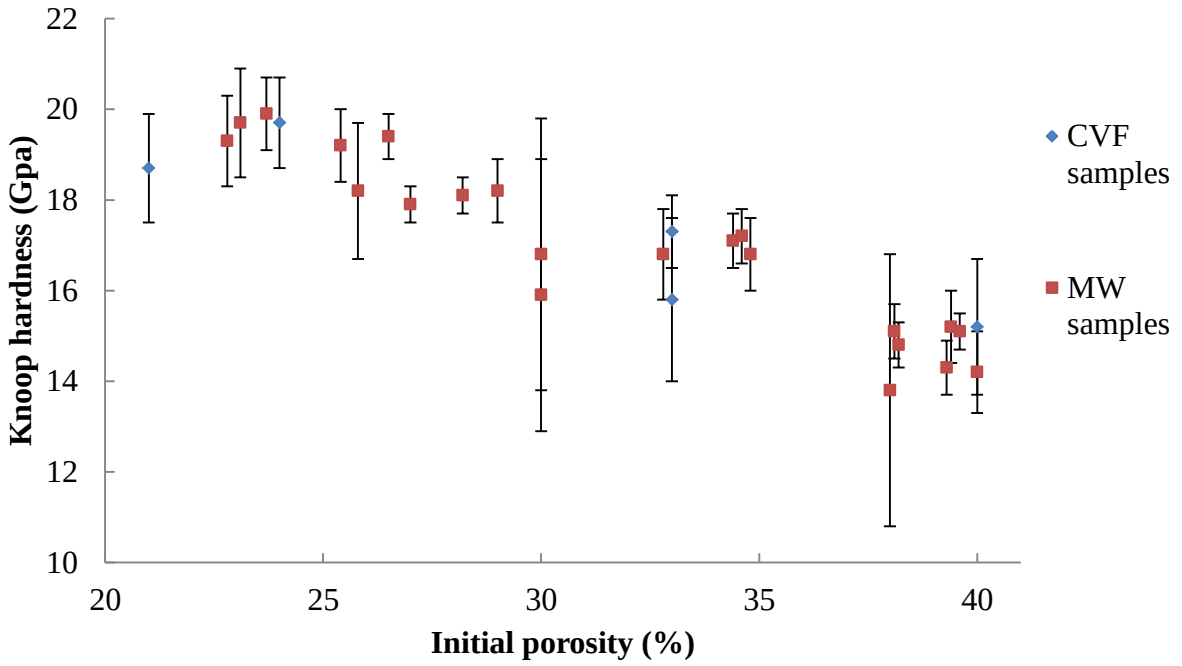

Figure III)51: Resume graph of compared hardness in function of the initial porosity

To find the differences origin, we made a test in conventional furnace in Ar/H_2 atmosphere. This test allows us to separate the effect of the atmosphere and the effect related to the furnace (electromagnetic field and thermal gradient between compounds). It appears that the microstructure differences came from the atmosphere it is probably due to the cleaning of the boron carbide particles and silicon surface. In that case, less oxidizes silicon is infiltrated in the more reactive boron carbide preform. The reaction can take place in more surfaces so more carbon is free which produces more silicon carbide clusters, which leads to small polygonal grains.

Conclusion Chapter III

In part A, the feasibility of the adaptation of the reaction bonding technique in microwave furnace was demonstrated. To fulfill the infiltration, the heat treatment had to be done under hydrogenous argon (1.4bar), at a heating rate of 10°C/min. Apart from these two constraining conditions, it is possible to develop RBBC by heating under a microwave field, because the phases involved: boron carbide and silicon couple with the waves, The use of susceptors in the crucible is unnecessary for parts with a size superior of 35 mm diameter and 10mm height (10g of B_4C). It should be noted that the phase coupling difference results in a melting of the silicon when the preform is at a lower temperature, which can have consequences on the microstructures.

In part B, the major identified parameters were scanned to understand their prominence. It appears that initial porosity state is the main parameter to achieve high mechanical properties (20GPa of hardness). The pre-sintering step is also substantial parameter because it prevents the displacement of the particles, so, piece keeps it shape. These test also defined minimum silicon overload to fill all the porosity (20wt.%). The temperature and dwell time parameters have low influence on the reaction which is rapid after infiltration of the molten silicon.

In part C, specificities of the microwave heating were studied to better understand the reactivity in such condition. The comparison of the compositions of the samples obtained by the conventional and microwave heating methods, for various thermal cycles, shows that the reaction is more advanced in microwaves. In fact, more than the action of the electromagnetic field, it is shown that it is the atmosphere that could have an influence on the reaction. Indeed, it appears that Ar/H_2 facilitate the reaction probably because surfaces are cleaned from all oxidation. This was confirmed by the reactive thickness study where the B12 (rim phase) width is always higher in microwave furnace than in conventional furnace. Mechanical properties also appear to be similar for both heating conditions even if their microstructures are completely different: in particular, the silicon carbide known to grow in needles in the case of conventional heating is in the form of micro grains composed of nanometric crystals in the case of the microwave process. The study of cracks propagation shows that there are differences between conventional way of fabrication and micro-wave furnace heated samples. However, the microwave furnace, allows quicker cooling rate than conventional furnace, which drastically decrease the process time. Indeed, in micro-wave furnace the thermal cycle (heating, dwell time and cooling to temperature lower than 100°C) took 3hours while in conventional furnace it took at least 8 hours to do the same thing. But it is important to note that the effects of high cooling rate were not studied in this work. This could damage bigger piece by thermal choc.

Bibliography:

[BAR13] : BARICK P., JANA D.C., THIYAGARAJAN N., "Effect of particle size on the mechanical properties of reaction bonded boron carbide ceramics", Cer. Int., 39, p. 763-770, 2013

[DAR12] : DARIEL M.P, FRAGE N., "Reacition bonded Boron carbide: recent developments", Advanced in Applied Ceramics, vol 111, n°5&6, p. 301-310, 2012

[HAY06] : HYUN S., FRAGE N., DARIEL M.P., "The morphology of ceramic phases in BxC-SiC-Si infiltrated composites", Journal of solid state chemistry, 179, p. 2875-2879, 2006

[HAY09a] : Frage et al, “The effect of particle size distribution on the microstructure and the mechanical properties of boron carbide based reaction-bonded composite”, Int. J. Appl. Ceram. Technol., 6[4] 492-500 (2009)

[HAY09b] : HAYUN S., WEIZMANN A., DARIEL M.P., FRAGE N., "Rim region growth and its composition in the raction bonded boron carbide composites with core-rim structure.", 16th International Symposium of Boron, Borides and Related materials, Journal of Physics: Conference Series, 176, 012009, 2009

[HAY09t] : HAYUN S., Thesis, "The Inter-relationships between the static and dynamic mechanical properties and microstructure of reaction bonded boron carbide composites", Ben Gurion University of Neguev, Septembre 2009

[HAY10a] : HAYUN S., WEIZMANN A., DARIEL M.P., FRAGE N., "Microstructural evolution during the infiltration of boron carbide with molten silicon", J. Eur. Cer. Soc., 30, p. 1007-1014, 2010

[HAY10b] : HAYUN S., DARIEL M.P., FRAGE N., ZARETSKY E., "The high-strain-rate dynamic response of boron carbide-based composites: The effect of microstructure", Acta Materialia, 58, p.1721-1731, 2010

[HAY10c] : HAYUN S., DILMAN H., DARIEL M.P., FRAGE N., DUB S., "The effect of carbon source on the microstructure and the mechanical properties of reaction bonded boron carbide", Advances in sintering science and technology, Book series: Ceramic Transaction, 209, p. 29-39, 2010

[LEE02] : LEE H., SPEYER R.F., "Sintering of boron carbide heat-treated with hydrogen", J. Ame.Cer.Soc, 85, [8], p.2131-2133, 2002

[TAR04t] : TARIOLLE S.,Thesis, "Carbure de bore monolithique poreux et composites lamellaires elaboration, proprietes, renforcement", E.N.S des Mines de Saint-Etienne, order n°328TD, 2004

[THU13] : THUAULT A., MARINEL S., SAVARY E., HEUGUET R., SAUNIER S., GOEURIOT D., AGRAWAL D., "Processing of reaction-bonded B4C-SiC composites in a single-mode microwave cavity, Cer. Int., 39, [2], p. 1215-1219, 2013

[WAN14] : WANG J., LIN W., JIANG Z., DUAN L., YANG G., "The preparation and properties of SiCw/B4C composites infiltrated with molten silicon", Cer. Int., 40, p. 6793-6798, 2014

[WU12] : WU H., ZHANG S., GAO M., ZHU D., PAN Y., LIU Y., PAN H., OLIVEIRA F.J., VIEIRA J.M., "Microstructure and mechanical properties of multi-carbides/(Al,Si) composites derived from porous B4C preforms by reactive melt infiltration", Mat. Sci. Eng. A, 551, p. 200-208, 2012

[ZHA14a] : ZHANG C., RU H., WANG W., YUE X., ZHAO J., "The role of the infiltration temperature in the reaction bonding of boron carbide by silicon infiltration", J. Am. Ceram. Soc., 97, [10], p. 3286-3293, 2014

[ZHA14b] : ZHANG Z., DU X., LI Z., WANG W., ZHANG J., FU Z., "Microstructures and mechanical properties of B4C-SiC intergranular/intragranular nanocomposite ceramics fabricated from B4C, Si, and graphite powders", J. Eur. Cer. Soc., 34, p. 2153-2161, 2014

[ZUO13a] : ZUO F., SAUNIER S., MARINEL S., GOEURIOT D., “Comparison of the microwave and conventional sintering of alumina: effect of MgO Doping and particle size”, J. Am. Ceram. Soc., 96, [6], p. 1732-1737, 2013

ZUO13b] : ZUO F., SAUNIER S., MEUNIER C., GOEURIOT D., “Non-thermal effect on densification kinetics during microwave sintering of α-alumina”, Scripta Materialia, 69, p. 331-333, 2013

CONCLUSION

The thesis presents the adaptation of the reaction bonded boron carbide, permeation of molten silicon into porous boron carbide preform, in a microwave furnace. Obtained microstructure and properties were studied in the light of those obtained conventionally. Several parameters in the process were studied, like the atmosphere condition (composition and pressure). Once the working atmosphere was clearly found, then parametric studies were conducted to find optimal infiltration condition to obtain the highest mechanical properties. After that, these properties were linked to the obtained microstructure and compared with conventional samples. A possible phenomenology, explaining the difference between conventionally made samples and microwave heated samples, was advanced.

1-Process

An optimized crucible was designed to stabilize and homogenize the required temperature. It consists in alumino-silicate box with a layer of silicon carbide under boron carbide preform and silicon chip on the top. The working atmosphere was Ar/H_2 (10%) at an absolute pressure of 1.4 bars to prevent at a maximum the plasma formation. This atmosphere limits the heating rate at 10°C/min. In microwave furnace, temperature was measured on the B_4C and a differential temperature was observed between Silicon lump and B_4C. Silicon started to melt (1414°C) when boron carbide was between 1300-1350°C. This was caused by a difference in the coupling effect. Moreover, constant incident power test showed that molten silicon is easily heated by microwave. This decreases the power consumption at high temperature.

2-Microstrucure and properties

As in conventional furnaces, the microwave heated obtained composites consisted in four different phases: silicon carbide, residual silicon, boron carbide and $B_{12}(B,C,Si)_3$. This microstructure differed according to which heating methods were used for the infiltration step. Smaller SiC grains were obtained in microwave furnace than in conventional furnace. This difference came from the gas utilized not from any specific microwave effect. The reactivity between Si and B_4C seemed slightly better in microwave than in conventional furnace because the reactions rates are higher in microwave than in conventional furnace and the B_{12} layer width is higher in microwave than in conventional furnace for the same amount of time. Despite of these differences, mechanical properties were equal for both heating methods. The composite obtained have high hardness (13-19GPa) this mostly depends on the initial porosity than on the temperature. The dwell time at high temperature had no effect, either on the microstructure or on properties. At a temperature lesser than 1400°C, a dwell time is needed to fully infiltrate the boron carbide preform. Despite the SiC microstructure difference, fracture toughness values are similar whatever the atmosphere. This is due to the cracks propagation inside the composite. Indeed, cracks were almost not

deflected, neither by big needles (vacuum) nor by small aggregate (Ar/H_2 atmosphere) because of the interfacial cohesion. In all cases, the pre-sintering was crucial step to achieve high mechanical properties and microstructure homogeneity.

3-Phenomenology

Differences in microstructure were investigated to found their exact origins. One test was carried out in conventional furnace but under slightly reduced, Ar/H_2, atmosphere (CTF) to separate "heating" methods from atmosphere condition. The microstructure was the same in CTF than in MW. The microstructure was more influenced by the atmosphere than by the heating methods. B_4C and Si had a better surface state in the case of the atmosphere infiltration than in the conventional furnace. Ar/H_2 removed silicon oxide and boron oxide from Si and B_4C respectively. Both phases are more reactive so the equilibrium was reached faster.

4-Prospect

This thesis was the first attempt to study RBBC in a microwave furnace. In conclusion; it appears that the RBBC formation process is facilitated under microwave heating conditions. However, particular atmosphere conditions are imposed by the microwave technique: hydrogenous argon. This atmosphere influences the process more than microwaves. Therefore, we cannot say that the electromagnetic field has a strong influence on the genesis of the microstructure, and thus the properties. The obtained composites have similar mechanical properties that those prepared by conventional furnace.

Nevertheless, this technique remains interesting from an application point of view, saving time and energy for industry. The logical next step seems to be to develop targets to test ballistically, especially since the hardness of the composites obtained is quite high. Moreover, since the coupling to the microwave of the part depends on its mass, the production of larger diameter parts is conceivable.

APPENDIX

Appendix I Abstract board on the preforms manufacturing condition:

Source	Composition	Pressure	Heat treatment (°C)	Final porosity (%)	Comments
S.Hayun, N.Frage, M.P.Dariel, "The morphology of ceramic phase in B_xC-SiC-Si infiltrated composite", Journal of solid state chemistry 179 (2006) 2875-2879	B_4C		1900-2100 (30min)	20-40	
Details	B_4C (5µm, Modan Jang) compact 20 mm of diameter, 3 mm thickness, shaped by uniaxial pressure. Compact is sintered between 1900-2100°C during 30 minutes. The authors obtained a final porosity between 20-40%. To add carbon the authors infiltrated an aqueous sugar solution (50/50). Then compact is dried and heated at 500°C.				
A.Thuault, S.Marinel, E.Savary, R.Heuguet, S.Saunier, D.Goeuriot, D.Agrawal, "Processing of reaction bonded B_4C-SiC composite in a single-mode microwave cavity", Ceramic international 39 (2013) 1215-1219	85%B_4C+ 15%C	Unaxial 30.6kN (922MPa)	Compact No-sintered	35	
Details	85% in weight of B_4C (F20 Metap 5003) with 15% in weight of C (Alfa Aesar 99.9995%, D50≈74µm), an organic binder is added (Rhodoviol 4%, Prolabo). The pellet made 6.5mm of diameter and 5.4 mm of thickness and is uniaxialy pressed under 30.6kN. The density obtained is 65% of the theoretical density (B_4C-C).				
J.Wang, W.Lin, Z.Jiang, L.Duan, G.Yang, "The preparation and properties of SiC_w/B_4C composite infiltrated with molten Si", Ceramic international 40 (2014) 6793-6798	B_4C-SiC-C	100MPa	900 (5h)	Unknown	
Details	In first time B_4C(F100; purity 96-98%, d50:125µm;-F500; purity 94-95%, 12.8±1µm, Mudanjiang Jingganzuan Boron carbide Co) and C are mixed with paraffin (20% in weight)				

	and some dispersant (Tetramethylammoniumhydroxyde, TMAH) then ball milled during 24h. After a slurry of SiC (Guangzhou Jiechuan Trade Co) dispersed in distilled water and TMAH (25% in weight, jiangsu) is added in the previous mix during 6h. The final mix is dried at 60°C under vacuum. The compact is shaped by pressing at 100Mpa ($50*25*6mm^3$). Then compacts are heated at 900°C during 5h.				
S.Hayun, A.Weizmann, N.Frage, M.P.Dariel, "Microstructural evolution during the infiltration of boron carbide with molten silicon", Journal of the European ceramic society 30 (2010) 1007-1014	B_4C-5weight %C	Uniaxial 25MPa	Compact No-sintered	Unknown	
Details	B_4C(Mudanjiang abrasive and grinding tools Co, purity 95%) is shaped by uniaxial pressing at 25MPa(20mm of diameter and 3 mm of thickness). The carbon is added with an aqueous sugar solution (50/50). The compact is dried and heated at 500°C to pyrolyze the sugar.				
S.Tariolle, F.Thévenot, M.Aizenstein, M.P.Dariel, N.Furmin, N.Frage, "Boron carbide-Copper infiltrated cermets", Journal of solid state chemistry 177 (2004) 400-406	B_4C	Uniaxial 60MPa (EMSE) 80MPa (BGU) Isostatic 350MPa (EMSE)	Sous Ar 2150(1h) (EMSE) 2150-2200(1h) (BGU)	13-19 (EMSE) 5-30 (BGU)	
Details	EMSE: B_4C (Tetrebo 300F, ESK Kempten purity 98%, d50: 0.7-0.8µm, specific area: $12m^2/g$) powder is mixed with a dispersant (phosphoric ester, 1.5% in weight) and a solvent (methylethylcetone/ ethanol 66/34). Slip is disagglomerated by ultrasound then it is homogenized in a blender with SiC cylinder during 8h. A sintering agent (phenol-formaldehyde resin, Alnovol PN320) is added to the slurry the mix is homogenized again in the blender during one night. In some mix a pyrolysable pore-generating agent (corn starch, ref 695111, Roquette, france) is added and the mixture is homogenized in the blender during 4h at low speed. The slip is dried at 100°C under vacuum then 200µm				

	particles sizes are sifted out. Samples are shaped by uniaxial pressure (60MPa) followed by a cold isostatic pressure (350MPa), and unbound under Argon flow. The sintering is realized under argon flow at 2150°C during 1h. BGU: B_4C(MJ and Starck, d50: 0.8µm, the B/C ratio is 3.7-3.8, specific area 15-20m²/g) powder is shaped without binder by uniaxial pressure (80MPa) and then are sintering under argon flow at 2150-2200°C during 1h.				
S.Hayun, H.Dilman, M.P.Dariel, N.Frage, "The effect of aluminum on the microstructure and phase composition of boron carbide infiltrated with silicon", Materials chemistry and physics 118 (2009) 490-495	B_4C	Uniaxial 25MPa	Compact No-sintered	Unknown	
Details	Preforms made from coarse B_4C (106µm Mudan jiang, China) uniaxial pressure (25MPa).				
N.Frage, L.Levin, N.Furmin, M.Gelbstein, M.P.Dariel' "Manufacturing B_4C-(Al,Si) composite materials by metal alloy infiltration", Journal of materials processing technology 143-144 (2003) 486-490	B_4C	150MPa	Sous Ar 1900-2160	16-40	
Details	B_4C (Strack, grade HS,d50: 2µm) is compacted at 150MPa then sintered between 1900 and 2160°C (to vary the porosity rate) in an "Astro" furnace under argon flow.				
M.Cafri, H.Dilman, M.P.Dariel, N.Frage, "Boron carbide/magnesium composite: Processing, microstructure and properties", Journal of the European ceramic society 32 (2012) 3477-3483	Multimodal B_4C	Uniaxial 180 MPa	Compact No-Sintered	20	
Details	B_4C(Starck, grade HS, 3µm, purity 97.5% and MJ china, 50 and 100µm, purity 97%). Samples are prepared by a mix (16h) of B_4C (3µm-19%, 13µm-18%, 50µm-10%, 106µm-53% in volume). Preforms were cylinder of 20mm diameter and 4mm height, they are shaped by uniaxial pressure (180MPa).				
H.Wu, S.Zhang, M.Gao, D.Zhu, Y.Pan, Y.Liu, H.Pan, F.J.Oliveira, J.M.Vieira, "Microstructure and mechanical properties of multi-carbide/(Al,Si)	B_4C and B_4C-C	Uniaxial 96MPa	1550 (3h)	Unknown	

composite derived from porous B_4C preforms by reactive melt infiltration", Materials science and engineering A 551 (2012) 200-208					
Details	B_4C (Dalian Jinma Technology Co. Ltd., d50: 10-40 µm), carbon is added (100nm, 10% in weight) in some samples. These two types of sample are ball mixed in alcohol with agate ball at 650 rpm during 6h then dried under air at 80°C. Polyvinyl alcohol is added (3% in weight) as binder. Compacts (50*50*5mm) are obtained by uniaxial pressure (96MPa). The preforms are sintered at 1550°C during 3h. Al-Si alloy is laboratory made from powder with 99.99% purity. Ingots obtained are cut to obtain a sufficient quantity to fulfill preforms' pore.				
S.Hayun, N.Frage, M.P.Dariel, E.Zaretsky, "The high-strain-rate dynamic response of boron carbide-based composites: the effect of microstructure", Acta Materialia 58 (2010) 1721-1731	B_4C and B_4C-C	RB Uniaxial 140MPa RI and RIC RBM		RB 30 RI and RIC 30 RBM 25	
Details	4 samples' groups are formed (RI, RIC, RB, RBM): B_4C (Strack, grade Hs, d50: 1µm). RI and RIC are compacted to obtain a post-sintered porosity of 30%. In RIC, C is added with sugar solution (50/50) which is pyrolyzed under argon flow at 500°C. RB is shaped by uniaxial pressure (140MPa) and samples have a porosity of 30%. RBM is obtained by a multimodal mix of B_4C powder follow the protocol of the "Reaction bonded boron carbide/Magnesium-silicon composite" publication, this method allowed to obtain 25% of porosity.				
S.Hayun, A.Weizmann, N.Frage, M.P.Dariel, "The effect of particle size distribution on the microstructure and mechanical properties of reaction bonded B_4C", Journal of applied ceramic technology 6[4] (2009) 492-500	Multimodal B_4C	Uniaxial 40-180MPa	Compact No-Sintered	25-40	
Details	B_4C commercial (Mudanjiang abrasives and grinding tools, Mudanjiang, purity 95%) is sifted to separate different particles sizes (130, 70, 50, 13, 1µm). Preforms are prepared by different mix of previous powder. These mixes are mixed in dry condition in a				

	planetary mill during 8h. Glycerol (2% in weight) and alcohol (8% in weight) are added to the cold compaction. Mixes are shaped by uniaxial pressure between 40-180 MPa. Compacts (20mm diameter, 5mm thickness) are unbound.				
S.Hayun, H.Dilman, N.Frage, M.P.Dariel, S.dub "The effect of carbon source on the microstructure and the mechanical properties of reaction bonded B_4C", Advanced in sintering science and technology 209 (2010) 29-39	B_4C	Uniaxial 10 MPa	1900-2100 (30min)	20-40	
Details	B_4C powder is unaxialy pressed at 10MPa then partially sintered between 1900-2100°C during 30min to obtain a porosity of 20, 30 or 40%. Carbon is added with an aqueous sugar solution (50/50). Preforms are dried then sugar is pyrolyzed at 500°C under argon flow.				
M.Cafri, A.Malka, H.Dilman, M.P.Dariel, N.Frage, "Reaction bonded boron carbide/ Magnesium-silicon composite", International journal of applied ceramic technology 11[2] (2014) 273-279	Multimodal B_4C	Uniaxial 180MPa	Compact No-sintered	20	
Details	Samples are prepared from different commercial B_4C powder (H.C Strack 3µm, grade HS, 97.5%; Mudanjiang 13,50,100µm purity 97%) to reach a density of 80% by cold compression. Powder mix is the follow: 3µm-19%, 13µm-18%, 50µm-10%, 106µm-53%. Mixes are mixed in dry condition during 16h. Preforms of 20mm diameter, 4 mm thickness are shaped by uniaxial pressure 180MPa.				
S.Hayun, D.Rittel, N.Frage, M.P.Dariel , "Static and dynamic mechanical properties of infiltrated B_4C-Si composite", Materials science and engineering A 487 (2008) 405-409	B_4C	10MPa	2000-2100 (30min)	20 and 30	
Details	"Boron carbide (Starck, Grade HS) was compact at 10 MPa and sintered at 2000 and 2100°C for 30 min […] to obtain preforms with 20 and 30% of porosity."				
S.Hayun, A.Weizmann, H.Dilman, M.P.Dariel, N.Frage, "Rim region and its composition in reaction bonded boron carbide composites with	B_4C	25MPa	Compact No-sintered	Unknown	Coarse B_4C to study the interface reaction

core-rim structure", Journal of physics: conference series 176 (2009) 012009					
Details	Coarse B_4C (Mudan Jiang, size 106µm) is uniaxialy pressed at 25MPa.				
C.Zhang, H.Ru, w.Wang, X.Yue, J.Zhao, "The Role of the infiltration temperature in the reaction bonding of boron carbide by silicon infiltration", Journal of the American ceramic society 97[10] (2014) 3286-3293	B_4C +C	Uniaxial 200MPa	Compact No-sintered	Unknown	
Details	Commercial nano-powder of C is ultrasonically dispersed in distilled water. The dispersed C (10%) and commercial B_4C (90%) (Mudanjiang Abrasives and grinding Tools, 95% purity, d50=4.08µm) are mechanically mixed for 12h then dried at 90°C.The powder is crushed using a mortar and sieved at 250µm. PVA is added as binder agent for pressing step. Mixes are uniaxially pressed at 200MPa.				
P.Barick, D.Chandra Jana, N.Thiyagarajan, "Effect of the particle size on the mechanical properties of reaction bonded carbide ceramics", Ceramics international 39 (2013) 763-770	B_4C+C	Uniaxial 140MPa	Compact No-sintered	38-42	
Details	Commercial B_4C powder (Speedfam India (Pvt.) Limited, d50= 18.65, 33.70, 63.35) and C (Philips carbon black limited) are mixed like this: 87.2 wt% B_4C (one d50) 2.44wt% C and 10.37% of phenolic resin (36.04wt% of C in resin) finally the net amount of C is about 7wt%. The mix is ball milled in acetone using ZrO_2 balls. Resin is added 2h prior of the completion of milling. Acetone is removed from the mix. The dry powder is screened through a 60BSS sieve. The powder is uniaxially compacted at 140MPa.				
B.A.Almeida, M.C.Ferro, A.Ravanan, P.M.F.Grave, H-Y.Wu, M-X.Gao, Y.Pan, F.J. Oliveira, A.B.Lopes, J.M.Vieira, "Study of multi-carbide B_4C-SiC/(Al,Si) reaction infiltrated composites by SEM with EBSD", Materials science and engineering 55 (2014) 012001	B_4C	Uniaxial 60MPa Isostatic 196MPa	Compact No-sintered	50	
Details	B_4C (d50=10µm), is mixed with PVA and unixially pressed at 60MPa then is isostatcally pressed at				

	196MPa. 99.9% of pure Al and 99.99% of pure Si are melted to produce the different batches (Al-Si (25 and 35%)). Melting is carried out on a graphite furnace under 50kPa of Ar. Another batch is produce with 25% Si but it’s melted twice than once.

Appendix II Abstract board on the infiltration condition:

Source	Infiltrating	Preform	Porosity (%)	Temperature (°C)	Atmosphere	Comment
S.Hayun, N.Frage, M.P.Dariel, "The morphology of ceramic phase in B_xC-SiC-Si infiltrated composite", Journal of solid state chemistry 179 (2006) 2875-2879	Si (lump)	B_4C(-C)	20-40	1450	Vacuum 10^{-4} torr (≈10Pa≈10^{-4} mbar)	
Results	SiC is produced with or without carbon addition in equivalent quantity. In the case of carbon addition SiC precipitated in the interface between melt and graphite and "appears as white plate like particles". In the carbon free case SiC precipitated on the interface between melt and B_4C particles and appear in majority as "an irregular polygonal form". There are "core-rim" structures with BxSiyC composition.					
A.Thuault, S.Marinel, E.Savary, R.Heuguet, S.Saunier, D.Goeuriot, D.Agrawal, "Processing of reaction bonded B_4C-SiC composite in a single-mode microwave cavity", Ceramic international 39 (2013) 1215-1219	Si (pellet) Alfa Aesar (99.9% 0.149nm)	B_4C-C	35	1500	Ar(95%)-H2(5%)	
Results	There is a little shrinkage in height. Microstructure consists in B_4C and SiC grains surround by Silicon matrix and present low residual porosity. SiC grains have a polygonal shape form.					
J.Wang, W.Lin, Z.Jiang, L.Duan, G.Yang, "The preparation and properties of SiC_w/B_4C composite infiltrated with molten Si", Ceramic international 40 (2014) 6793-6798	Si	B_4C-SiC-Si	Unknown	1500	Vacuum	
Results	The bulk density increases firstly with the initial addition of SiC_w then decreases slowly. Maximum					

	value is obtained with 18% (weight) addition of SiC_w. The hardness and bending strength decrease with the initial addition of SiC_w, while fracture toughness increase.					
S.Hayun, A.Weizmann, N.Frage, M.P.Dariel, "Microstructural evolution during the infiltration of boron carbide with molten silicon", Journal of the European ceramic society 30 (2010) 1007-1014	Si(lump)	B_4C(-C)	unknown	1450	Vacuum 10^{-5} torr (≈1Pa≈10^{-5} mbar)	Development of a $B_{12}(B,C,Si)_3$ phase 3-7µm thickness between B_4C and SiC/Si. If the initial diameter of B_4C<5µm there are no more B_4C at the end of infiltration.
Results	Reaction between B_4C and Si formed $B_{12}(B,C,Si)_3$ phase and SiC. Two type of morphologies for SiC are observed which is related to the carbon source. The mechanism proposed is a dissolution-precipitation process. Si melt is saturated by C and B when infiltration is proceeding.					
S.Tariolle, F.Thévenot, M.Aizenstein, M.P.Dariel, N.Furmin, N.Frage, "Boron carbide-Copper infiltrated cermets", Journal of solid state chemistry 177 (2004) 400-406	Cu (Alfa Aesar 5N)-Si (electronic purity)	B_4C	EMSE (13-19) BGU (5-30)	750-1100	Ar	Eutectic Cu-Si (35% Si) TF : 850-900°C Liquid Cu solubilized B in the B_4C which can permit to improve the mechanic attach
Results	Cu-Si alloy can penetrated in the preform while pure Cu can't. SiC is formed and surrounded B_4C grains, but there is a thin layer of Cu-Si alloy between SiC and B_4C. SiC act like a barrier around the carbon particles or the B_4C particles these lead at a limited increase of hardness as a function of the heat treatment duration.					
S.Hayun, H.Dilman, M.P.Dariel, N.Frage, "The effect of aluminum on the microstructure and phase composition of boron carbide	Si (Alfa Aesar purity 99.9999%)	B_4C	Unknown	1450-1480 (10-240 min)	Vacuum 10^{-5} torr (≈1Pa≈10^{-5} mbar)	Vaporization of the Al_2O_3 under vacuum-> contamination of

infiltrated with silicon", Materials chemistry and physics 118 (2009) 490-495						the composite by Al in the liquid phase witch improved the B solubility.
Results	When infiltration is proceeding without Al_2O_3 the final microstructure is composed by four phase (B_4C, SiC, Si and $B_{12}(B,C,Si)_3$). If the infiltration is proceeding with Al2O3 after 30 minutes at the infiltration temperature Al phase can be detect by XRD method. Both type of infiltration lead to core-rim structure. EDS analysis show high aluminum content in molten Si, this phase is smother than pure Si. The solubility of B increase with the increase of Al in the melt, while B activity in the melt decreases.					
N.Frage, L.Levin, N.Furmin, M.Gelbstein, M.P.Dariel' "Manufacturing B_4C-(Al,Si) composite materials by metal alloy infiltration", Journal of materials processing technology 143-144 (2003) 486-490	Al-Si(13-40% in weight)	B_4C	16-40	1100°C infiltration+ Heat treatment at 1200°C (10h)	Vacuum 10^{-4} torr (≈10Pa≈10^{-4} mbar)	
Results	The addition of Al in the alloy affects the kinetics of wetting during infiltration process. The presence of Si improves the wetting and reduces the infiltration temperature by 30-60°C. Reactivity of Si improves the wetting and accelerated the penetration of molten alloy. Pure aluminum didn't penetrate in the preform while Al-40%Si completely penetrated in it. There no reaction between B_4C and Al in the case of pure Al. For Al-Si alloy different phase appear AlB2, Al4C3 and SiC. Heat treatment leads to the formation of $AlB_{12}C_2$, $Al_8C_7B_4$ and $Al_4C_4B_x$. Amount of Aluminum carbide is maximum for 13% Si beyond this value it disappears. The hardness is strongly dependent of the ceramic/metal ratio. Heat treatment increases hardness by increases the amount of SiC.					
M.Cafri, H.Dilman, M.P.Dariel, N.Frage, "Boron carbide/magnesium composite: Processing, microstructure and properties", Journal of the European ceramic	Mg or alloy AZ91(9% Al and 1% Zn) (piece) Twice more	B_4C	20	850(20min)	Semi-hermetical (≈1Pa) 6.6KPa de Mg	Eutectic Mg-Si : (55% Si) TF : 939°C

society 32 (2012) 3477-3483	than necessary to fulfill pore					
Results	The wetting of Mg alloy is better than pure Mg, but these two types of contact lead to the formation of new phase at the interface. The final composite is composed by residual Mg, MgB_2 and B_4C for pure Mg infiltration, and residual Mg, MgB_2C, $Mg_{17}Al_{12}$ and B_4C for alloy infiltration. The newly formed phase wet perfectly the B_4C. The mechanical properties of alloy infiltration is better than pure Mg infiltration for micro hardness and young modulus because of the metal/ceramic ratio , but they are significantly lower than pure Si infiltration.					
H.Wu, S.Zhang, M.Gao, D.Zhu, Y.Pan, Y.Liu, H.Pan, F.J.Oliveira, J.M.Vieira, "Microstructure and mechanical properties of multi-carbide/(Al,Si) composite derived from porous B_4C preforms by reactive melt infiltration", Materials science and engineering A 551 (2012) 200-208	Al-Si alloy (36-55-80%) Piece 3 case	B_4C and B_4C-C	Unknown	200°C higher than Tf of the alloy	10^{-2} Pa	
Results	All the composites are composed by SiC, Al, Si, B_4C, $AlB_{12}C_2$, and $Al_3B_{48}C_2$. Al-Si alloy are able to spontaneously infiltrated B_4C and B_4C/C preform. The better mechanical properties are obtained for Al-55%Si Flexural strength 328±8 MPa, Hardness 17±3GPa, Young modulus 291±3GPa).					
S.Hayun, N.Frage, M.P.Dariel, E.Zaretsky, "The high-strain-rate dynamic response of boron carbide-based composites: the effect of microstructure", Acta Materialia 58 (2010) 1721-1731	Si(98.4% Alfa Aesar)	B_4C	25-30	1480 (20min)	Vacuum 10^{-5} torr (≈1Pa≈10^{-5} mbar)	
Results	Regardless of the composition or of the history of the preform the composition of the final composite is the same: B_4C, $B_{12}(B,C,Si)_3$, SiC, Si. However the shape of SiC particle, the amount of Si and the size of B4C grains are different for composite obtain by different approach. Multimodal preform has lower mechanical properties. The difference of mechanical properties between					

	composite with free carbon and no free carbon is due to the shape of SiC. The presintering stage seems to have no effect on mechanical properties.					
S.Hayun, A.Weizmann, N.Frage, M.P.Dariel, "The effect of particle size distribution on the microstructure and mechanical properties of reaction bonded B_4C", Journal of applied ceramic technology 6[4] (2009) 492-500	Si (Alfa Aesar, Ward Mill, MA, purity 98.4%)	B_4C	25-40	1450 (15min)	Vacuum 10^{-4} torr (≈10Pa≈10^{-4} mbar)	
Results	No influence of the mixture (monosized and multimodal preform) on the infiltration behavior. The composite is composed by B_4C, $B_{12}(B,C,Si)_3$, SiC, Si. Mechanical properties: Hardness 2300±250 HV, young modulus 400±10GPa, Flexural strength 318±20 MPa.					
S.Hayun, H.Dilman, N.Frage, M.P.Dariel, S.dub, "The effect of carbon source on the microstructure and the mechanical properties of reaction bonded B_4C", Advanced in sintering science and technology 209 (2010) 29-39	Si (Alfa Aesar98.4%)	B_4C(-C)	20-40	1480 (20min)	Vacuum 10^{-5} torr (≈1Pa≈10^{-5} mbar)	SiC formed without free carbon improved mechanical properties beside of SiC formed with free carbon
Results	Regardless of carbon source the composite composition is the same: B_4C, $B_{12}(B,C,Si)_3$, SiC, Si. If there is no free carbon in the preform Si reacts with B_4C to form plate-like particles SiC , if there is free carbon Si reacts with C to form irregular polygonal SiC. The amount of SiC is approximately the same. B_4C and $B_{12}(B,C,Si)_3$ have the same mechanical properties. The boundary between B_4C and $B_{12}(B,C,Si)_3$ is semi coherent boundary. The Young modulus and hardness decrease with increase of residual Si. Flexural strength didn't depend of the amount of residual silicon but strongly depend of the carbon source (SiC's shape) it is higher for infiltration without free carbon than infiltration with free carbon.					
M.Cafri, A.Malka, H.Dilman, M.P.Dariel, N.Frage, "Reaction bonded boron carbide/ Magnesium-	Mg-Si (eutectic 53% atomic Si) or	B_4C	20	1000 (20min)	0.01 Pa	B_4C infiltrated by the eutectic alloy has good ballistic

silicon composite", International journal of applied ceramic technology 11[2] (2014) 273-279	AZ91 (9%Al,0.7% Zn, 0.3% Mn in weight)-Si (53% atomic)					properties (16% weaker than pure Si) comparatively at its cost
Results	Composite is composed by B_4C, SiC, Mg_2Si and $Mg_x(Al,Si)_y(B,C)_z$. Mechanical properties : Hardness 1700HV, Young's modulus 356MPa, bending strength 230MPa. Ballistic efficiency is higher than alumina and only 16% weaker than pure Si infiltration.					
B.A.Almeida, M.C.Ferro, A.Ravanan, P.M.F.Grave, H-Y.Wu, M-X.Gao, Y.Pan, F.J. Oliveira, A.B.Lopes, J.M.Vieira, "Study of multi-carbide B_4C-SiC/(Al,Si) reaction infiltrated composites by SEM with EBSD", Materials science and engineering 55 (2014) 012001	Al-Si (25 and 35% Si) And Al-25%Si with 2 melting	B_4C	50	1200-1350 (5-60 min)	+50kPa Ar	The shape of B_4C isn't specify
Results	XRD analysis shows four phases: Al(44 vol%), Si(19vol%), B_4C(33vol%), SiC(4vol%). EBSD images show Al and Si are separated, B4C grains are not preferentially wet by one or the other metal. For EBSD analysis mechanical polishing followed by chemical etching (30s-1min in 25 vol% HNO_3 75 vol% methanol) give goods results.					
S.Hayun, A.Weizmann, H.Dilman, M.P.Dariel, N.Frage, "Rim region growth and its composition in reaction bonded boron carbide composites with core-rim structure", Journal of physics: conference series 176 (2009) 012009	Si	B_4C	Unknown	1480 (10-240 min)	Vacuum 10^{-5} torr ($\approx$1Pa$\approx10^{-5}$ mbar)	Direct contact between B_4C and SiC. Reaction between Al2O3 and C even if they aren't in direct contact. Al in liquid Si modifies the core-rim structure. The B_4C can be

						completely consumed by Si/Al liquid in contrast of Si liquid.
Results	If there is alumina in the furnace, some aluminum could interact in the preform, modify the kinetics of rim region growth and enhance the transformation of B_4C in $B_x(C,Si,Al)_y$. Aluminum in rim region stabilize it in KOH attack.					
C.Zhang, H.Ru, w.Wang, X.Yue, J.Zhao, "The Role of the infiltration temperature in the reaction bonding of boron carbide by silicon infiltration", Journal of the American ceramic society 97[10] (2014) 3286-3293	Si	B_4C +C	Unknown	1450-1650 (1h)	Vacuum 50Pa	
Results	The volume % of B_4C decreases while those of SiC and Si increase with the increase of the temperature infiltration. The morphology of SiC depends of the infiltration temperature. Condition which leads at the higher mechanical properties is in 1600°C to infiltrate Si. Mechanicals properties: hardness 19GPa, flexural strength 344MPa and fracture toughness 3.8MPa.$m^{1/2}$.					
M.Kouzeli, C.San Marchi, A.Mortensen, "Effect of reaction on the tensile behavior of infiltrated boron carbide-aluminum composites", Materials science and engineering A 337 (2002) 264-273	Al	B_4C	Unknown	750 (2 and 15min)	Vacuum 2Pa then Ar 8MPa	
Results	The purpose of the manipulation is to obtain B_4C particle in an Al matrix. Phase obtain: B_4C, AlB_2, Al_3BC. The Young's modulus depends on the volume fraction ceramic. The Young's modulus depends the duration of interaction (time at high temperature).					
P.Barick, D.Chandra Jana, N.Thiyagarajan, "Effect of the particle size on the mechanical	Si	B_4C+C	38-42	1550 (30min)	Vacuum $65*10^{-6}$ Torr (($\approx$6.5Pa$\approx$$6.5*10^{-5}$	

properties of reaction bonded carbide ceramics", Ceramics international 39 (2013) 763-770					mbar	
Results	Large starting particles and a small amount of residual Si is good for hardness, while small grain and large amount of residual silicon is good for fracture toughness and K_{1C}.					
S.Hayun, D.Rittel, N.Frage, M.P.Dariel , "Static and dynamic mechanical properties of infiltrated B_4C-Si composite", Materials science and engineering A 487 (2008) 405-409	Si	B_4C	20 and 30	1480 (20 min)	Vacuum 10^{-4} torr (≈10Pa≈10^{-4} mbar)	
Results	Composite is composed by three phases B_4C, SiC, Si. Mechanical properties depend of the amount of residual Si, they decrease (Young's modulus and Hardness) when residual Si increases or they increase (Flexural Strength and K_{1C}) when residual Si increases.					

Appendix III Abstract board on the wettability test

Source	Substrate	Wetting	Test temperature (°C)	Test duration (min)	Test atmosphere (pressure)	Results
R.Pampuch, E.Walasek, J.Bialoskorski, "Reaction Mechanism in Carbon-liquid silicon systems at elevated temperatures", Ceramics international 12 (1986) 99-106	C	Si	1500±50	1-30	Vacuum (1.33Pa)	
R.Pampuch, E.Walasek, J.Bialoskorski, "Mechanism of reaction in the Si+C system and the self-propagating high-temperature synthesis of silicon carbide", Ceramics international 13 (1987) 63-68	C	Si	1450	2-3	Unknown	Si diffuses 10 times faster than C in SiC-> growth of the SiC layer at the SiC/C interface.
J.G.Li, H.Hausner, "Contact angle and work of adhesion isotherms of silicon-tin alloys on monocrystalline silicon carbide", Materials letters 11 (1991) 10-12	α-SiC	Si-Sn	1430	60	Unknown	
J.G.Li, H.Hausner, "Wetting and adhesion in liquid silicon /ceramic systems", Materials letters 14 (1992) 329-332	Al_2O_3 SiO_2 SiC	Si	1430	60	Unknown	
J.G.Li, H.Hausner, "Wetting and infiltration of graphite materials by molten silicon", Scripta metallurgica et materialia 32 [3] (1995) 377-382	Graphite	Si	1430	60	Ar (1 atm)	Si is washed in HF (40%) then it rinsed in water and acetone. Infiltration is made at 1430° and has 60min of duration. The melting of Si takes 1.5min generally. Vertical infiltration

						seems to be independent of the contact angle; lateral infiltration is dependent of the contact angle.
J.G.Li, H.Hausner, "Reactive Wetting in the liquid-silicon/Solid-Carbon System",Journal of the American ceramic society 79 [4] (1996) 873-880	Vitreous carbon	Si	1430	60	Ar (1 atm)	
K.Landry,C.Rado, R.Voitovich, N.Eustathopoulos, "Mechanism of reactive wetting: the question of triple line configuration", Acta materialia 45 [7] (1997) 3079-3085	Vitreous carbon and SiC	Cu-40%Si Cu-1%Cr	1150 1100	1.40	Vacuum (10^{-6} Pa 10^{-3} Pa He)	
A.Mortensen, F.Hodaj, N.Eustathopoulos, "On thermal effect in reactive wetting", Scripta materialia 38 [9] (1998) 1411-1417	Theoretical work					
S.Kalogeropoulu, C.Rado, N.Eustathopoulos, "Mechanism of reactive wetting : the wetting to non-wetting case", Scripta materialia 41 [7] (1999) 723-728	SiC	Ag	1200	15	Unknown	
C.Rado, S.Kalogeropoulou, N.Eustathopoulos, "Wetting and Adhesion in Metal-Silicon Carbide systems: the effect of surface polarity of SiC", Scripta materialia 42 (2000) 203-208	SiC	Si, Ni-40%Si, Cu-25%Si	1430 1360 1100	Few minutes or tens of minutes	Unknown	There are a significant difference between the two crystals orientation (approximately 9°)
F.G.Yost, "Kinetics of reactive wetting", Scripta materialia 42 (2000) 801-806	Theoretical work					
O.Dezellus, F.Hodaj, S.Janaqi, N.Eustathopoulos, "Influence of evaporation-condensation in reactive spreading", Acta materialia 50 (2002)	Vitreous carbon	Cu-40%Si Cu-1.5%Si	1150	Unknown	Unknown	

4727-4740						
O.Dezellus, F.Hodaj, S.Janaqi, N.Eustathopoulos, "Chemical reaction-limited spreading: the triple line velocity versus contact angle reaction", Acta materialia 50 (2002) 4741-4753	Vitreous carbon	Cu-40%Si Ni-63%Si	1200	Unknown	Vacuum (10^{-5} Pa)	The advanced speed of the triple line is independent of the time and the drop's size (almost) it depend only on the contact angle.
N.Fourmin, N.Frage, M.Aizenshtein M.P.Dariel, "Ceramic metal interaction and wetting phenomena in the B_4C/Cu system", Journal of the European ceramic society 23 (2003) 2821-2828	B_4C	Cu-xB	1150	60	Vacuum (10^{-3} Pa)	
N.Fourmin, N.Frage, M.Aizenshtein M.P.Dariel, "Interface reaction in the B_4C/(Cu-Si) system", Acta materialia 52 (2004) 2625-2635	B_4C	Cu-xSi x (0-60%)	1150	120	Vacuum (10^{-5} Torr $\approx 10^{-3}$ Pa)	
Y.Nadich, "About liquid metal/ceramic interface interaction mechanism and mode of a new intermediate compound formation", Current opinion in solid state and materials science 9 (2005) 161-166	Al2O3 Graphite	Cu(Ti) Cu(Cr) CuSnTi	1150	15-60 5-90	Vacuum ($5x10^{-4}$ Pa)	
M.Aizenshtein, I.Mizrahi,N.Fourmin, S.Hayun, M.P.Dariel, N.Frage, "Interface interaction in the B_4C/(Fe-B-C) system", Materials science and engineering A 495 (2008) 70-74	B_4C	Fe-B Fe-C Fe-B-C	1450	15	Vacuum (10^{-3} Pa)	
N.Eustathopoulos, R.Israel, B.Drevet, D.Camel, "Reactive infiltration by Si: Infiltration versus wetting",Scripta materialia 62 (2010) 966-971	Graphite Si3N4(oxide)	Si	1430-1460	10	Unknown	
N.Eustathopoulos, B.Drevet, "Surface tension of liquid silicon: High or low value?", Journal of	BN Levitation	Si	Near the melting point	NA	Unknown	σ0 at 1645K 840±45mN/m

crystal growth 371 (2013) 77-83	with field or a gas effect		(1420-1450)			Young-Dupré equation: $cos\theta = \left(\frac{W}{\sigma}\right) - 1$ Where W is adhesion work, σ is surface tension and θ is the contact angle. BN is not wet by Si (contact angle between 105-145°). $\sigma = 840(\pm 45) - 0.19(\pm 0.09)(T - 1685)$ With σ in mN/m and T in K
H.Wu, F.Zeng, T.Yuan, F.Zhang, X.Xiong, "Wettability of 2519Al on B_4C at 1000-1250°C and mechanical properties of infiltrated B_4C-2519Al composite", Ceramics international 40 (2014) 2073-2081	B_4C	2519Al	1000-1250	30	Unknown	θ_f=141.2-0.086T

Samples	Initiale density (%)	Initial porosity (%)	Temperature (°C)	Dwel time (min)	Atmosphere	Final density (g/cm^3)	Hardness (GPa)
CVF	79	21	1480	20	Vacuum		18,7±1,2
CVF	76	24	1480	20	Vacuum	2,56	19,7±1
CVF	67	33	1480	20	Vacuum	2,51	15,8±1,8
CVF	67	33	1480	20	Vacuum	2,56	17,3±0,8
CVF	60	40	1480	20	Vacuum	2,51	15,2±1,5
CVF	60	40	1480	20	Vacuum		
CTF	73,5	26,5	1450	15	Ar/H_2	2,58	18,3±0,5
MW	74,6	25,4	1500	15	Ar/H_2		19,2±0,8
MW	74,2	25,8	1400	15	Ar/H_2	2,41	18,2±1,5
MW	65,6	34,4	1550	15	Ar/H_2	2,53	17,1±0,6
MW	67,2	32,8	1450	15	Ar/H_2	2,55	16,8±1
MW	65,2	34,8	1350	15	Ar/H_2	2,42	16,8±0,8
MW	60,7	39,3	1500	15	Ar/H_2	2,46	14,3±0,6
MW	60,6	39,4	1400	15	Ar/H_2	2,24	15,2±0,8
MW	65,4	34,6	1500	15	Ar/H_2	2,58	17,2±0,6
MW	71	29	1450	120	Ar/H_2	2,57	18,2±0,7
MW	71,8	28,2	1400	5	Ar/H_2	2,56	18,1±0,4
MW	73	27	1400	60	Ar/H_2	2,59	17,9±0,4
MW	61,8	38,2	1400	0	Ar/H_2	2,56	14,8±0,5
MW	62	38	1500	0	Ar/H_2	2,56	13,8±3
MW	55,6	44,4	?Monomode	15	Ar/H_2	2,55	13,8±0,4
MW	70	30	1450	15	Ar/H_2	2,43	15,9±3
MW	70	30	1450	15	Ar/H_2	2,42	16,8±3
MW	60,9	39,1	?Monomode	15	Ar/H_2	2,47	
MW	61,5	38,5	?Monomode	15	Ar/H_2	2,55	14,6±0,5
MW	61,5	38,5	?Monomode	15	Ar/H_2	2,51	15,4±0,4
MW	61,9	38,1	1450	15	Ar/H_2	2,56	15,1±0,6
MW	60,4	39,6	1450	15	Ar/H_2	2,56	15,1±0,4
MW	74,4	25,6	1350	15	Ar/H_2	2,5	

Young Modulus (±5GPa)	Flexural strength (MPa)	Toughness ($MPa.m^{1/2}$)	Poisson coefficient (±0,02)	Shear modulus (±3 GPa)	XRD + Chemical removing			Calculated density (g/cm^3)
					Vol.%Si	Vol.%SiC	Vol.% B_4C+B_{12}	
					6,4	8,4	85,1	2,57
370	553,2±52	2,55±0,35	0,21	152	10,9	7,2	81,9	2,55
341	346±127	2,55±0,43	0,16	145,75	25,8	6	68,2	2,51
356	492±44		0,18	150	23,4	6,1	70,4	2,52
333	427±62	2,4±0,19	0,17	142	36,6	8,2	55,2	2,51
					28,7	8,1	63,2	2,52
403	446±81	2,51±0,35	0,16	172,5	12	14	74	2,59
					4,5	13,4	82,1	2,60
					6,7	11,5	81,8	2,59
					25,3	9,8	64,9	2,54
395	352±125	2,84±0,22	0,17	167,75	28,5	9,4	62,1	2,53
					26,3	9,1	64,6	2,53
					30,3	8,3	61,4	2,52
					27	9,4	63,6	2,53
364		3,23±0,72			16,5	10,2	73,3	2,56
382		3,31±0,59	0,19	160	9	13	77	2,59
364	464±60	2,68±0,25	0,19	152	12	12	76	2,58
396		2,56±0,33	0,18	166,25	14	12	74	2,58
344		2,16±0,22	0,19	143,5	30	10	60	2,53
334		2,62±0,11	0,2	139	28	10	62	2,54
321		2,67±0,17	0,17	136,5				
323			0,13	142,5				
320		2,07±0,39	0,17	136,5				
316			0,16	135,25				
340		2,27±0,19	0,19	142				
341		2,21±0,17	0,2	142,25				
340	400±117	2,25±0,31	0,19	142				
390		3,1±0,12	0,18	164,75				
380	260±36		0,13	167	11	10,1	78,9	2,57

École Nationale Supérieure des Mines
de Saint-Étienne

NNT : 2017LYSEM021

Mathieu DUTTO

Reaction Bonded Boron Carbide Processed by Microwave Heating for Ballistic Applications.

Specialty: Materials Science

Keywords: Microwave, Reaction bonding, Boron carbide, Silicon carbide, high hardness

Abstract:

Many studies have shown the feasibility of processing silicon-boron carbide composite by infiltration of molten silicon through a porous preform made of boron carbide (Reaction Bonding Process). Using this method, the obtained composite contains a large amount of boron carbide, which is the hardest and the most interesting phase for ballistic application. In our developed process, the maximum processing temperature is 1600°C, which is far below the usual high temperature stage/pressure conditions commonly used to sinter B_4C by conventional method (respectively 2200°C and40MPa). The main goal of this thesis is to develop a novel reaction bonded process based on microwave heating. Microwaves heating has many interesting features, including fast heating process, selective heating mechanism (in case of heating multi-materials) and volumetric heating distribution. . To fulfill our goal, many technological issues need to be addressed (working in controlled atmosphere and under microwave field, high temperature ...). This thesis reports the development of this novel process, and materials made from it, exhibit similar properties compared to those made conventionally. However, some microstructural differences were observed in SiC resulting phases. This thesis has allowed to

-find out the boron carbide composite piece fabrication conditions in microwave cavity (Argon/Hydrogen10%, slight overpressure: 14bars)

-show that mechanical properties (hardness, Young's modulus…) obtained are comparable to those measured on conventionally reaction bonded produced materials.

-show that formed SiC has some microstructural peculiarities, between vacuum samples (for conventional) and ones obtained in hydrogenous argon (using microwave).

-show that it is possible to produce larger size piece (66mm of diameter). These results are shown to be promising for ballistic applications, including the fabrication of bulletproof jacket and light armor

École Nationale Supérieure des Mines
de Saint-Étienne

NNT : 2017LYSEM021

Mathieu DUTTO

Procédé micro-ondes pour l'élaboration de composites B_4C-SiC par infiltration et réaction de silicium, en vue d'applications balistiques.

Spécialité: Science des matériaux

Mots clefs : Micro-onde, Reaction bonding, Carbure de bore, Carbure de silicium, haute dureté

Résumé :

De nombreuses études ont montré la faisabilité de la fabrication de pièces composites en carbure de bore et de silicium par l'infiltration de silicium fondu dans une préforme poreuse en carbure de bore (Reaction bonding). Cette méthode permet l'obtention d'un composite fortement chargé en carbure de bore (phase qui nous intéresse pour les applications balistiques), sans pour autant avoir besoin de monter à des températures de frittage de plus de 2200°C (température habituellement utilisée pour fritter le B_4C). Dans notre cas la température maximale est comprise entre 1400-1600°C. Cette thèse s'intéresse plus particulièrement à l'adaptation du procédé de « reaction bonding » au chauffage sous champ micro-ondes. Les micro-ondes sont particulièrement intéressantes en ce qui concerne la rapidité du cycle thermique et le chauffage préférentiel de certaines phases (dans le cas des multi-matériaux). Pour ce faire, plusieurs verrous technologiques ont dû être levés (travail sous atmosphère et sous champs électromagnétiques, température élevée, …). Les composites obtenus sont comparés à leurs équivalents en chauffage conventionnel. Des différences microstructurales ont été observées au niveau du SiC formé lors de la réaction. Cette thèse nous a donc permis de :

-trouver des conditions de fabrication de pièces en carbure de bore par chauffage micro-ondes (Argon/Hydrogéné10%, légère surpression : 1.4 bars)

-montrer que les propriétés mécaniques (dureté, module d'Young,…) obtenues en four micro-ondes sont équivalentes à celles obtenus en four conventionnel (dureté : 14-20GPa)

-montrer d'importante différences microstructurales du carbure de silicium formé, entre les échantillons obtenus sous vide (four conventionnel) et ceux obtenus sous atmosphère contrôlée (micro-ondes et four conventionnel).

-montrer que le passage à des plus grandes tailles est possible, il est même plus simple d'infiltrer de grandes pièces que de petites à cause de l'effet de la masse sur la réponse du matériau aux champs électromagnétiques des micro-ondes.

Ces résultats sont très prometteurs pour des applications balistiques : fabrication de gilets pare-balles et blindages légers.